

# **INTERNATIONAL LINEAR COLLIDER REFERENCE DESIGN REPORT**

**ILC Global Design Effort and  
World Wide Study**

**AUGUST, 2007**

## **Volume 1: EXECUTIVE SUMMARY**

**Editors:**

**James Brau, Yasuhiro Okada, Nicholas Walker**

## **Volume 2: PHYSICS AT THE ILC**

**Editors:**

**Abdelhak Djouadi, Joseph Lykken, Klaus Mönig  
Yasuhiro Okada, Mark Oreglia, Satoru Yamashita**

## **Volume 3: ACCELERATOR**

**Editors:**

**Nan Phinney, Nobukazu Toge, Nicholas Walker**

## **Volume 4: DETECTORS**

**Editors:**

**Ties Behnke, Chris Damerell, John Jaros, Akiya Miyamoto**

# **Volume 1: EXECUTIVE SUMMARY**

**Editors:**

**James Brau, Yasuhiro Okada, Nicholas Walker**



# List of Contributors

Gerald Aarons<sup>203</sup>, Toshinori Abe<sup>290</sup>, Jason Abernathy<sup>293</sup>, Medina Ablikim<sup>87</sup>, Halina Abramowicz<sup>216</sup>, David Adey<sup>236</sup>, Catherine Adloff<sup>128</sup>, Chris Adolphsen<sup>203</sup>, Konstantin Afanaciev<sup>11,47</sup>, Ilya Agapov<sup>192,35</sup>, Jung-Keun Ahn<sup>187</sup>, Hiroaki Aihara<sup>290</sup>, Mitsuo Akemoto<sup>67</sup>, Maria del Carmen Alabau<sup>130</sup>, Justin Albert<sup>293</sup>, Hartwig Albrecht<sup>47</sup>, Michael Albrecht<sup>273</sup>, David Alesini<sup>134</sup>, Gideon Alexander<sup>216</sup>, Jim Alexander<sup>43</sup>, Wade Allison<sup>276</sup>, John Amann<sup>203</sup>, Ramila Amirikas<sup>47</sup>, Qi An<sup>283</sup>, Shozo Anami<sup>67</sup>, B. Ananthanarayan<sup>74</sup>, Terry Anderson<sup>54</sup>, Ladislav Andricek<sup>147</sup>, Marc Anduze<sup>50</sup>, Michael Anerella<sup>19</sup>, Nikolai Anfimov<sup>115</sup>, Deepa Angal-Kalinin<sup>38,26</sup>, Sergei Antipov<sup>8</sup>, Claire Antoine<sup>28,54</sup>, Mayumi Aoki<sup>86</sup>, Atsushi Aoza<sup>193</sup>, Steve Aplin<sup>47</sup>, Rob Appleby<sup>38,265</sup>, Yasuo Arai<sup>67</sup>, Sakae Araki<sup>67</sup>, Tug Arkan<sup>54</sup>, Ned Arnold<sup>8</sup>, Ray Arnold<sup>203</sup>, Richard Arnowitt<sup>217</sup>, Xavier Artru<sup>81</sup>, Kunal Arya<sup>245,244</sup>, Alexander Aryshev<sup>67</sup>, Eri Asakawa<sup>149,67</sup>, Fred Asiri<sup>203</sup>, David Asner<sup>24</sup>, Muzaffer Atac<sup>54</sup>, Grigor Atoian<sup>323</sup>, David Attié<sup>28</sup>, Jean-Eudes Augustin<sup>302</sup>, David B. Augustine<sup>54</sup>, Bradley Ayres<sup>78</sup>, Tariq Aziz<sup>211</sup>, Derek Baars<sup>150</sup>, Frederique Badaud<sup>131</sup>, Nigel Baddams<sup>35</sup>, Jonathan Bagger<sup>114</sup>, Sha Bai<sup>87</sup>, David Bailey<sup>265</sup>, Ian R. Bailey<sup>38,263</sup>, David Baker<sup>25,203</sup>, Nikolai I. Balalykin<sup>115</sup>, Juan Pablo Balbuena<sup>34</sup>, Jean-Luc Baldy<sup>35</sup>, Markus Ball<sup>255,47</sup>, Maurice Ball<sup>54</sup>, Alessandro Ballestrero<sup>103</sup>, Jamie Ballin<sup>72</sup>, Charles Baltay<sup>323</sup>, Philip Bambade<sup>130</sup>, Syuichi Ban<sup>67</sup>, Henry Band<sup>297</sup>, Karl Bane<sup>203</sup>, Bakul Banerjee<sup>54</sup>, Serena Barbanotti<sup>96</sup>, Daniele Barbareschi<sup>313,54,99</sup>, Angela Barbaro-Galtieri<sup>137</sup>, Desmond P. Barber<sup>47,38,263</sup>, Mauricio Barbi<sup>281</sup>, Dmitri Y. Bardin<sup>115</sup>, Barry Barish<sup>23,59</sup>, Timothy L. Barklow<sup>203</sup>, Roger Barlow<sup>38,265</sup>, Virgil E. Barnes<sup>186</sup>, Maura Barone<sup>54,59</sup>, Christoph Bartels<sup>47</sup>, Valeria Bartsch<sup>230</sup>, Rahul Basu<sup>88</sup>, Marco Battaglia<sup>137,239</sup>, Yuri Batygin<sup>203</sup>, Jerome Baudot<sup>84,301</sup>, Ulrich Baur<sup>205</sup>, D. Elwyn Baynham<sup>27</sup>, Carl Beard<sup>38,26</sup>, Chris Bebek<sup>137</sup>, Philip Bechtel<sup>47</sup>, Ulrich J. Becker<sup>146</sup>, Franco Bedeschi<sup>102</sup>, Marc Bedjidian<sup>299</sup>, Prafulla Behera<sup>261</sup>, Ties Behnke<sup>47</sup>, Leo Bellantoni<sup>54</sup>, Alain Bellerive<sup>24</sup>, Paul Bellomo<sup>203</sup>, Lynn D. Bentson<sup>203</sup>, Mustapha Benyamna<sup>131</sup>, Thomas Bergauer<sup>177</sup>, Edmond Berger<sup>8</sup>, Matthias Bergholz<sup>48,17</sup>, Suman Beri<sup>178</sup>, Martin Berndt<sup>203</sup>, Werner Bernreuther<sup>190</sup>, Alessandro Bertolini<sup>47</sup>, Marc Besancon<sup>28</sup>, Auguste Besson<sup>84,301</sup>, Andre Beteille<sup>132</sup>, Simona Bettoni<sup>134</sup>, Michael Beyer<sup>305</sup>, R.K. Bhandari<sup>315</sup>, Vinod Bharadwaj<sup>203</sup>, Vipin Bhatnagar<sup>178</sup>, Satyaki Bhattacharya<sup>248</sup>, Gautam Bhattacharyya<sup>194</sup>, Biplob Bhattacharjee<sup>22</sup>, Ruchika Bhuyan<sup>76</sup>, Xiao-Jun Bi<sup>87</sup>, Marica Biagini<sup>134</sup>, Wilhelm Bialowons<sup>47</sup>, Otmar Biebel<sup>144</sup>, Thomas Bieler<sup>150</sup>, John Bierwagen<sup>150</sup>, Alison Birch<sup>38,26</sup>, Mike Bisset<sup>31</sup>, S.S. Biswal<sup>74</sup>, Victoria Blackmore<sup>276</sup>, Grahame Blair<sup>192</sup>, Guillaume Blanchard<sup>131</sup>, Gerald Blazey<sup>171</sup>, Andrew Blue<sup>254</sup>, Johannes Blümlein<sup>48</sup>, Christian Boffo<sup>54</sup>, Courtlandt Bohn<sup>171,\*</sup>, V. I. Boiko<sup>115</sup>, Veronique Boisvert<sup>192</sup>, Eduard N. Bondarchuk<sup>45</sup>, Roberto Boni<sup>134</sup>, Giovanni Bonvicini<sup>321</sup>,

Stewart Boogert<sup>192</sup>, Maarten Boonekamp<sup>28</sup>, Gary Boorman<sup>192</sup>, Kerstin Borrás<sup>47</sup>,  
 Daniela Bortoletto<sup>186</sup>, Alessio Bosco<sup>192</sup>, Carlo Bosio<sup>308</sup>, Pierre Bosland<sup>28</sup>, Angelo Bosotti<sup>96</sup>,  
 Vincent Boudry<sup>50</sup>, Djamel-Eddine Boumediene<sup>131</sup>, Bernard Bouquet<sup>130</sup>, Serguei Bourov<sup>47</sup>,  
 Gordon Bowden<sup>203</sup>, Gary Bower<sup>203</sup>, Adam Boyarski<sup>203</sup>, Ivanka Bozovic-Jelisavcic<sup>316</sup>,  
 Concezio Bozzi<sup>97</sup>, Axel Brachmann<sup>203</sup>, Tom W. Bradshaw<sup>27</sup>, Andrew Brandt<sup>288</sup>,  
 Hans Peter Brasser<sup>6</sup>, Benjamin Brau<sup>243</sup>, James E. Brau<sup>275</sup>, Martin Breidenbach<sup>203</sup>,  
 Steve Bricker<sup>150</sup>, Jean-Claude Brient<sup>50</sup>, Ian Brock<sup>303</sup>, Stanley Brodsky<sup>203</sup>,  
 Craig Brooksby<sup>138</sup>, Timothy A. Broome<sup>27</sup>, David Brown<sup>137</sup>, David Brown<sup>264</sup>,  
 James H. Brownell<sup>46</sup>, Mélanie Bruchon<sup>28</sup>, Heiner Brueck<sup>47</sup>, Amanda J. Brummitt<sup>27</sup>,  
 Nicole Brun<sup>131</sup>, Peter Buchholz<sup>306</sup>, Yulian A. Budagov<sup>115</sup>, Antonio Bulgheroni<sup>310</sup>,  
 Eugene Bulyak<sup>118</sup>, Adriana Bungau<sup>38,265</sup>, Jochen Bürger<sup>47</sup>, Dan Burke<sup>28,24</sup>,  
 Craig Burkhart<sup>203</sup>, Philip Burrows<sup>276</sup>, Graeme Burt<sup>38</sup>, David Burton<sup>38,136</sup>,  
 Karsten Büsser<sup>47</sup>, John Butler<sup>16</sup>, Jonathan Butterworth<sup>230</sup>, Alexei Buzulutskov<sup>21</sup>,  
 Enric Cabruja<sup>34</sup>, Massimo Caccia<sup>311,96</sup>, Yunhai Cai<sup>203</sup>, Alessandro Calcaterra<sup>134</sup>,  
 Stephane Caliiier<sup>130</sup>, Tiziano Camporesi<sup>35</sup>, Jun-Jie Cao<sup>66</sup>, J.S. Cao<sup>87</sup>, Ofelia Capatina<sup>35</sup>,  
 Chiara Cappellini<sup>96,311</sup>, Ruben Carcagno<sup>54</sup>, Marcela Carena<sup>54</sup>, Cristina Carloganu<sup>131</sup>,  
 Roberto Carosi<sup>102</sup>, F. Stephen Carr<sup>27</sup>, Francisco Carrion<sup>54</sup>, Harry F. Carter<sup>54</sup>,  
 John Carter<sup>192</sup>, John Carwardine<sup>8</sup>, Richard Cassel<sup>203</sup>, Ronald Cassell<sup>203</sup>,  
 Giorgio Cavallari<sup>28</sup>, Emanuela Cavallo<sup>107</sup>, Jose A. R. Cembranos<sup>241,269</sup>,  
 Dhiman Chakraborty<sup>171</sup>, Frederic Chandez<sup>131</sup>, Matthew Charles<sup>261</sup>, Brian Chase<sup>54</sup>,  
 Subhasis Chattopadhyay<sup>315</sup>, Jacques Chauveau<sup>302</sup>, Maximilien Chefdeville<sup>160,28</sup>,  
 Robert Chehab<sup>130</sup>, Stéphane Chel<sup>28</sup>, Georgy Chelkov<sup>115</sup>, Chiping Chen<sup>146</sup>,  
 He Sheng Chen<sup>87</sup>, Huai Bi Chen<sup>31</sup>, Jia Er Chen<sup>10</sup>, Sen Yu Chen<sup>87</sup>, Shaomin Chen<sup>31</sup>,  
 Shenjian Chen<sup>157</sup>, Xun Chen<sup>147</sup>, Yuan Bo Chen<sup>87</sup>, Jian Cheng<sup>87</sup>, M. Chevallier<sup>81</sup>,  
 Yun Long Chi<sup>87</sup>, William Chickering<sup>239</sup>, Gi-Chol Cho<sup>175</sup>, Moo-Hyun Cho<sup>182</sup>,  
 Jin-Hyuk Choi<sup>182</sup>, Jong Bum Choi<sup>37</sup>, Seong Youl Choi<sup>37</sup>, Young-Il Choi<sup>208</sup>,  
 Brajesh Choudhary<sup>248</sup>, Debajyoti Choudhury<sup>248</sup>, S. Rai Choudhury<sup>109</sup>, David Christian<sup>54</sup>,  
 Glenn Christian<sup>276</sup>, Grojean Christophe<sup>35,29</sup>, Jin-Hyuk Chung<sup>30</sup>, Mike Church<sup>54</sup>,  
 Jacek Ciborowski<sup>294</sup>, Selcuk Cihangir<sup>54</sup>, Gianluigi Ciovati<sup>220</sup>, Christine Clarke<sup>276</sup>,  
 Don G. Clarke<sup>26</sup>, James A. Clarke<sup>38,26</sup>, Elizabeth Clements<sup>54,59</sup>, Cornelia Coca<sup>2</sup>,  
 Paul Coe<sup>276</sup>, John Cogan<sup>203</sup>, Paul Colas<sup>28</sup>, Caroline Collard<sup>130</sup>, Claude Colledani<sup>84</sup>,  
 Christophe Combaret<sup>299</sup>, Albert Comerma<sup>232</sup>, Chris Compton<sup>150</sup>, Ben Constance<sup>276</sup>,  
 John Conway<sup>240</sup>, Ed Cook<sup>138</sup>, Peter Cooke<sup>38,263</sup>, William Cooper<sup>54</sup>, Sean Corcoran<sup>318</sup>,  
 Rémi Cornat<sup>131</sup>, Laura Corner<sup>276</sup>, Eduardo Cortina Gil<sup>33</sup>, W. Clay Corvin<sup>203</sup>,  
 Angelo Cotta Ramusino<sup>97</sup>, Ray Cowan<sup>146</sup>, Curtis Crawford<sup>43</sup>, Lucien M Cremaldi<sup>270</sup>,  
 James A. Crittenden<sup>43</sup>, David Cussans<sup>237</sup>, Jaroslav Cvach<sup>90</sup>, Wilfrid Da Silva<sup>302</sup>,  
 Hamid Dabiri Khah<sup>276</sup>, Anne Dabrowski<sup>172</sup>, Wladyslaw Dabrowski<sup>3</sup>, Olivier Dadoun<sup>130</sup>,  
 Jian Ping Dai<sup>87</sup>, John Dainton<sup>38,263</sup>, Colin Daly<sup>296</sup>, Chris Damerell<sup>27</sup>, Mikhail Danilov<sup>92</sup>,  
 Witold Daniluk<sup>219</sup>, Sarojini Daram<sup>269</sup>, Anindya Datta<sup>22</sup>, Paul Dauncey<sup>72</sup>, Jacques David<sup>302</sup>,  
 Michel Davier<sup>130</sup>, Ken P. Davies<sup>26</sup>, Sally Dawson<sup>19</sup>, Wim De Boer<sup>304</sup>, Stefania De Curtis<sup>98</sup>,  
 Nicolo De Groot<sup>160</sup>, Christophe De La Taille<sup>130</sup>, Antonio de Lira<sup>203</sup>, Albert De Roeck<sup>35</sup>,  
 Riccardo De Sangro<sup>134</sup>, Stefano De Santis<sup>137</sup>, Laurence Deacon<sup>192</sup>, Aldo Deandrea<sup>299</sup>,  
 Klaus Dehmelt<sup>47</sup>, Eric Delagnes<sup>28</sup>, Jean-Pierre Delahaye<sup>35</sup>, Pierre Delebecque<sup>128</sup>,  
 Nicholas Delerue<sup>276</sup>, Olivier Delferriere<sup>28</sup>, Marcel Demarteau<sup>54</sup>, Zhi Deng<sup>31</sup>,  
 Yu. N. Denisov<sup>115</sup>, Christopher J. Densham<sup>27</sup>, Klaus Desch<sup>303</sup>, Nilendra Deshpande<sup>275</sup>,  
 Guillaume Devanz<sup>28</sup>, Erik Devetak<sup>276</sup>, Amos Dexter<sup>38</sup>, Vito Di Benedetto<sup>107</sup>,  
 Ángel Diéguez<sup>232</sup>, Ralf Diener<sup>255</sup>, Nguyen Dinh Dinh<sup>89,135</sup>, Madhu Dixit<sup>24,226</sup>,

Sudhir Dixit<sup>276</sup>, Abdelhak Djouadi<sup>133</sup>, Zdenek Dolezal<sup>36</sup>, Ralph Dollan<sup>69</sup>, Dong Dong<sup>87</sup>,  
 Hai Yi Dong<sup>87</sup>, Jonathan Dorfan<sup>203</sup>, Andrei Dorokhov<sup>84</sup>, George Doucas<sup>276</sup>,  
 Robert Downing<sup>188</sup>, Eric Doyle<sup>203</sup>, Guy Doziere<sup>84</sup>, Alessandro Drago<sup>134</sup>, Alex Dragt<sup>266</sup>,  
 Gary Drake<sup>8</sup>, Zbynek Drásal<sup>36</sup>, Herbert Dreiner<sup>303</sup>, Persis Drell<sup>203</sup>, Chafik Driouichi<sup>165</sup>,  
 Alexandr Drozhdin<sup>54</sup>, Vladimir Drugakov<sup>47,11</sup>, Shuxian Du<sup>87</sup>, Gerald Dugan<sup>43</sup>,  
 Viktor Duginov<sup>115</sup>, Wojciech Dulinski<sup>84</sup>, Frederic Dulucq<sup>130</sup>, Sukanta Dutta<sup>249</sup>,  
 Jishnu Dwivedi<sup>189</sup>, Alexandre Dychkant<sup>171</sup>, Daniel Dzahini<sup>132</sup>, Guenter Eckerlin<sup>47</sup>,  
 Helen Edwards<sup>54</sup>, Wolfgang Ehrenfeld<sup>255,47</sup>, Michael Ehrlichman<sup>269</sup>, Heiko Ehrlichmann<sup>47</sup>,  
 Gerald Eigen<sup>235</sup>, Andrey Elagin<sup>115,217</sup>, Luciano Elementi<sup>54</sup>, Peder Eliasson<sup>35</sup>, John Ellis<sup>35</sup>,  
 George Ellwood<sup>38,26</sup>, Eckhard Elsen<sup>47</sup>, Louis Emery<sup>8</sup>, Kazuhiro Enami<sup>67</sup>, Kuninori Endo<sup>67</sup>,  
 Atsushi Enomoto<sup>67</sup>, Fabien Eozénu<sup>28</sup>, Robin Erbacher<sup>240</sup>, Roger Erickson<sup>203</sup>,  
 K. Oleg Eyser<sup>47</sup>, Vitaliy Fadeyev<sup>245</sup>, Shou Xian Fang<sup>87</sup>, Karen Fant<sup>203</sup>, Alberto Fasso<sup>203</sup>,  
 Michele Fauci Giannelli<sup>192</sup>, John Fehlberg<sup>184</sup>, Lutz Feld<sup>190</sup>, Jonathan L. Feng<sup>241</sup>,  
 John Ferguson<sup>35</sup>, Marcos Fernandez-Garcia<sup>95</sup>, J. Luis Fernandez-Hernando<sup>38,26</sup>,  
 Pavel Fiala<sup>18</sup>, Ted Fieguth<sup>203</sup>, Alexander Finch<sup>136</sup>, Giuseppe Finocchiaro<sup>134</sup>,  
 Peter Fischer<sup>257</sup>, Peter Fisher<sup>146</sup>, H. Eugene Fisk<sup>54</sup>, Mike D. Fitton<sup>27</sup>, Ivor Fleck<sup>306</sup>,  
 Manfred Fleischer<sup>47</sup>, Julien Fleury<sup>130</sup>, Kevin Flood<sup>297</sup>, Mike Foley<sup>54</sup>, Richard Ford<sup>54</sup>,  
 Dominique Fortin<sup>242</sup>, Brian Foster<sup>276</sup>, Nicolas Fourches<sup>28</sup>, Kurt Francis<sup>171</sup>, Ariane Frey<sup>147</sup>,  
 Raymond Frey<sup>275</sup>, Horst Friedsam<sup>8</sup>, Josef Frisch<sup>203</sup>, Anatoli Frishman<sup>107</sup>, Joel Fuerst<sup>8</sup>,  
 Keisuke Fujii<sup>67</sup>, Junpei Fujimoto<sup>67</sup>, Masafumi Fukuda<sup>67</sup>, Shigeki Fukuda<sup>67</sup>,  
 Yoshisato Funahashi<sup>67</sup>, Warren Funk<sup>220</sup>, Julia Furltova<sup>47</sup>, Kazuro Furukawa<sup>67</sup>,  
 Fumio Furuta<sup>67</sup>, Takahiro Fusayasu<sup>154</sup>, Juan Fuster<sup>94</sup>, Karsten Gadow<sup>47</sup>, Frank Gaede<sup>47</sup>,  
 Renaud Gaglione<sup>299</sup>, Wei Gai<sup>8</sup>, Jan Gajewski<sup>3</sup>, Richard Galik<sup>43</sup>, Alexei Galkin<sup>174</sup>,  
 Valery Galkin<sup>174</sup>, Laurent Gallin-Martel<sup>132</sup>, Fred Gannaway<sup>276</sup>, Jian She Gao<sup>87</sup>, Jie Gao<sup>87</sup>,  
 Yuanning Gao<sup>31</sup>, Peter Garbincius<sup>54</sup>, Luis Garcia-Tabares<sup>33</sup>, Lynn Garren<sup>54</sup>,  
 Luís Garrido<sup>232</sup>, Erika Garutti<sup>47</sup>, Terry Garvey<sup>130</sup>, Edward Garwin<sup>203</sup>, David Gascón<sup>232</sup>,  
 Martin Gastal<sup>35</sup>, Corrado Gatto<sup>100</sup>, Raoul Gatto<sup>300,35</sup>, Pascal Gay<sup>131</sup>, Lixin Ge<sup>203</sup>,  
 Ming Qi Ge<sup>87</sup>, Rui Ge<sup>87</sup>, Achim Geiser<sup>47</sup>, Andreas Gellrich<sup>47</sup>, Jean-Francois Genat<sup>302</sup>,  
 Zhe Qiao Geng<sup>87</sup>, Simonetta Gentile<sup>308</sup>, Scot Gerbick<sup>8</sup>, Rod Gerig<sup>8</sup>, Dilip Kumar Ghosh<sup>248</sup>,  
 Kirtiman Ghosh<sup>22</sup>, Lawrence Gibbons<sup>43</sup>, Arnaud Giganon<sup>28</sup>, Allan Gillespie<sup>250</sup>,  
 Tony Gillman<sup>27</sup>, Ilya Ginzburg<sup>173,201</sup>, Ioannis Giomataris<sup>28</sup>, Michele Giunta<sup>102,312</sup>,  
 Peter Gladkikh<sup>118</sup>, Janusz Gluza<sup>284</sup>, Rohini Godbole<sup>74</sup>, Stephen Godfrey<sup>24</sup>,  
 Gerson Goldhaber<sup>137,239</sup>, Joel Goldstein<sup>237</sup>, George D. Gollin<sup>260</sup>,  
 Francisco Javier Gonzalez-Sanchez<sup>95</sup>, Maurice Goodrick<sup>246</sup>, Yuri Gornushkin<sup>115</sup>,  
 Mikhail Gostkin<sup>115</sup>, Erik Gottschalk<sup>54</sup>, Philippe Goudket<sup>38,26</sup>, Ivo Gough Eschrich<sup>241</sup>,  
 Filimon Gournaris<sup>230</sup>, Ricardo Graciani<sup>232</sup>, Norman Graf<sup>203</sup>, Christian Grah<sup>48</sup>,  
 Francesco Grancagnolo<sup>99</sup>, Damien Grandjean<sup>84</sup>, Paul Grannis<sup>206</sup>, Anna Grassellino<sup>279</sup>,  
 Eugeni Graugés<sup>232</sup>, Stephen Gray<sup>43</sup>, Michael Green<sup>192</sup>, Justin Greenhalgh<sup>38,26</sup>,  
 Timothy Greenshaw<sup>263</sup>, Christian Grefe<sup>255</sup>, Ingrid-Maria Gregor<sup>47</sup>, Gerald Grenier<sup>299</sup>,  
 Mark Grimes<sup>237</sup>, Terry Grimm<sup>150</sup>, Philippe Gris<sup>131</sup>, Jean-Francois Grivaz<sup>130</sup>,  
 Marius Groll<sup>255</sup>, Jeffrey Gronberg<sup>138</sup>, Denis Grondin<sup>132</sup>, Donald Groom<sup>137</sup>, Eilam Gross<sup>322</sup>,  
 Martin Grunewald<sup>231</sup>, Claus Grupen<sup>306</sup>, Grzegorz Grzelak<sup>294</sup>, Jun Gu<sup>87</sup>, Yun-Ting Gu<sup>61</sup>,  
 Monoranjan Guchait<sup>211</sup>, Susanna Guiducci<sup>134</sup>, Ali Murat Guler<sup>151</sup>, Hayg Guler<sup>50</sup>,  
 Erhan Gulmez<sup>261,15</sup>, John Gunion<sup>240</sup>, Zhi Yu Guo<sup>10</sup>, Atul Gurtu<sup>211</sup>, Huy Bang Ha<sup>135</sup>,  
 Tobias Haas<sup>47</sup>, Andy Haase<sup>203</sup>, Naoyuki Haba<sup>176</sup>, Howard Haber<sup>245</sup>, Stephan Haensel<sup>177</sup>,  
 Lars Hage<sup>47</sup>, Hiroyuki Hagura<sup>67,117</sup>, Csaba Hajdu<sup>70</sup>, Gunther Haller<sup>203</sup>,  
 Johannes Haller<sup>255</sup>, Lea Hallermann<sup>47,255</sup>, Valerie Halyo<sup>185</sup>, Koichi Hamaguchi<sup>290</sup>,

Larry Hammond<sup>54</sup>, Liang Han<sup>283</sup>, Tao Han<sup>297</sup>, Louis Hand<sup>43</sup>, Virender K. Handu<sup>13</sup>,  
 Hitoshi Hano<sup>290</sup>, Christian Hansen<sup>293</sup>, Jørn Dines Hansen<sup>165</sup>, Jorgen Beck Hansen<sup>165</sup>,  
 Kazufumi Hara<sup>67</sup>, Kristian Harder<sup>27</sup>, Anthony Hartin<sup>276</sup>, Walter Hartung<sup>150</sup>,  
 Carsten Hast<sup>203</sup>, John Hauptman<sup>107</sup>, Michael Hauschild<sup>35</sup>, Claude Hauviller<sup>35</sup>,  
 Miroslav Havranek<sup>90</sup>, Chris Hawkes<sup>236</sup>, Richard Hawkings<sup>35</sup>, Hitoshi Hayano<sup>67</sup>,  
 Masashi Hazumi<sup>67</sup>, An He<sup>87</sup>, Hong Jian He<sup>31</sup>, Christopher Hearty<sup>238</sup>, Helen Heath<sup>237</sup>,  
 Thomas Hebbeker<sup>190</sup>, Vincent Hedberg<sup>145</sup>, David Hedin<sup>171</sup>, Samuel Heifets<sup>203</sup>,  
 Sven Heinemeyer<sup>95</sup>, Sebastien Heini<sup>84</sup>, Christian Helebrant<sup>47,255</sup>, Richard Helms<sup>43</sup>,  
 Brian Heltsley<sup>43</sup>, Sophie Henrot-Versille<sup>130</sup>, Hans Henschel<sup>48</sup>, Carsten Hensel<sup>262</sup>,  
 Richard Hermel<sup>128</sup>, Atilà Herms<sup>232</sup>, Gregor Herten<sup>4</sup>, Stefan Hesselbach<sup>285</sup>,  
 Rolf-Dieter Heuer<sup>47,255</sup>, Clemens A. Heusch<sup>245</sup>, Joanne Hewett<sup>203</sup>, Norio Higashi<sup>67</sup>,  
 Takatoshi Higashi<sup>193</sup>, Yasuo Higashi<sup>67</sup>, Toshiyasu Higo<sup>67</sup>, Michael D. Hildreth<sup>273</sup>,  
 Karlheinz Hiller<sup>48</sup>, Sonja Hillert<sup>276</sup>, Stephen James Hillier<sup>236</sup>, Thomas Himel<sup>203</sup>,  
 Abdelkader Himmi<sup>84</sup>, Ian Hinchliffe<sup>137</sup>, Zenro Hioki<sup>289</sup>, Koichiro Hirano<sup>112</sup>,  
 Tachishige Hirose<sup>320</sup>, Hiromi Hisamatsu<sup>67</sup>, Junji Hisano<sup>86</sup>, Chit Thu Hlaing<sup>239</sup>,  
 Kai Meng Hock<sup>38,263</sup>, Martin Hoferkamp<sup>272</sup>, Mark Hohlfeld<sup>303</sup>, Yousuke Honda<sup>67</sup>,  
 Juho Hong<sup>182</sup>, Tae Min Hong<sup>243</sup>, Hiroyuki Honma<sup>67</sup>, Yasuyuki Horii<sup>222</sup>, Dezso Horvath<sup>70</sup>,  
 Kenji Hosoyama<sup>67</sup>, Jean-Yves Hostachy<sup>132</sup>, Mi Hou<sup>87</sup>, Wei-Shu Hou<sup>164</sup>, David Howell<sup>276</sup>,  
 Maxine Hronek<sup>54,59</sup>, Yee B. Hsiung<sup>164</sup>, Bo Hu<sup>156</sup>, Tao Hu<sup>87</sup>, Jung-Yun Huang<sup>182</sup>,  
 Tong Ming Huang<sup>87</sup>, Wen Hui Huang<sup>31</sup>, Emil Huedem<sup>54</sup>, Peter Huggard<sup>27</sup>,  
 Cyril Hugonie<sup>127</sup>, Christine Hu-Guo<sup>84</sup>, Katri Huitu<sup>258,65</sup>, Youngseok Hwang<sup>30</sup>,  
 Marek Idzik<sup>3</sup>, Alexandr Ignatenko<sup>11</sup>, Fedor Ignatov<sup>21</sup>, Hirokazu Ikeda<sup>111</sup>,  
 Katsumasa Ikematsu<sup>47</sup>, Tatiana Ilicheva<sup>115,60</sup>, Didier Imbault<sup>302</sup>, Andreas Imhof<sup>255</sup>,  
 Marco Incagli<sup>102</sup>, Ronen Ingbir<sup>216</sup>, Hitoshi Inoue<sup>67</sup>, Youichi Inoue<sup>221</sup>, Gianluca Introzzi<sup>278</sup>,  
 Katerina Ioakeimidi<sup>203</sup>, Satoshi Ishihara<sup>259</sup>, Akimasa Ishikawa<sup>193</sup>, Tadashi Ishikawa<sup>67</sup>,  
 Vladimir Issakov<sup>323</sup>, Kazutoshi Ito<sup>222</sup>, V. V. Ivanov<sup>115</sup>, Valentin Ivanov<sup>54</sup>,  
 Yury Ivanyushenkov<sup>27</sup>, Masako Iwasaki<sup>290</sup>, Yoshihisa Iwashita<sup>85</sup>, David Jackson<sup>276</sup>,  
 Frank Jackson<sup>38,26</sup>, Bob Jacobsen<sup>137,239</sup>, Ramaswamy Jaganathan<sup>88</sup>, Steven Jamison<sup>38,26</sup>,  
 Matthias Enno Janssen<sup>47,255</sup>, Richard Jaramillo-Echeverria<sup>95</sup>, John Jaros<sup>203</sup>,  
 Clement Jauffret<sup>50</sup>, Suresh B. Jawale<sup>13</sup>, Daniel Jeans<sup>120</sup>, Ron Jedziniak<sup>54</sup>, Ben Jeffery<sup>276</sup>,  
 Didier Jehanno<sup>130</sup>, Leo J. Jenner<sup>38,263</sup>, Chris Jensen<sup>54</sup>, David R. Jensen<sup>203</sup>,  
 Hairong Jiang<sup>150</sup>, Xiao Ming Jiang<sup>87</sup>, Masato Jimbo<sup>223</sup>, Shan Jin<sup>87</sup>, R. Keith Jobe<sup>203</sup>,  
 Anthony Johnson<sup>203</sup>, Erik Johnson<sup>27</sup>, Matt Johnson<sup>150</sup>, Michael Johnston<sup>276</sup>,  
 Paul Joireman<sup>54</sup>, Stevan Jokic<sup>316</sup>, James Jones<sup>38,26</sup>, Roger M. Jones<sup>38,265</sup>,  
 Erik Jongewaard<sup>203</sup>, Leif Jönsson<sup>145</sup>, Gopal Joshi<sup>13</sup>, Satish C. Joshi<sup>189</sup>, Jin-Young Jung<sup>137</sup>,  
 Thomas Junk<sup>260</sup>, Aurelio Juste<sup>54</sup>, Marumi Kado<sup>130</sup>, John Kadyk<sup>137</sup>, Daniela Käfer<sup>47</sup>,  
 Eiji Kako<sup>67</sup>, Puneeth Kalavase<sup>243</sup>, Alexander Kalinin<sup>38,26</sup>, Jan Kalinowski<sup>295</sup>,  
 Takuya Kamitani<sup>67</sup>, Yoshio Kamiya<sup>106</sup>, Yukihide Kamiya<sup>67</sup>, Jun-ichi Kamoshita<sup>55</sup>,  
 Sergey Kananov<sup>216</sup>, Kazuyuki Kanaya<sup>292</sup>, Ken-ichi Kanazawa<sup>67</sup>, Shinya Kanemura<sup>225</sup>,  
 Heung-Sik Kang<sup>182</sup>, Wen Kang<sup>87</sup>, D. Kanjial<sup>105</sup>, Frédéric Kapusta<sup>302</sup>, Pavel Karataev<sup>192</sup>,  
 Paul E. Karchin<sup>321</sup>, Dean Karlen<sup>293,226</sup>, Yannis Karyotakis<sup>128</sup>, Vladimir Kashikhin<sup>54</sup>,  
 Shigeru Kashiwagi<sup>176</sup>, Paul Kasley<sup>54</sup>, Hiroaki Katagiri<sup>67</sup>, Takashi Kato<sup>167</sup>, Yukihiro Kato<sup>119</sup>,  
 Judith Katzy<sup>47</sup>, Alexander Kaukher<sup>305</sup>, Manjit Kaur<sup>178</sup>, Kiyotomo Kawagoe<sup>120</sup>,  
 Hiroyuki Kawamura<sup>191</sup>, Sergei Kazakov<sup>67</sup>, V. D. Kekelidze<sup>115</sup>, Lewis Keller<sup>203</sup>,  
 Michael Kelley<sup>39</sup>, Marc Kelly<sup>265</sup>, Michael Kelly<sup>8</sup>, Kurt Kennedy<sup>137</sup>, Robert Kephart<sup>54</sup>,  
 Justin Keung<sup>279,54</sup>, Oleg Khainovski<sup>239</sup>, Sameen Ahmed Khan<sup>195</sup>, Prashant Khare<sup>189</sup>,  
 Nikolai Khovansky<sup>115</sup>, Christian Kiesling<sup>147</sup>, Mitsuo Kikuchi<sup>67</sup>, Wolfgang Kilian<sup>306</sup>,



Martin Killenberg<sup>303</sup>, Donghee Kim<sup>30</sup>, Eun San Kim<sup>30</sup>, Eun-Joo Kim<sup>37</sup>, Guinyun Kim<sup>30</sup>,  
 Hongjoo Kim<sup>30</sup>, Hyoungsuk Kim<sup>30</sup>, Hyun-Chui Kim<sup>187</sup>, Jonghoon Kim<sup>203</sup>, Kwang-Je Kim<sup>8</sup>,  
 Kyung Sook Kim<sup>30</sup>, Peter Kim<sup>203</sup>, Seunghwan Kim<sup>182</sup>, Shin-Hong Kim<sup>292</sup>, Sun Kee Kim<sup>197</sup>,  
 Tae Jeong Kim<sup>125</sup>, Youngim Kim<sup>30</sup>, Young-Kee Kim<sup>54,52</sup>, Maurice Kimmitt<sup>252</sup>,  
 Robert Kirby<sup>203</sup>, François Kircher<sup>28</sup>, Danuta Kisielewska<sup>3</sup>, Olaf Kittel<sup>303</sup>,  
 Robert Klanner<sup>255</sup>, Arkadiy L. Klebaner<sup>54</sup>, Claus Kleinwort<sup>47</sup>, Tatsiana Klimkovich<sup>47</sup>,  
 Esben Klinkby<sup>165</sup>, Stefan Kluth<sup>147</sup>, Marc Knecht<sup>32</sup>, Peter Kneisel<sup>220</sup>, In Soo Ko<sup>182</sup>,  
 Kwok Ko<sup>203</sup>, Makoto Kobayashi<sup>67</sup>, Nobuko Kobayashi<sup>67</sup>, Michael Kobel<sup>214</sup>,  
 Manuel Koch<sup>303</sup>, Peter Kodys<sup>36</sup>, Uli Koetz<sup>47</sup>, Robert Kohrs<sup>303</sup>, Yuuji Kojima<sup>67</sup>,  
 Hermann Kolanoski<sup>69</sup>, Karol Kolodziej<sup>284</sup>, Yury G. Kolomensky<sup>239</sup>, Sachio Komamiya<sup>106</sup>,  
 Xiang Cheng Kong<sup>87</sup>, Jacobo Konigsberg<sup>253</sup>, Volker Korb<sup>47</sup>, Shane Koscielniak<sup>226</sup>,  
 Sergey Kostromin<sup>115</sup>, Robert Kowalewski<sup>293</sup>, Sabine Kraml<sup>35</sup>, Manfred Krammer<sup>177</sup>,  
 Anatoly Krasnykh<sup>203</sup>, Thorsten Krautscheid<sup>303</sup>, Maria Krawczyk<sup>295</sup>, H. James Krebs<sup>203</sup>,  
 Kurt Krempetz<sup>54</sup>, Graham Kribs<sup>275</sup>, Srinivas Krishnagopal<sup>189</sup>, Richard Kriske<sup>269</sup>,  
 Andreas Kronfeld<sup>54</sup>, Jürgen Kroseberg<sup>245</sup>, Uladzimir Kruchonak<sup>115</sup>, Dirk Kruecker<sup>47</sup>,  
 Hans Krüger<sup>303</sup>, Nicholas A. Krumpa<sup>26</sup>, Zinovii Krumshstein<sup>115</sup>, Yu Ping Kuang<sup>31</sup>,  
 Kiyoshi Kubo<sup>67</sup>, Vic Kuchler<sup>54</sup>, Noboru Kudoh<sup>67</sup>, Szymon Kulis<sup>3</sup>, Masayuki Kumada<sup>161</sup>,  
 Abhay Kumar<sup>189</sup>, Tatsuya Kume<sup>67</sup>, Anirban Kundu<sup>22</sup>, German Kurevlev<sup>38,265</sup>,  
 Yoshimasa Kurihara<sup>67</sup>, Masao Kuriki<sup>67</sup>, Shigeru Kuroda<sup>67</sup>, Hirotoshi Kuroiwa<sup>67</sup>,  
 Shin-ichi Kurokawa<sup>67</sup>, Tomonori Kusano<sup>222</sup>, Pradeep K. Kush<sup>189</sup>, Robert Kutschke<sup>54</sup>,  
 Ekaterina Kuznetsova<sup>308</sup>, Peter Kvasnicka<sup>36</sup>, Youngjoon Kwon<sup>324</sup>, Luis Labarga<sup>228</sup>,  
 Carlos Lacasta<sup>94</sup>, Sharon Lackey<sup>54</sup>, Thomas W. Lackowski<sup>54</sup>, Remi Lafaye<sup>128</sup>,  
 George Lafferty<sup>265</sup>, Eric Lagorio<sup>132</sup>, Imad Laktineh<sup>299</sup>, Shankar Lal<sup>189</sup>, Maurice Laloum<sup>83</sup>,  
 Briant Lam<sup>203</sup>, Mark Lancaster<sup>230</sup>, Richard Lander<sup>240</sup>, Wolfgang Lange<sup>48</sup>,  
 Ulrich Langenfeld<sup>303</sup>, Willem Langeveld<sup>203</sup>, David Larbalestier<sup>297</sup>, Ray Larsen<sup>203</sup>,  
 Tomas Lastovicka<sup>276</sup>, Gordana Lastovicka-Medin<sup>271</sup>, Andrea Latina<sup>35</sup>, Emmanuel Latour<sup>50</sup>,  
 Lisa Laurent<sup>203</sup>, Ba Nam Le<sup>62</sup>, Duc Ninh Le<sup>89,129</sup>, Francois Le Diberder<sup>130</sup>,  
 Patrick Le Du<sup>28</sup>, Hervé Lebbolo<sup>83</sup>, Paul Lebrun<sup>54</sup>, Jacques Lecoq<sup>131</sup>, Sung-Won Lee<sup>218</sup>,  
 Frank Lehner<sup>47</sup>, Jerry Leibfritz<sup>54</sup>, Frank Lenkszus<sup>8</sup>, Tadeusz Lesiak<sup>219</sup>, Aharon Levy<sup>216</sup>,  
 Jim Lewandowski<sup>203</sup>, Greg Leyh<sup>203</sup>, Cheng Li<sup>283</sup>, Chong Sheng Li<sup>10</sup>, Chun Hua Li<sup>87</sup>,  
 Da Zhang Li<sup>87</sup>, Gang Li<sup>87</sup>, Jin Li<sup>31</sup>, Shao Peng Li<sup>87</sup>, Wei Ming Li<sup>162</sup>, Weiguo Li<sup>87</sup>,  
 Xiao Ping Li<sup>87</sup>, Xue-Qian Li<sup>158</sup>, Yuanjing Li<sup>31</sup>, Yulan Li<sup>31</sup>, Zenghai Li<sup>203</sup>, Zhong Quan Li<sup>87</sup>,  
 Jian Tao Liang<sup>212</sup>, Yi Liao<sup>158</sup>, Lutz Lilje<sup>47</sup>, J. Guilherme Lima<sup>171</sup>, Andrew J. Lintern<sup>27</sup>,  
 Ronald Lipton<sup>54</sup>, Benno List<sup>255</sup>, Jenny List<sup>47</sup>, Chun Liu<sup>93</sup>, Jian Fei Liu<sup>199</sup>, Ke Xin Liu<sup>10</sup>,  
 Li Qiang Liu<sup>212</sup>, Shao Zhen Liu<sup>87</sup>, Sheng Guang Liu<sup>67</sup>, Shubin Liu<sup>283</sup>, Wanming Liu<sup>8</sup>,  
 Wei Bin Liu<sup>87</sup>, Ya Ping Liu<sup>87</sup>, Yu Dong Liu<sup>87</sup>, Nigel Lockyer<sup>226,238</sup>, Heather E. Logan<sup>24</sup>,  
 Pavel V. Logatchev<sup>21</sup>, Wolfgang Lohmann<sup>48</sup>, Thomas Lohse<sup>69</sup>, Smaragda Lola<sup>277</sup>,  
 Amparo Lopez-Virto<sup>95</sup>, Peter Loveridge<sup>27</sup>, Manuel Lozano<sup>34</sup>, Cai-Dian Lu<sup>87</sup>,  
 Changguo Lu<sup>185</sup>, Gong-Lu Lu<sup>66</sup>, Wen Hui Lu<sup>212</sup>, Henry Lubatti<sup>296</sup>, Arnaud Lucotte<sup>132</sup>,  
 Björn Lundberg<sup>145</sup>, Tracy Lundin<sup>63</sup>, Mingxing Luo<sup>325</sup>, Michel Luong<sup>28</sup>, Vera Luth<sup>203</sup>,  
 Benjamin Lutz<sup>47,255</sup>, Pierre Lutz<sup>28</sup>, Thorsten Lux<sup>229</sup>, Pawel Luzniak<sup>91</sup>, Alexey Lyapin<sup>230</sup>,  
 Joseph Lykken<sup>54</sup>, Clare Lynch<sup>237</sup>, Li Ma<sup>87</sup>, Lili Ma<sup>38,26</sup>, Qiang Ma<sup>87</sup>, Wen-Gan Ma<sup>283,87</sup>,  
 David Macfarlane<sup>203</sup>, Arthur Maciel<sup>171</sup>, Allan MacLeod<sup>233</sup>, David MacNair<sup>203</sup>,  
 Wolfgang Mader<sup>214</sup>, Stephen Magill<sup>8</sup>, Anne-Marie Magnan<sup>72</sup>, Bino Maiheu<sup>230</sup>,  
 Manas Maity<sup>319</sup>, Millicent Majchrzak<sup>269</sup>, Gobinda Majumder<sup>211</sup>, Roman Makarov<sup>115</sup>,  
 Dariusz Makowski<sup>213,47</sup>, Bogdan Malaescu<sup>130</sup>, C. Mallik<sup>315</sup>, Usha Mallik<sup>261</sup>,  
 Stephen Malton<sup>230,192</sup>, Oleg B. Malyshev<sup>38,26</sup>, Larisa I. Malysheva<sup>38,263</sup>,

John Mammosser<sup>220</sup>, Mamta<sup>249</sup>, Judita Mamuzic<sup>48,316</sup>, Samuel Manen<sup>131</sup>,  
 Massimo Manghisoni<sup>307,101</sup>, Steven Manly<sup>282</sup>, Fabio Marcellini<sup>134</sup>, Michal Marcisovsky<sup>90</sup>,  
 Thomas W. Markiewicz<sup>203</sup>, Steve Marks<sup>137</sup>, Andrew Marone<sup>19</sup>, Felix Marti<sup>150</sup>,  
 Jean-Pierre Martin<sup>42</sup>, Victoria Martin<sup>251</sup>, Gisèle Martin-Chassard<sup>130</sup>, Manel Martinez<sup>229</sup>,  
 Celso Martinez-Rivero<sup>95</sup>, Dennis Martsch<sup>255</sup>, Hans-Ulrich Martyn<sup>190,47</sup>,  
 Takashi Maruyama<sup>203</sup>, Mika Masuzawa<sup>67</sup>, Hervé Mathez<sup>299</sup>, Takeshi Matsuda<sup>67</sup>,  
 Hiroshi Matsumoto<sup>67</sup>, Shuji Matsumoto<sup>67</sup>, Toshihiro Matsumoto<sup>67</sup>, Hiroyuki Matsunaga<sup>106</sup>,  
 Peter Mättig<sup>298</sup>, Thomas Mattison<sup>238</sup>, Georgios Mavromanolakis<sup>246,54</sup>,  
 Kentarou Mawatari<sup>124</sup>, Anna Mazzacane<sup>313</sup>, Patricia McBride<sup>54</sup>, Douglas McCormick<sup>203</sup>,  
 Jeremy McCormick<sup>203</sup>, Kirk T. McDonald<sup>185</sup>, Mike McGee<sup>54</sup>, Peter McIntosh<sup>38,26</sup>,  
 Bobby McKee<sup>203</sup>, Robert A. McPherson<sup>293</sup>, Mandi Meidlinger<sup>150</sup>, Karlheinz Meier<sup>257</sup>,  
 Barbara Mele<sup>308</sup>, Bob Meller<sup>43</sup>, Isabell-Alissandra Melzer-Pellmann<sup>47</sup>, Hector Mendez<sup>280</sup>,  
 Adam Mercer<sup>38,265</sup>, Mikhail Merkin<sup>141</sup>, I. N. Meshkov<sup>115</sup>, Robert Messner<sup>203</sup>,  
 Jessica Metcalfe<sup>272</sup>, Chris Meyer<sup>244</sup>, Hendrik Meyer<sup>47</sup>, Joachim Meyer<sup>47</sup>, Niels Meyer<sup>47</sup>,  
 Norbert Meyners<sup>47</sup>, Paolo Michelato<sup>96</sup>, Shinichiro Michizono<sup>67</sup>, Daniel Mihalcea<sup>171</sup>,  
 Satoshi Mihara<sup>106</sup>, Takanori Mihara<sup>126</sup>, Yoshinari Mikami<sup>236</sup>,  
 Alexander A. Mikhailichenko<sup>43</sup>, Catia Milardi<sup>134</sup>, David J. Miller<sup>230</sup>, Owen Miller<sup>236</sup>,  
 Roger J. Miller<sup>203</sup>, Caroline Milstene<sup>54</sup>, Toshihiro Mimashi<sup>67</sup>, Irakli Minashvili<sup>115</sup>,  
 Ramon Miquel<sup>229,80</sup>, Shekhar Mishra<sup>54</sup>, Winfried Mitaroff<sup>177</sup>, Chad Mitchell<sup>266</sup>,  
 Takako Miura<sup>67</sup>, Akiya Miyamoto<sup>67</sup>, Hitoshi Miyata<sup>166</sup>, Ulf Mjörnmark<sup>145</sup>,  
 Joachim Mnich<sup>47</sup>, Klaus Moenig<sup>48</sup>, Kenneth Moffeit<sup>203</sup>, Nikolai Mokhov<sup>54</sup>,  
 Stephen Molloy<sup>203</sup>, Laura Monaco<sup>96</sup>, Paul R. Monasterio<sup>239</sup>, Alessandro Montanari<sup>47</sup>,  
 Sung Ik Moon<sup>182</sup>, Gudrid A. Moortgat-Pick<sup>38,49</sup>, Paulo Mora De Freitas<sup>50</sup>, Federic Morel<sup>84</sup>,  
 Stefano Moretti<sup>285</sup>, Vasily Morgunov<sup>47,92</sup>, Toshinori Mori<sup>106</sup>, Laurent Morin<sup>132</sup>,  
 François Morisseau<sup>131</sup>, Yoshiyuki Morita<sup>67</sup>, Youhei Morita<sup>67</sup>, Yuichi Morita<sup>106</sup>,  
 Nikolai Morozov<sup>115</sup>, Yuichi Morozumi<sup>67</sup>, William Morse<sup>19</sup>, Hans-Guenther Moser<sup>147</sup>,  
 Gilbert Moulta<sup>127</sup>, Sekazi Mtingwa<sup>146</sup>, Mihajlo Mudrinic<sup>316</sup>, Alex Mueller<sup>81</sup>,  
 Wolfgang Mueller<sup>82</sup>, Astrid Muennich<sup>190</sup>, Milada Margarete Muhlleitner<sup>129,35</sup>,  
 Bhaskar Mukherjee<sup>47</sup>, Biswarup Mukhopadhyaya<sup>64</sup>, Thomas Müller<sup>304</sup>, Morrison Munro<sup>203</sup>,  
 Hitoshi Murayama<sup>239,137</sup>, Toshiya Muto<sup>222</sup>, Ganapati Rao Myneni<sup>220</sup>, P.Y. Nabhiraj<sup>315</sup>,  
 Sergei Nagaitsev<sup>54</sup>, Tadashi Nagamine<sup>222</sup>, Ai Nagano<sup>292</sup>, Takashi Naito<sup>67</sup>, Hirotaka Nakai<sup>67</sup>,  
 Hiromitsu Nakajima<sup>67</sup>, Isamu Nakamura<sup>67</sup>, Tomoya Nakamura<sup>290</sup>, Tsutomu Nakanishi<sup>155</sup>,  
 Katsumi Nakao<sup>67</sup>, Noriaki Nakao<sup>54</sup>, Kazuo Nakayoshi<sup>67</sup>, Sang Nam<sup>182</sup>, Yoshihito Namito<sup>67</sup>,  
 Won Namkung<sup>182</sup>, Chris Nantista<sup>203</sup>, Olivier Napoly<sup>28</sup>, Meenakshi Narain<sup>20</sup>,  
 Beate Naroska<sup>255</sup>, Uriel Nauenberg<sup>247</sup>, Ruchika Nayyar<sup>248</sup>, Homer Neal<sup>203</sup>,  
 Charles Nelson<sup>204</sup>, Janice Nelson<sup>203</sup>, Timothy Nelson<sup>203</sup>, Stanislav Nemecek<sup>90</sup>,  
 Michael Neubauer<sup>203</sup>, David Neuffer<sup>54</sup>, Myriam Q. Newman<sup>276</sup>, Oleg Nezhevenko<sup>54</sup>,  
 Cho-Kuen Ng<sup>203</sup>, Anh Ky Nguyen<sup>89,135</sup>, Minh Nguyen<sup>203</sup>, Hong Van Nguyen Thi<sup>1,89</sup>,  
 Carsten Niebuhr<sup>47</sup>, Jim Niehoff<sup>54</sup>, Piotr Niezurawski<sup>294</sup>, Tomohiro Nishitani<sup>112</sup>,  
 Osamu Nitoh<sup>224</sup>, Shuichi Noguchi<sup>67</sup>, Andrei Nomerotski<sup>276</sup>, John Noonan<sup>8</sup>,  
 Edward Norbeck<sup>261</sup>, Yuri Nosochkov<sup>203</sup>, Dieter Notz<sup>47</sup>, Grazyna Nowak<sup>219</sup>,  
 Hannelies Nowak<sup>48</sup>, Matthew Noy<sup>72</sup>, Mitsuaki Nozaki<sup>67</sup>, Andreas Nyffeler<sup>64</sup>,  
 David Nygren<sup>137</sup>, Piermaria Oddone<sup>54</sup>, Joseph O'Dell<sup>38,26</sup>, Jong-Seok Oh<sup>182</sup>,  
 Sun Kun Oh<sup>122</sup>, Kazumasa Ohkuma<sup>56</sup>, Martin Ohlerich<sup>48,17</sup>, Kazuhito Ohmi<sup>67</sup>,  
 Yukiyo Ohnishi<sup>67</sup>, Satoshi Ohsawa<sup>67</sup>, Norihito Ohuchi<sup>67</sup>, Katsunobu Oide<sup>67</sup>,  
 Nobuchika Okada<sup>67</sup>, Yasuhiro Okada<sup>67,202</sup>, Takahiro Okamura<sup>67</sup>, Toshiyuki Okugi<sup>67</sup>,  
 Shoji Okumi<sup>155</sup>, Ken-ichi Okumura<sup>222</sup>, Alexander Olchevski<sup>115</sup>, William Oliver<sup>227</sup>,

Bob Olivier<sup>147</sup>, James Olsen<sup>185</sup>, Jeff Olsen<sup>203</sup>, Stephen Olsen<sup>256</sup>, A. G. Olshevsky<sup>115</sup>,  
 Jan Olsson<sup>47</sup>, Tsunehiko Omori<sup>67</sup>, Yasar Onel<sup>261</sup>, Gulsen Onengut<sup>44</sup>, Hiroaki Ono<sup>168</sup>,  
 Dmitry Onoprienko<sup>116</sup>, Mark Oreglia<sup>52</sup>, Will Oren<sup>220</sup>, Toyoko J. Orimoto<sup>239</sup>,  
 Marco Oriunno<sup>203</sup>, Marius Ciprian Orlandea<sup>2</sup>, Masahiro Oroku<sup>290</sup>, Lynne H. Orr<sup>282</sup>,  
 Robert S. Orr<sup>291</sup>, Val Oshea<sup>254</sup>, Anders Oskarsson<sup>145</sup>, Per Osland<sup>235</sup>, Dmitri Ossetski<sup>174</sup>,  
 Lennart Österman<sup>145</sup>, Francois Ostiguy<sup>54</sup>, Hidetoshi Otono<sup>290</sup>, Brian Ottewell<sup>276</sup>,  
 Qun Ouyang<sup>87</sup>, Hasan Padamsee<sup>43</sup>, Cristobal Padilla<sup>229</sup>, Carlo Pagani<sup>96</sup>, Mark A. Palmer<sup>43</sup>,  
 Wei Min Pam<sup>87</sup>, Manjiri Pande<sup>13</sup>, Rajni Pande<sup>13</sup>, V.S. Pandit<sup>315</sup>, P.N. Pandita<sup>170</sup>,  
 Mila Pandurovic<sup>316</sup>, Alexander Pankov<sup>180,179</sup>, Nicola Panzeri<sup>96</sup>, Zisis Papandreou<sup>281</sup>,  
 Rocco Paparella<sup>96</sup>, Adam Para<sup>54</sup>, Hwanbae Park<sup>30</sup>, Brett Parker<sup>19</sup>, Chris Parkes<sup>254</sup>,  
 Vittorio Parma<sup>35</sup>, Zohreh Parsa<sup>19</sup>, Justin Parsons<sup>261</sup>, Richard Partridge<sup>20,203</sup>,  
 Ralph Pasquinelli<sup>54</sup>, Gabriella Pásztor<sup>242,70</sup>, Ewan Paterson<sup>203</sup>, Jim Patrick<sup>54</sup>,  
 Piero Patteri<sup>134</sup>, J. Ritchie Patterson<sup>43</sup>, Giovanni Pauletta<sup>314</sup>, Nello Paver<sup>309</sup>,  
 Vince Pavlicek<sup>54</sup>, Bogdan Pawlik<sup>219</sup>, Jacques Payet<sup>28</sup>, Norbert Pchalek<sup>47</sup>, John Pedersen<sup>35</sup>,  
 Guo Xi Pei<sup>87</sup>, Shi Lun Pei<sup>87</sup>, Jerzy Pelka<sup>183</sup>, Giulio Pellegrini<sup>34</sup>, David Pellett<sup>240</sup>,  
 G.X. Peng<sup>87</sup>, Gregory Penn<sup>137</sup>, Aldo Penzo<sup>104</sup>, Colin Perry<sup>276</sup>, Michael Peskin<sup>203</sup>,  
 Franz Peters<sup>203</sup>, Troels Christian Petersen<sup>165,35</sup>, Daniel Peterson<sup>43</sup>, Thomas Peterson<sup>54</sup>,  
 Maureen Petterson<sup>245,244</sup>, Howard Pfeffer<sup>54</sup>, Phil Pfund<sup>54</sup>, Alan Phelps<sup>286</sup>,  
 Quang Van Phi<sup>89</sup>, Jonathan Phillips<sup>250</sup>, Nan Phinney<sup>203</sup>, Marcello Piccolo<sup>134</sup>,  
 Livio Piemontese<sup>97</sup>, Paolo Pierini<sup>96</sup>, W. Thomas Piggott<sup>138</sup>, Gary Pike<sup>54</sup>, Nicolas Pillet<sup>84</sup>,  
 Talini Pinto Jayawardena<sup>27</sup>, Phillippe Piot<sup>171</sup>, Kevin Pitts<sup>260</sup>, Mauro Pivi<sup>203</sup>,  
 Dave Plate<sup>137</sup>, Marc-Andre Pleier<sup>303</sup>, Andrei Poblaguev<sup>323</sup>, Michael Poehler<sup>323</sup>,  
 Matthew Poelker<sup>220</sup>, Paul Poffenberger<sup>293</sup>, Igor Pogorelsky<sup>19</sup>, Freddy Poirier<sup>47</sup>,  
 Ronald Poling<sup>269</sup>, Mike Poole<sup>38,26</sup>, Sorina Popescu<sup>2</sup>, John Popielarski<sup>150</sup>, Roman Pöschl<sup>130</sup>,  
 Martin Postranecky<sup>230</sup>, Prakash N. Potukochi<sup>105</sup>, Julie Prast<sup>128</sup>, Serge Prat<sup>130</sup>,  
 Miro Preger<sup>134</sup>, Richard Prepost<sup>297</sup>, Michael Price<sup>192</sup>, Dieter Proch<sup>47</sup>,  
 Avinash Puntambekar<sup>189</sup>, Qing Qin<sup>87</sup>, Hua Min Qu<sup>87</sup>, Arnulf Quadt<sup>58</sup>,  
 Jean-Pierre Quesnel<sup>35</sup>, Veljko Radeka<sup>19</sup>, Rahmat Rahmat<sup>275</sup>, Santosh Kumar Rai<sup>258</sup>,  
 Pantaleo Raimondi<sup>134</sup>, Erik Ramberg<sup>54</sup>, Kirti Ranjan<sup>248</sup>, Sista V.L.S. Rao<sup>13</sup>,  
 Alexei Raspereza<sup>147</sup>, Alessandro Ratti<sup>137</sup>, Lodovico Ratti<sup>278,101</sup>, Tor Raubenheimer<sup>203</sup>,  
 Ludovic Raux<sup>130</sup>, V. Ravindran<sup>64</sup>, Sreerup Raychaudhuri<sup>77,211</sup>, Valerio Re<sup>307,101</sup>,  
 Bill Rease<sup>142</sup>, Charles E. Reece<sup>220</sup>, Meinhard Regler<sup>177</sup>, Kay Rehlich<sup>47</sup>, Ina Reichel<sup>137</sup>,  
 Armin Reichold<sup>276</sup>, John Reid<sup>54</sup>, Ron Reid<sup>38,26</sup>, James Reidy<sup>270</sup>, Marcel Reinhard<sup>50</sup>,  
 Uwe Renz<sup>4</sup>, Jose Repond<sup>8</sup>, Javier Resta-Lopez<sup>276</sup>, Lars Reuen<sup>303</sup>, Jacob Ribnik<sup>243</sup>,  
 Tyler Rice<sup>244</sup>, François Richard<sup>130</sup>, Sabine Riemann<sup>48</sup>, Tord Riemann<sup>48</sup>, Keith Riles<sup>268</sup>,  
 Daniel Riley<sup>43</sup>, Cécile Rimbault<sup>130</sup>, Saurabh Rindani<sup>181</sup>, Louis Rinolfi<sup>35</sup>, Fabio Risigo<sup>96</sup>,  
 Imma Riu<sup>229</sup>, Dmitri Rizhikov<sup>174</sup>, Thomas Rizzo<sup>203</sup>, James H. Rochford<sup>27</sup>,  
 Ponciano Rodriguez<sup>203</sup>, Martin Roeben<sup>138</sup>, Gigi Rolandi<sup>35</sup>, Aaron Roodman<sup>203</sup>,  
 Eli Rosenberg<sup>107</sup>, Robert Roser<sup>54</sup>, Marc Ross<sup>54</sup>, François Rossel<sup>302</sup>, Robert Rossmanith<sup>7</sup>,  
 Stefan Roth<sup>190</sup>, André Rouge<sup>50</sup>, Allan Rowe<sup>54</sup>, Amit Roy<sup>105</sup>, Sendhunil B. Roy<sup>189</sup>,  
 Sourov Roy<sup>73</sup>, Laurent Royer<sup>131</sup>, Perrine Royole-Degieux<sup>130,59</sup>, Christophe Royon<sup>28</sup>,  
 Manqi Ruan<sup>31</sup>, David Rubin<sup>43</sup>, Ingo Ruehl<sup>35</sup>, Alberto Ruiz Jimeno<sup>95</sup>, Robert Ruland<sup>203</sup>,  
 Brian Rusnak<sup>138</sup>, Sun-Young Ryu<sup>187</sup>, Gian Luca Sabbi<sup>137</sup>, Iftach Sadeh<sup>216</sup>,  
 Ziraddin Y Sadygov<sup>115</sup>, Takayuki Saeki<sup>67</sup>, David Sagan<sup>43</sup>, Vinod C. Sahn<sup>189,13</sup>,  
 Arun Saini<sup>248</sup>, Kenji Saito<sup>67</sup>, Kiwamu Saito<sup>67</sup>, Gerard Sajot<sup>132</sup>, Shogo Sakanaka<sup>67</sup>,  
 Kazuyuki Sakaue<sup>320</sup>, Zen Salata<sup>203</sup>, Sabah Salih<sup>265</sup>, Fabrizio Salvatore<sup>192</sup>,  
 Joergen Samson<sup>47</sup>, Toshiya Sanami<sup>67</sup>, Allister Levi Sanchez<sup>50</sup>, William Sands<sup>185</sup>,

John Santic<sup>54,\*</sup>, Tomoyuki Sanuki<sup>222</sup>, Andrey Saprnov<sup>115,48</sup>, Utpal Sarkar<sup>181</sup>,  
 Noboru Sasao<sup>126</sup>, Kotaro Satoh<sup>67</sup>, Fabio Sauli<sup>35</sup>, Claude Saunders<sup>8</sup>, Valeri Saveliev<sup>174</sup>,  
 Aurore Savoy-Navarro<sup>302</sup>, Lee Sawyer<sup>143</sup>, Laura Saxton<sup>150</sup>, Oliver Schäfer<sup>305</sup>,  
 Andreas Schällicke<sup>48</sup>, Peter Schade<sup>47,255</sup>, Sebastien Schaetzel<sup>47</sup>, Glenn Scheitrum<sup>203</sup>,  
 Émilie Schibler<sup>299</sup>, Rafe Schindler<sup>203</sup>, Markus Schlösser<sup>47</sup>, Ross D. Schlueter<sup>137</sup>,  
 Peter Schmid<sup>48</sup>, Ringo Sebastian Schmidt<sup>48,17</sup>, Uwe Schneekloth<sup>47</sup>,  
 Heinz Juergen Schreiber<sup>48</sup>, Siegfried Schreiber<sup>47</sup>, Henning Schroeder<sup>305</sup>, K. Peter Schüler<sup>47</sup>,  
 Daniel Schulte<sup>35</sup>, Hans-Christian Schultz-Coulon<sup>257</sup>, Markus Schumacher<sup>306</sup>,  
 Steffen Schumann<sup>215</sup>, Bruce A. Schumm<sup>244,245</sup>, Reinhard Schwienhorst<sup>150</sup>,  
 Rainer Schwierz<sup>214</sup>, Duncan J. Scott<sup>38,26</sup>, Fabrizio Scuri<sup>102</sup>, Felix Sefkow<sup>47</sup>, Rachid Sefri<sup>83</sup>,  
 Nathalie Seguin-Moreau<sup>130</sup>, Sally Seidel<sup>272</sup>, David Seidman<sup>172</sup>, Sezen Sekmen<sup>151</sup>,  
 Sergei Seletskiy<sup>203</sup>, Eibun Senaha<sup>159</sup>, Rohan Senanayake<sup>276</sup>, Hiroshi Sendai<sup>67</sup>,  
 Daniele Sertore<sup>96</sup>, Andrei Seryi<sup>203</sup>, Ronald Settles<sup>147,47</sup>, Ramazan Sever<sup>151</sup>,  
 Nicholas Shales<sup>38,136</sup>, Ming Shao<sup>283</sup>, G. A. Shelkov<sup>115</sup>, Ken Shepard<sup>8</sup>,  
 Claire Shepherd-Themistocleous<sup>27</sup>, John C. Sheppard<sup>203</sup>, Cai Tu Shi<sup>87</sup>, Tetsuo Shidara<sup>67</sup>,  
 Yeo-Jeong Shim<sup>187</sup>, Hirotaka Shimizu<sup>68</sup>, Yasuhiro Shimizu<sup>123</sup>, Yuuki Shimizu<sup>193</sup>,  
 Tetsushi Shimogawa<sup>193</sup>, Seunghwan Shin<sup>30</sup>, Masaomi Shioden<sup>71</sup>, Ian Shipsey<sup>186</sup>,  
 Grigori Shirkov<sup>115</sup>, Toshio Shishido<sup>67</sup>, Ram K. Shivpuri<sup>248</sup>, Purushottam Shrivastava<sup>189</sup>,  
 Sergey Shulga<sup>115,60</sup>, Nikolai Shumeiko<sup>11</sup>, Sergey Shuvalov<sup>47</sup>, Zongguo Si<sup>198</sup>,  
 Azher Majid Siddiqui<sup>110</sup>, James Siegrist<sup>137,239</sup>, Claire Simon<sup>28</sup>, Stefan Simrock<sup>47</sup>,  
 Nikolai Sinev<sup>275</sup>, Bhartendu K. Singh<sup>12</sup>, Jasbir Singh<sup>178</sup>, Pitamber Singh<sup>13</sup>, R.K. Singh<sup>129</sup>,  
 S.K. Singh<sup>5</sup>, Monito Singini<sup>278</sup>, Anil K. Sinha<sup>13</sup>, Nita Sinha<sup>88</sup>, Rahul Sinha<sup>88</sup>,  
 Klaus Sinram<sup>47</sup>, A. N. Sissakian<sup>115</sup>, N. B. Skachkov<sup>115</sup>, Alexander Skrinsky<sup>21</sup>,  
 Mark Slater<sup>246</sup>, Wojciech Slominski<sup>108</sup>, Ivan Smiljanic<sup>316</sup>, A J Stewart Smith<sup>185</sup>,  
 Alex Smith<sup>269</sup>, Brian J. Smith<sup>27</sup>, Jeff Smith<sup>43,203</sup>, Jonathan Smith<sup>38,136</sup>, Steve Smith<sup>203</sup>,  
 Susan Smith<sup>38,26</sup>, Tonee Smith<sup>203</sup>, W. Neville Snodgrass<sup>26</sup>, Blanka Sobloher<sup>47</sup>,  
 Young-Uk Sohn<sup>182</sup>, Ruelson Solidum<sup>153,152</sup>, Nikolai Solyak<sup>54</sup>, Dongchul Son<sup>30</sup>,  
 Nasuf Sonmez<sup>51</sup>, Andre Sopczak<sup>38,136</sup>, V. Soskov<sup>139</sup>, Cherrill M. Spencer<sup>203</sup>,  
 Panagiotis Spentzouris<sup>54</sup>, Valeria Speziali<sup>278</sup>, Michael Spira<sup>209</sup>, Daryl Sprehn<sup>203</sup>,  
 K. Sridhar<sup>211</sup>, Asutosh Srivastava<sup>248,14</sup>, Steve St. Lorant<sup>203</sup>, Achim Stahl<sup>190</sup>,  
 Richard P. Stanek<sup>54</sup>, Marcel Stanitzki<sup>27</sup>, Jacob Stanley<sup>245,244</sup>, Konstantin Stefanov<sup>27</sup>,  
 Werner Stein<sup>138</sup>, Herbert Steiner<sup>137</sup>, Evert Stenlund<sup>145</sup>, Amir Stern<sup>216</sup>, Matt Sternberg<sup>275</sup>,  
 Dominik Stockinger<sup>254</sup>, Mark Stockton<sup>236</sup>, Holger Stoeck<sup>287</sup>, John Strachan<sup>26</sup>,  
 V. Strakhovenko<sup>21</sup>, Michael Strauss<sup>274</sup>, Sergei I. Striganov<sup>54</sup>, John Strologas<sup>272</sup>,  
 David Strom<sup>275</sup>, Jan Strube<sup>275</sup>, Gennady Stupakov<sup>203</sup>, Dong Su<sup>203</sup>, Yuji Sudo<sup>292</sup>,  
 Taikan Suehara<sup>290</sup>, Toru Suehiro<sup>290</sup>, Yusuke Suetsugu<sup>67</sup>, Ryuhei Sugahara<sup>67</sup>,  
 Yasuhiro Sugimoto<sup>67</sup>, Akira Sugiyama<sup>193</sup>, Jun Suhk Suh<sup>30</sup>, Goran Sukovic<sup>271</sup>, Hong Sun<sup>87</sup>,  
 Stephen Sun<sup>203</sup>, Werner Sun<sup>43</sup>, Yi Sun<sup>87</sup>, Yipeng Sun<sup>87,10</sup>, Leszek Suszycki<sup>3</sup>,  
 Peter Sutcliffe<sup>38,263</sup>, Rameshwar L. Suthar<sup>13</sup>, Tsuyoshi Suwada<sup>67</sup>, Atsuto Suzuki<sup>67</sup>,  
 Chihiro Suzuki<sup>155</sup>, Shiro Suzuki<sup>193</sup>, Takashi Suzuki<sup>292</sup>, Richard Swent<sup>203</sup>,  
 Krzysztof Swientek<sup>3</sup>, Christina Swinson<sup>276</sup>, Evgeny Syresin<sup>115</sup>, Michal Szleper<sup>172</sup>,  
 Alexander Tadday<sup>257</sup>, Rika Takahashi<sup>67,59</sup>, Tohru Takahashi<sup>68</sup>, Mikio Takano<sup>196</sup>,  
 Fumihiko Takasaki<sup>67</sup>, Seishi Takeda<sup>67</sup>, Tateru Takenaka<sup>67</sup>, Tohru Takeshita<sup>200</sup>,  
 Yosuke Takubo<sup>222</sup>, Masami Tanaka<sup>67</sup>, Chuan Xiang Tang<sup>31</sup>, Takashi Taniguchi<sup>67</sup>,  
 Sami Tantawi<sup>203</sup>, Stefan Tapprogge<sup>113</sup>, Michael A. Tartaglia<sup>54</sup>,  
 Giovanni Francesco Tassielli<sup>313</sup>, Toshiaki Tauchi<sup>67</sup>, Laurent Tavian<sup>35</sup>, Hiroko Tawara<sup>67</sup>,  
 Geoffrey Taylor<sup>267</sup>, Alexandre V. Telnov<sup>185</sup>, Valery Telnov<sup>21</sup>, Peter Tenenbaum<sup>203</sup>,

Eliza Teodorescu<sup>2</sup>, Akio Terashima<sup>67</sup>, Giuseppina Terracciano<sup>99</sup>, Nobuhiro Terunuma<sup>67</sup>,  
 Thomas Teubner<sup>263</sup>, Richard Teuscher<sup>293,291</sup>, Jay Theilacker<sup>54</sup>, Mark Thomson<sup>246</sup>,  
 Jeff Tice<sup>203</sup>, Maury Tigner<sup>43</sup>, Jan Timmermans<sup>160</sup>, Maxim Titov<sup>28</sup>, Nobukazu Toge<sup>67</sup>,  
 N. A. Tokareva<sup>115</sup>, Kirsten Tollefson<sup>150</sup>, Lukas Tomasek<sup>90</sup>, Savo Tomovic<sup>271</sup>,  
 John Tompkins<sup>54</sup>, Manfred Tonutti<sup>190</sup>, Anita Topkar<sup>13</sup>, Dragan Toprek<sup>38,265</sup>,  
 Fernando Toral<sup>33</sup>, Eric Torrence<sup>275</sup>, Gianluca Traversi<sup>307,101</sup>, Marcel Trimpl<sup>54</sup>,  
 S. Mani Tripathi<sup>240</sup>, William Trischuk<sup>291</sup>, Mark Trodden<sup>210</sup>, G. V. Trubnikov<sup>115</sup>,  
 Robert Tschirhart<sup>54</sup>, Edisher Tskhadadze<sup>115</sup>, Kiyosumi Tsuchiya<sup>67</sup>,  
 Toshifumi Tsukamoto<sup>67</sup>, Akira Tsunemi<sup>207</sup>, Robin Tucker<sup>38,136</sup>, Renato Turchetta<sup>27</sup>,  
 Mike Tyndel<sup>27</sup>, Nobuhiro Uekusa<sup>258,65</sup>, Kenji Ueno<sup>67</sup>, Kensei Umemori<sup>67</sup>,  
 Martin Ummenhofer<sup>303</sup>, David Underwood<sup>8</sup>, Satoru Uozumi<sup>200</sup>, Junji Urakawa<sup>67</sup>,  
 Jeremy Urban<sup>43</sup>, Didier Uriot<sup>28</sup>, David Urner<sup>276</sup>, Andrei Ushakov<sup>48</sup>, Tracy Usher<sup>203</sup>,  
 Sergey Uzunyan<sup>171</sup>, Brigitte Vachon<sup>148</sup>, Linda Valerio<sup>54</sup>, Isabelle Valin<sup>84</sup>, Alex Valishev<sup>54</sup>,  
 Raghava Vamra<sup>75</sup>, Harry Van Der Graaf<sup>160,35</sup>, Rick Van Kooten<sup>79</sup>, Gary Van Zandbergen<sup>54</sup>,  
 Jean-Charles Vanel<sup>50</sup>, Alessandro Variola<sup>130</sup>, Gary Varner<sup>256</sup>, Mayda Velasco<sup>172</sup>,  
 Ulrich Velte<sup>47</sup>, Jaap Velthuis<sup>237</sup>, Sundir K. Vempati<sup>74</sup>, Marco Venturini<sup>137</sup>,  
 Christophe Vescovi<sup>132</sup>, Henri Videau<sup>50</sup>, Ivan Vila<sup>95</sup>, Pascal Vincent<sup>302</sup>, Jean-Marc Virey<sup>32</sup>,  
 Bernard Visentin<sup>28</sup>, Michele Viti<sup>48</sup>, Thanh Cuong Vo<sup>317</sup>, Adrian Vogel<sup>47</sup>, Harald Vogt<sup>48</sup>,  
 Eckhard Von Toerne<sup>303,116</sup>, S. B. Vorozhtsov<sup>115</sup>, Marcel Vos<sup>94</sup>, Margaret Votava<sup>54</sup>,  
 Vaclav Vrba<sup>90</sup>, Doreen Wackerroth<sup>205</sup>, Albrecht Wagner<sup>47</sup>, Carlos E. M. Wagner<sup>8,52</sup>,  
 Stephen Wagner<sup>247</sup>, Masayoshi Wake<sup>67</sup>, Roman Walczak<sup>276</sup>, Nicholas J. Walker<sup>47</sup>,  
 Wolfgang Walkowiak<sup>306</sup>, Samuel Wallon<sup>133</sup>, Roberval Walsh<sup>251</sup>, Sean Walston<sup>138</sup>,  
 Wolfgang Waltenberger<sup>177</sup>, Dieter Walz<sup>203</sup>, Chao En Wang<sup>163</sup>, Chun Hong Wang<sup>87</sup>,  
 Dou Wang<sup>87</sup>, Faya Wang<sup>203</sup>, Guang Wei Wang<sup>87</sup>, Haitao Wang<sup>8</sup>, Jiang Wang<sup>87</sup>,  
 Jiu Qing Wang<sup>87</sup>, Juwen Wang<sup>203</sup>, Lanfa Wang<sup>203</sup>, Lei Wang<sup>244</sup>, Min-Zu Wang<sup>164</sup>,  
 Qing Wang<sup>31</sup>, Shu Hong Wang<sup>87</sup>, Xiaolian Wang<sup>283</sup>, Xue-Lei Wang<sup>66</sup>, Yi Fang Wang<sup>87</sup>,  
 Zheng Wang<sup>87</sup>, Rainer Wanzenberg<sup>47</sup>, Bennie Ward<sup>9</sup>, David Ward<sup>246</sup>,  
 Barbara Warmbein<sup>47,59</sup>, David W. Warner<sup>40</sup>, Matthew Warren<sup>230</sup>, Masakazu Washio<sup>320</sup>,  
 Isamu Watanabe<sup>169</sup>, Ken Watanabe<sup>67</sup>, Takashi Watanabe<sup>121</sup>, Yuichi Watanabe<sup>67</sup>,  
 Nigel Watson<sup>236</sup>, Nanda Wattimena<sup>47,255</sup>, Mitchell Wayne<sup>273</sup>, Marc Weber<sup>27</sup>,  
 Harry Weerts<sup>8</sup>, Georg Weiglein<sup>49</sup>, Thomas Weiland<sup>82</sup>, Stefan Weinzierl<sup>113</sup>, Hans Weise<sup>47</sup>,  
 John Weisend<sup>203</sup>, Manfred Wendt<sup>54</sup>, Oliver Wendt<sup>47,255</sup>, Hans Wenzel<sup>54</sup>,  
 William A. Wenzel<sup>137</sup>, Norbert Wermes<sup>303</sup>, Ulrich Werthenbach<sup>306</sup>, Steve Wesseln<sup>54</sup>,  
 William Wester<sup>54</sup>, Andy White<sup>288</sup>, Glen R. White<sup>203</sup>, Katarzyna Wichmann<sup>47</sup>,  
 Peter Wienemann<sup>303</sup>, Wojciech Wierba<sup>219</sup>, Tim Wilksen<sup>43</sup>, William Willis<sup>41</sup>,  
 Graham W. Wilson<sup>262</sup>, John A. Wilson<sup>236</sup>, Robert Wilson<sup>40</sup>, Matthew Wing<sup>230</sup>,  
 Marc Winter<sup>84</sup>, Brian D. Wirth<sup>239</sup>, Stephen A. Wolbers<sup>54</sup>, Dan Wolff<sup>54</sup>,  
 Andrzej Wolski<sup>38,263</sup>, Mark D. Woodley<sup>203</sup>, Michael Woods<sup>203</sup>, Michael L. Woodward<sup>27</sup>,  
 Timothy Woolliscroft<sup>263,27</sup>, Steven Worm<sup>27</sup>, Guy Wormser<sup>130</sup>, Dennis Wright<sup>203</sup>,  
 Douglas Wright<sup>138</sup>, Andy Wu<sup>220</sup>, Tao Wu<sup>192</sup>, Yue Liang Wu<sup>93</sup>, Stefania Xella<sup>165</sup>,  
 Guoxing Xia<sup>47</sup>, Lei Xia<sup>8</sup>, Aimin Xiao<sup>8</sup>, Liling Xiao<sup>203</sup>, Jia Lin Xie<sup>87</sup>, Zhi-Zhong Xing<sup>87</sup>,  
 Lian You Xiong<sup>212</sup>, Gang Xu<sup>87</sup>, Qing Jing Xu<sup>87</sup>, Urjit A. Yajnik<sup>75</sup>, Vitaly Yakimenko<sup>19</sup>,  
 Ryuji Yamada<sup>54</sup>, Hiroshi Yamaguchi<sup>193</sup>, Akira Yamamoto<sup>67</sup>, Hitoshi Yamamoto<sup>222</sup>,  
 Masahiro Yamamoto<sup>155</sup>, Naoto Yamamoto<sup>155</sup>, Richard Yamamoto<sup>146</sup>,  
 Yasuchika Yamamoto<sup>67</sup>, Takashi Yamanaka<sup>290</sup>, Hiroshi Yamaoka<sup>67</sup>, Satoru Yamashita<sup>106</sup>,  
 Hideki Yamazaki<sup>292</sup>, Wenbiao Yan<sup>246</sup>, Hai-Jun Yang<sup>268</sup>, Jin Min Yang<sup>93</sup>, Jongmann Yang<sup>53</sup>,  
 Zhenwei Yang<sup>31</sup>, Yoshiharu Yano<sup>67</sup>, Efe Yazgan<sup>218,35</sup>, G. P. Yeh<sup>54</sup>, Hakan Yilmaz<sup>72</sup>,

Philip Yock<sup>234</sup>, Hakutaro Yoda<sup>290</sup>, John Yoh<sup>54</sup>, Kaoru Yokoya<sup>67</sup>, Hirokazu Yokoyama<sup>126</sup>,  
Richard C. York<sup>150</sup>, Mitsuhiro Yoshida<sup>67</sup>, Takuo Yoshida<sup>57</sup>, Tamaki Yoshioka<sup>106</sup>,  
Andrew Young<sup>203</sup>, Cheng Hui Yu<sup>87</sup>, Jaehoon Yu<sup>288</sup>, Xian Ming Yu<sup>87</sup>, Changzheng Yuan<sup>87</sup>,  
Chong-Xing Yue<sup>140</sup>, Jun Hui Yue<sup>87</sup>, Josef Zacek<sup>36</sup>, Igor Zagorodnov<sup>47</sup>, Jaroslav Zalesak<sup>90</sup>,  
Boris Zalikhanov<sup>115</sup>, Aleksander Filip Zarnecki<sup>294</sup>, Leszek Zawiejski<sup>219</sup>,  
Christian Zeitnitz<sup>298</sup>, Michael Zeller<sup>323</sup>, Dirk Zerwas<sup>130</sup>, Peter Zerwas<sup>47,190</sup>,  
Mehmet Zeyrek<sup>151</sup>, Ji Yuan Zhai<sup>87</sup>, Bao Cheng Zhang<sup>10</sup>, Bin Zhang<sup>31</sup>, Chuang Zhang<sup>87</sup>,  
He Zhang<sup>87</sup>, Jiawen Zhang<sup>87</sup>, Jing Zhang<sup>87</sup>, Jing Ru Zhang<sup>87</sup>, Jinlong Zhang<sup>8</sup>,  
Liang Zhang<sup>212</sup>, X. Zhang<sup>87</sup>, Yuan Zhang<sup>87</sup>, Zhige Zhang<sup>27</sup>, Zhiqing Zhang<sup>130</sup>,  
Ziping Zhang<sup>283</sup>, Haiwen Zhao<sup>270</sup>, Ji Jiu Zhao<sup>87</sup>, Jing Xia Zhao<sup>87</sup>, Ming Hua Zhao<sup>199</sup>,  
Sheng Chu Zhao<sup>87</sup>, Tianchi Zhao<sup>296</sup>, Tong Xian Zhao<sup>212</sup>, Zhen Tang Zhao<sup>199</sup>,  
Zhengguo Zhao<sup>268,283</sup>, De Min Zhou<sup>87</sup>, Feng Zhou<sup>203</sup>, Shun Zhou<sup>87</sup>, Shou Hua Zhu<sup>10</sup>,  
Xiong Wei Zhu<sup>87</sup>, Valery Zhukov<sup>304</sup>, Frank Zimmermann<sup>35</sup>, Michael Ziolkowski<sup>306</sup>,  
Michael S. Zisman<sup>137</sup>, Fabian Zomer<sup>130</sup>, Zhang Guo Zong<sup>87</sup>, Osman Zorba<sup>72</sup>,  
Vishnu Zutshi<sup>171</sup>

# List of Institutions

- <sup>1</sup> *Abdus Salam International Centre for Theoretical Physics, Strada Costiera 11, 34014 Trieste, Italy*
- <sup>2</sup> *Academy, RPR, National Institute of Physics and Nuclear Engineering ‘Horia Hulubei’ (IFIN-HH), Str. Atomistilor no. 407, P.O. Box MG-6, R-76900 Bucharest - Magurele, Romania*
- <sup>3</sup> *AGH University of Science and Technology Akademia Gorniczo-Hutnicza im. Stanislaw Staszica w Krakowie al. Mickiewicza 30 PL-30-059 Cracow, Poland*
- <sup>4</sup> *Albert-Ludwigs Universität Freiburg, Physikalisches Institut, Hermann-Herder Str. 3, D-79104 Freiburg, Germany*
- <sup>5</sup> *Aligarh Muslim University, Aligarh, Uttar Pradesh 202002, India*
- <sup>6</sup> *Amberg Engineering AG, Trockenloostr. 21, P.O.Box 27, 8105 Regensdorf-Watt, Switzerland*
- <sup>7</sup> *Angstromquelle Karlsruhe (ANKA), Forschungszentrum Karlsruhe, Hermann-von-Helmholtz-Platz 1, D-76344 Eggenstein-Leopoldshafen, Germany*
- <sup>8</sup> *Argonne National Laboratory (ANL), 9700 S. Cass Avenue, Argonne, IL 60439, USA*
- <sup>9</sup> *Baylor University, Department of Physics, 101 Bagby Avenue, Waco, TX 76706, USA*
- <sup>10</sup> *Beijing University, Department of Physics, Beijing, China 100871*
- <sup>11</sup> *Belarusian State University, National Scientific & Educational Center, Particle & HEP Physics, M. Bogdanovich St., 153, 240040 Minsk, Belarus*
- <sup>12</sup> *Benares Hindu University, Benares, Varanasi 221005, India*
- <sup>13</sup> *Bhabha Atomic Research Centre, Trombay, Mumbai 400085, India*
- <sup>14</sup> *Birla Institute of Technology and Science, EEE Dept., Pilani, Rajasthan, India*
- <sup>15</sup> *Bogazici University, Physics Department, 34342 Bebek / Istanbul, 80820 Istanbul, Turkey*
- <sup>16</sup> *Boston University, Department of Physics, 590 Commonwealth Avenue, Boston, MA 02215, USA*
- <sup>17</sup> *Brandenburg University of Technology, Postfach 101344, D-03013 Cottbus, Germany*
- <sup>18</sup> *Brno University of Technology, Antonínská; 548/1, CZ 601 90 Brno, Czech Republic*
- <sup>19</sup> *Brookhaven National Laboratory (BNL), P.O.Box 5000, Upton, NY 11973-5000, USA*
- <sup>20</sup> *Brown University, Department of Physics, Box 1843, Providence, RI 02912, USA*
- <sup>21</sup> *Budkar Institute for Nuclear Physics (BINP), 630090 Novosibirsk, Russia*
- <sup>22</sup> *Calcutta University, Department of Physics, 92 A.P.C. Road, Kolkata 700009, India*
- <sup>23</sup> *California Institute of Technology, Physics, Mathematics and Astronomy (PMA), 1200 East California Blvd, Pasadena, CA 91125, USA*
- <sup>24</sup> *Carleton University, Department of Physics, 1125 Colonel By Drive, Ottawa, Ontario, Canada K1S 5B6*

- <sup>25</sup> Carnegie Mellon University, Department of Physics, Wean Hall 7235, Pittsburgh, PA 15213, USA
- <sup>26</sup> CCLRC Daresbury Laboratory, Daresbury, Warrington, Cheshire WA4 4AD, UK
- <sup>27</sup> CCLRC Rutherford Appleton Laboratory, Chilton, Didcot, Oxton OX11 0QX, UK
- <sup>28</sup> CEA Saclay, DAPNIA, F-91191 Gif-sur-Yvette, France
- <sup>29</sup> CEA Saclay, Service de Physique Théorique, CEA/DSM/SPhT, F-91191 Gif-sur-Yvette Cedex, France
- <sup>30</sup> Center for High Energy Physics (CHEP) / Kyungpook National University, 1370 Sankyuk-dong, Buk-gu, Daegu 702-701, Korea
- <sup>31</sup> Center for High Energy Physics (TUHEP), Tsinghua University, Beijing, China 100084
- <sup>32</sup> Centre de Physique Theorique, CNRS - Luminy, Universiti d'Aix - Marseille II, Campus of Luminy, Case 907, 13288 Marseille Cedex 9, France
- <sup>33</sup> Centro de Investigaciones Energéticas, Medioambientales y Tecnológicas, CIEMAT, Avenia Complutense 22, E-28040 Madrid, Spain
- <sup>34</sup> Centro Nacional de Microelectrónica (CNM), Instituto de Microelectrónica de Barcelona (IMB), Campus UAB, 08193 Cerdanyola del Vallès (Bellaterra), Barcelona, Spain
- <sup>35</sup> CERN, CH-1211 Genève 23, Switzerland
- <sup>36</sup> Charles University, Institute of Particle & Nuclear Physics, Faculty of Mathematics and Physics, V Holesovickach 2, CZ-18000 Praque 8, Czech Republic
- <sup>37</sup> Chonbuk National University, Physics Department, Chonju 561-756, Korea
- <sup>38</sup> Cockcroft Institute, Daresbury, Warrington WA4 4AD, UK
- <sup>39</sup> College of William and Mary, Department of Physics, Williamsburg, VA, 23187, USA
- <sup>40</sup> Colorado State University, Department of Physics, Fort Collins, CO 80523, USA
- <sup>41</sup> Columbia University, Department of Physics, New York, NY 10027-6902, USA
- <sup>42</sup> Concordia University, Department of Physics, 1455 De Maisonneuve Blvd. West, Montreal, Quebec, Canada H3G 1M8
- <sup>43</sup> Cornell University, Laboratory for Elementary-Particle Physics (LEPP), Ithaca, NY 14853, USA
- <sup>44</sup> Cukurova University, Department of Physics, Fen-Ed. Fakultesi 01330, Balcali, Turkey
- <sup>45</sup> D. V. Efremov Research Institute, SINTEZ, 196641 St. Petersburg, Russia
- <sup>46</sup> Dartmouth College, Department of Physics and Astronomy, 6127 Wilder Laboratory, Hanover, NH 03755, USA
- <sup>47</sup> DESY-Hamburg site, Deutsches Elektronen-Synchrotron in der Helmholtz-Gemeinschaft, Notkestrasse 85, 22607 Hamburg, Germany
- <sup>48</sup> DESY-Zeuthen site, Deutsches Elektronen-Synchrotron in der Helmholtz-Gemeinschaft, Platanenallee 6, D-15738 Zeuthen, Germany
- <sup>49</sup> Durham University, Department of Physics, Ogen Center for Fundamental Physics, South Rd., Durham DH1 3LE, UK
- <sup>50</sup> Ecole Polytechnique, Laboratoire Leprince-Ringuet (LLR), Route de Saclay, F-91128 Palaiseau Cedex, France
- <sup>51</sup> Ege University, Department of Physics, Faculty of Science, 35100 Izmir, Turkey
- <sup>52</sup> Enrico Fermi Institute, University of Chicago, 5640 S. Ellis Avenue, RI-183, Chicago, IL 60637, USA
- <sup>53</sup> Ewha Womans University, 11-1 Daehyun-Dong, Seodaemun-Gu, Seoul, 120-750, Korea
- <sup>54</sup> Fermi National Accelerator Laboratory (FNAL), P.O.Box 500, Batavia, IL 60510-0500, USA
- <sup>55</sup> Fujita Gakuen Health University, Department of Physics, Toyoake, Aichi 470-1192, Japan



- <sup>56</sup> Fukui University of Technology, 3-6-1 Gakuen, Fukui-shi, Fukui 910-8505, Japan
- <sup>57</sup> Fukui University, Department of Physics, 3-9-1 Bunkyo, Fukui-shi, Fukui 910-8507, Japan
- <sup>58</sup> Georg-August-Universität Göttingen, II. Physikalisches Institut, Friedrich-Hund-Platz 1,  
37077 Göttingen, Germany
- <sup>59</sup> Global Design Effort
- <sup>60</sup> Gomel State University, Department of Physics, Ul. Sovietskaya 104, 246699 Gomel,  
Belarus
- <sup>61</sup> Guangxi University, College of Physics science and Engineering Technology, Nanning,  
China 530004
- <sup>62</sup> Hanoi University of Technology, 1 Dai Co Viet road, Hanoi, Vietnam
- <sup>63</sup> Hanson Professional Services, Inc., 1525 S. Sixth St., Springfield, IL 62703, USA
- <sup>64</sup> Harish-Chandra Research Institute, Chhatnag Road, Jhusi, Allahabad 211019, India
- <sup>65</sup> Helsinki Institute of Physics (HIP), P.O. Box 64, FIN-00014 University of Helsinki,  
Finland
- <sup>66</sup> Henan Normal University, College of Physics and Information Engineering, Xinxiang,  
China 453007
- <sup>67</sup> High Energy Accelerator Research Organization, KEK, 1-1 Oho, Tsukuba, Ibaraki  
305-0801, Japan
- <sup>68</sup> Hiroshima University, Department of Physics, 1-3-1 Kagamiyama, Higashi-Hiroshima,  
Hiroshima 739-8526, Japan
- <sup>69</sup> Humboldt Universität zu Berlin, Fachbereich Physik, Institut für  
Elementarteilchenphysik, Newtonstr. 15, D-12489 Berlin, Germany
- <sup>70</sup> Hungarian Academy of Sciences, KFKI Research Institute for Particle and Nuclear  
Physics, P.O. Box 49, H-1525 Budapest, Hungary
- <sup>71</sup> Ibaraki University, College of Technology, Department of Physics, Nakanarusawa 4-12-1,  
Hitachi, Ibaraki 316-8511, Japan
- <sup>72</sup> Imperial College, Blackett Laboratory, Department of Physics, Prince Consort Road,  
London, SW7 2BW, UK
- <sup>73</sup> Indian Association for the Cultivation of Science, Department of Theoretical Physics and  
Centre for Theoretical Sciences, Kolkata 700032, India
- <sup>74</sup> Indian Institute of Science, Centre for High Energy Physics, Bangalore 560012,  
Karnataka, India
- <sup>75</sup> Indian Institute of Technology, Bombay, Powai, Mumbai 400076, India
- <sup>76</sup> Indian Institute of Technology, Guwahati, Guwahati, Assam 781039, India
- <sup>77</sup> Indian Institute of Technology, Kanpur, Department of Physics, IIT Post Office, Kanpur  
208016, India
- <sup>78</sup> Indiana University - Purdue University, Indianapolis, Department of Physics, 402 N.  
Blackford St., LD 154, Indianapolis, IN 46202, USA
- <sup>79</sup> Indiana University, Department of Physics, Swain Hall West 117, 727 E. 3rd St.,  
Bloomington, IN 47405-7105, USA
- <sup>80</sup> Institutio Catalana de Recerca i Estudis, ICREA, Passeig Lluís Companys, 23, Barcelona  
08010, Spain
- <sup>81</sup> Institut de Physique Nucléaire, F-91406 Orsay, France
- <sup>82</sup> Institut für Theorie Elektromagnetischer Felder (TEMF), Technische Universität  
Darmstadt, Schloßgartenstr. 8, D-64289 Darmstadt, Germany
- <sup>83</sup> Institut National de Physique Nucleaire et de Physique des Particules, 3, Rue Michel-  
Ange, 75794 Paris Cedex 16, France

- <sup>84</sup> *Institut Pluridisciplinaire Hubert Curien, 23 Rue du Loess - BP28, 67037 Strasbourg Cedex 2, France*
- <sup>85</sup> *Institute for Chemical Research, Kyoto University, Gokasho, Uji, Kyoto 611-0011, Japan*
- <sup>86</sup> *Institute for Cosmic Ray Research, University of Tokyo, 5-1-5 Kashiwa-no-Ha, Kashiwa, Chiba 277-8582, Japan*
- <sup>87</sup> *Institute of High Energy Physics - IHEP, Chinese Academy of Sciences, P.O. Box 918, Beijing, China 100049*
- <sup>88</sup> *Institute of Mathematical Sciences, Taramani, C.I.T. Campus, Chennai 600113, India*
- <sup>89</sup> *Institute of Physics and Electronics, Vietnamese Academy of Science and Technology (VAST), 10 Dao-Tan, Ba-Dinh, Hanoi 10000, Vietnam*
- <sup>90</sup> *Institute of Physics, ASCR, Academy of Science of the Czech Republic, Division of Elementary Particle Physics, Na Slovance 2, CS-18221 Prague 8, Czech Republic*
- <sup>91</sup> *Institute of Physics, Pomorska 149/153, PL-90-236 Lodz, Poland*
- <sup>92</sup> *Institute of Theoretical and Experimental Physics, B. Chermushkinskawa, 25, RU-117259, Moscow, Russia*
- <sup>93</sup> *Institute of Theoretical Physics, Chinese Academy of Sciences, P.O.Box 2735, Beijing, China 100080*
- <sup>94</sup> *Instituto de Fisica Corpuscular (IFIC), Centro Mixto CSIC-UVEG, Edificio Investigacion Paterna, Apartado 22085, 46071 Valencia, Spain*
- <sup>95</sup> *Instituto de Fisica de Cantabria, (IFCA, CSIC-UC), Facultad de Ciencias, Avda. Los Castros s/n, 39005 Santander, Spain*
- <sup>96</sup> *Instituto Nazionale di Fisica Nucleare (INFN), Laboratorio LASA, Via Fratelli Cervi 201, 20090 Segrate, Italy*
- <sup>97</sup> *Instituto Nazionale di Fisica Nucleare (INFN), Sezione di Ferrara, via Paradiso 12, I-44100 Ferrara, Italy*
- <sup>98</sup> *Instituto Nazionale di Fisica Nucleare (INFN), Sezione di Firenze, Via G. Sansone 1, I-50019 Sesto Fiorentino (Firenze), Italy*
- <sup>99</sup> *Instituto Nazionale di Fisica Nucleare (INFN), Sezione di Lecce, via Arnesano, I-73100 Lecce, Italy*
- <sup>100</sup> *Instituto Nazionale di Fisica Nucleare (INFN), Sezione di Napoli, Complesso Università di Monte Sant'Angelo, via, I-80126 Naples, Italy*
- <sup>101</sup> *Instituto Nazionale di Fisica Nucleare (INFN), Sezione di Pavia, Via Bassi 6, I-27100 Pavia, Italy*
- <sup>102</sup> *Instituto Nazionale di Fisica Nucleare (INFN), Sezione di Pisa, Edificio C - Polo Fibonacci Largo B. Pontecorvo, 3, I-56127 Pisa, Italy*
- <sup>103</sup> *Instituto Nazionale di Fisica Nucleare (INFN), Sezione di Torino, c/o Università' di Torino facoltà' di Fisica, via P Giuria 1, 10125 Torino, Italy*
- <sup>104</sup> *Instituto Nazionale di Fisica Nucleare (INFN), Sezione di Trieste, Padriciano 99, I-34012 Trieste (Padriciano), Italy*
- <sup>105</sup> *Inter-University Accelerator Centre, Aruna Asaf Ali Marg, Post Box 10502, New Delhi 110067, India*
- <sup>106</sup> *International Center for Elementary Particle Physics, University of Tokyo, Hongo 7-3-1, Bunkyo District, Tokyo 113-0033, Japan*
- <sup>107</sup> *Iowa State University, Department of Physics, High Energy Physics Group, Ames, IA 50011, USA*
- <sup>108</sup> *Jagiellonian University, Institute of Physics, Ul. Reymonta 4, PL-30-059 Cracow, Poland*

- <sup>109</sup> *Jamia Millia Islamia, Centre for Theoretical Physics, Jamia Nagar, New Delhi 110025, India*
- <sup>110</sup> *Jamia Millia Islamia, Department of Physics, Jamia Nagar, New Delhi 110025, India*
- <sup>111</sup> *Japan Aerospace Exploration Agency, Sagamihara Campus, 3-1-1 Yoshinodai, Sagamihara, Kanagawa 220-8510, Japan*
- <sup>112</sup> *Japan Atomic Energy Agency, 4-49 Muramatsu, Tokai-mura, Naka-gun, Ibaraki 319-1184, Japan*
- <sup>113</sup> *Johannes Gutenberg Universität Mainz, Institut für Physik, 55099 Mainz, Germany*
- <sup>114</sup> *Johns Hopkins University, Applied Physics Laboratory, 11100 Johns Hopkins RD., Laurel, MD 20723-6099, USA*
- <sup>115</sup> *Joint Institute for Nuclear Research (JINR), Joliot-Curie 6, 141980, Dubna, Moscow Region, Russia*
- <sup>116</sup> *Kansas State University, Department of Physics, 116 Cardwell Hall, Manhattan, KS 66506, USA*
- <sup>117</sup> *KCS Corp., 2-7-25 Muramatsukita, Tokai, Ibaraki 319-1108, Japan*
- <sup>118</sup> *Kharkov Institute of Physics and Technology, National Science Center, 1, Akademicheskaya St., Kharkov, 61108, Ukraine*
- <sup>119</sup> *Kinki University, Department of Physics, 3-4-1 Kowakae, Higashi-Osaka, Osaka 577-8502, Japan*
- <sup>120</sup> *Kobe University, Faculty of Science, 1-1 Rokkodai-cho, Nada-ku, Kobe, Hyogo 657-8501, Japan*
- <sup>121</sup> *Kogakuin University, Department of Physics, Shinjuku Campus, 1-24-2 Nishi-Shinjuku, Shinjuku-ku, Tokyo 163-8677, Japan*
- <sup>122</sup> *Konkuk University, 93-1 Mojin-dong, Kwanglin-gu, Seoul 143-701, Korea*
- <sup>123</sup> *Korea Advanced Institute of Science & Technology, Department of Physics, 373-1 Kusong-dong, Yusong-gu, Taejon 305-701, Korea*
- <sup>124</sup> *Korea Institute for Advanced Study (KIAS), School of Physics, 207-43 Cheongryangri-dong, Dongdaemun-gu, Seoul 130-012, Korea*
- <sup>125</sup> *Korea University, Department of Physics, Seoul 136-701, Korea*
- <sup>126</sup> *Kyoto University, Department of Physics, Kitashirakawa-Oiwakecho, Sakyo-ku, Kyoto 606-8502, Japan*
- <sup>127</sup> *L.P.T.A., UMR 5207 CNRS-UM2, Université Montpellier II, Case Courrier 070, Bât. 13, place Eugène Bataillon, 34095 Montpellier Cedex 5, France*
- <sup>128</sup> *Laboratoire d'Annecy-le-Vieux de Physique des Particules (LAPP), Chemin de Bellevue, BP 110, F-74941 Annecy-le-Vieux Cedex, France*
- <sup>129</sup> *Laboratoire d'Annecy-le-Vieux de Physique Theorique (LAPTH), Chemin de Bellevue, BP 110, F-74941 Annecy-le-Vieux Cedex, France*
- <sup>130</sup> *Laboratoire de l'Accélérateur Linéaire (LAL), Université Paris-Sud 11, Bâtiment 200, 91898 Orsay, France*
- <sup>131</sup> *Laboratoire de Physique Corpusculaire de Clermont-Ferrand (LPC), Université Blaise Pascal, I.N.2.P.3./C.N.R.S., 24 avenue des Landais, 63177 Aubière Cedex, France*
- <sup>132</sup> *Laboratoire de Physique Subatomique et de Cosmologie (LPSC), Université Joseph Fourier (Grenoble 1), 53, ave. des Marthyrs, F-38026 Grenoble Cedex, France*
- <sup>133</sup> *Laboratoire de Physique Theorique, Université de Paris-Sud XI, Batiment 210, F-91405 Orsay Cedex, France*
- <sup>134</sup> *Laboratori Nazionali di Frascati, via E. Fermi, 40, C.P. 13, I-00044 Frascati, Italy*

- <sup>135</sup> *Laboratory of High Energy Physics and Cosmology, Department of Physics, Hanoi National University, 334 Nguyen Trai, Hanoi, Vietnam*
- <sup>136</sup> *Lancaster University, Physics Department, Lancaster LA1 4YB, UK*
- <sup>137</sup> *Lawrence Berkeley National Laboratory (LBNL), 1 Cyclotron Rd, Berkeley, CA 94720, USA*
- <sup>138</sup> *Lawrence Livermore National Laboratory (LLNL), Livermore, CA 94551, USA*
- <sup>139</sup> *Lebedev Physical Institute, Leninsky Prospect 53, RU-117924 Moscow, Russia*
- <sup>140</sup> *Liaoning Normal University, Department of Physics, Dalian, China 116029*
- <sup>141</sup> *Lomonosov Moscow State University, Skobeltsyn Institute of Nuclear Physics (MSU SINP), 1(2), Leninskie gory, GSP-1, Moscow 119991, Russia*
- <sup>142</sup> *Los Alamos National Laboratory (LANL), P.O.Box 1663, Los Alamos, NM 87545, USA*
- <sup>143</sup> *Louisiana Technical University, Department of Physics, Ruston, LA 71272, USA*
- <sup>144</sup> *Ludwig-Maximilians-Universität München, Department für Physik, Schellingstr. 4, D-80799 Munich, Germany*
- <sup>145</sup> *Lunds Universitet, Fysiska Institutionen, Avdelningen för Experimentell Högenergifysik, Box 118, 221 00 Lund, Sweden*
- <sup>146</sup> *Massachusetts Institute of Technology, Laboratory for Nuclear Science & Center for Theoretical Physics, 77 Massachusetts Ave., NW16, Cambridge, MA 02139, USA*
- <sup>147</sup> *Max-Planck-Institut für Physik (Werner-Heisenberg-Institut), Föhringer Ring 6, 80805 München, Germany*
- <sup>148</sup> *McGill University, Department of Physics, Ernest Rutherford Physics Bldg., 3600 University Ave., Montreal, Quebec, H3A 2T8 Canada*
- <sup>149</sup> *Meiji Gakuin University, Department of Physics, 2-37 Shirokanedai 1-chome, Minato-ku, Tokyo 244-8539, Japan*
- <sup>150</sup> *Michigan State University, Department of Physics and Astronomy, East Lansing, MI 48824, USA*
- <sup>151</sup> *Middle East Technical University, Department of Physics, TR-06531 Ankara, Turkey*
- <sup>152</sup> *Mindanao Polytechnic State College, Lapasan, Cagayan de Oro City 9000, Phillipines*
- <sup>153</sup> *MSU-Iligan Institute of Technology, Department of Physics, Andres Bonifacio Avenue, 9200 Iligan City, Phillipines*
- <sup>154</sup> *Nagasaki Institute of Applied Science, 536 Abamachi, Nagasaki-Shi, Nagasaki 851-0193, Japan*
- <sup>155</sup> *Nagoya University, Fundamental Particle Physics Laboratory, Division of Particle and Astrophysical Sciences, Furo-cho, Chikusa-ku, Nagoya, Aichi 464-8602, Japan*
- <sup>156</sup> *Nanchang University, Department of Physics, Nanchang, China 330031*
- <sup>157</sup> *Nanjing University, Department of Physics, Nanjing, China 210093*
- <sup>158</sup> *Nankai University, Department of Physics, Tianjin, China 300071*
- <sup>159</sup> *National Central University, High Energy Group, Department of Physics, Chung-li, Taiwan 32001*
- <sup>160</sup> *National Institute for Nuclear & High Energy Physics, PO Box 41882, 1009 DB Amsterdam, Netherlands*
- <sup>161</sup> *National Institute of Radiological Sciences, 4-9-1 Anagawa, Inaga, Chiba 263-8555, Japan*
- <sup>162</sup> *National Synchrotron Radiation Laboratory, University of Science and Technology of china, Hefei, Anhui, China 230029*
- <sup>163</sup> *National Synchrotron Research Center, 101 Hsin-Ann Rd., Hsinchu Science Part, Hsinchu, Taiwan 30076*

- <sup>164</sup> National Taiwan University, Physics Department, Taipei, Taiwan 106
- <sup>165</sup> Niels Bohr Institute (NBI), University of Copenhagen, Blegdamsvej 17, DK-2100 Copenhagen, Denmark
- <sup>166</sup> Niigata University, Department of Physics, Ikarashi, Niigata 950-218, Japan
- <sup>167</sup> Nikken Sekkai Ltd., 2-18-3 Iidabashi, Chiyoda-Ku, Tokyo 102-8117, Japan
- <sup>168</sup> Nippon Dental University, 1-9-20 Fujimi, Chiyoda-Ku, Tokyo 102-8159, Japan
- <sup>169</sup> North Asia University, Akita 010-8515, Japan
- <sup>170</sup> North Eastern Hill University, Department of Physics, Shillong 793022, India
- <sup>171</sup> Northern Illinois University, Department of Physics, DeKalb, Illinois 60115-2825, USA
- <sup>172</sup> Northwestern University, Department of Physics and Astronomy, 2145 Sheridan Road., Evanston, IL 60208, USA
- <sup>173</sup> Novosibirsk State University (NGU), Department of Physics, Pirogov st. 2, 630090 Novosibirsk, Russia
- <sup>174</sup> Obninsk State Technical University for Nuclear Engineering (IATE), Obninsk, Russia
- <sup>175</sup> Ochanomizu University, Department of Physics, Faculty of Science, 1-1 Otsuka 2, Bunkyo-ku, Tokyo 112-8610, Japan
- <sup>176</sup> Osaka University, Laboratory of Nuclear Studies, 1-1 Machikaneyama, Toyonaka, Osaka 560-0043, Japan
- <sup>177</sup> Österreichische Akademie der Wissenschaften, Institut für Hochenergiephysik, Nikolsdorfergasse 18, A-1050 Vienna, Austria
- <sup>178</sup> Panjab University, Chandigarh 160014, India
- <sup>179</sup> Pavel Sukhoi Gomel State Technical University, ICTP Affiliated Centre & Laboratory for Physical Studies, October Avenue, 48, 246746, Gomel, Belarus
- <sup>180</sup> Pavel Sukhoi Gomel State Technical University, Physics Department, October Ave. 48, 246746 Gomel, Belarus
- <sup>181</sup> Physical Research Laboratory, Navrangpura, Ahmedabad 380 009, Gujarat, India
- <sup>182</sup> Pohang Accelerator Laboratory (PAL), San-31 Hyoja-dong, Nam-gu, Pohang, Gyeongbuk 790-784, Korea
- <sup>183</sup> Polish Academy of Sciences (PAS), Institute of Physics, Al. Lotnikow 32/46, PL-02-668 Warsaw, Poland
- <sup>184</sup> Primera Engineers Ltd., 100 S Wacker Drive, Suite 700, Chicago, IL 60606, USA
- <sup>185</sup> Princeton University, Department of Physics, P.O. Box 708, Princeton, NJ 08542-0708, USA
- <sup>186</sup> Purdue University, Department of Physics, West Lafayette, IN 47907, USA
- <sup>187</sup> Pusan National University, Department of Physics, Busan 609-735, Korea
- <sup>188</sup> R. W. Downing Inc., 6590 W. Box Canyon Dr., Tucson, AZ 85745, USA
- <sup>189</sup> Raja Ramanna Center for Advanced Technology, Indore 452013, India
- <sup>190</sup> Rheinisch-Westfälische Technische Hochschule (RWTH), Physikalisches Institut, Physikzentrum, Sommerfeldstrasse 14, D-52056 Aachen, Germany
- <sup>191</sup> RIKEN, 2-1 Hirosawa, Wako, Saitama 351-0198, Japan
- <sup>192</sup> Royal Holloway, University of London (RHUL), Department of Physics, Egham, Surrey TW20 0EX, UK
- <sup>193</sup> Saga University, Department of Physics, 1 Honjo-machi, Saga-shi, Saga 840-8502, Japan
- <sup>194</sup> Saha Institute of Nuclear Physics, 1/AF Bidhan Nagar, Kolkata 700064, India
- <sup>195</sup> Salalah College of Technology (SCOT), Engineering Department, Post Box No. 608, Postal Code 211, Salalah, Sultanate of Oman
- <sup>196</sup> Saube Co., Hanabatake, Tsukuba, Ibaraki 300-3261, Japan

- <sup>197</sup> Seoul National University, San 56-1, Shinrim-dong, Kwanak-gu, Seoul 151-742, Korea
- <sup>198</sup> Shandong University, 27 Shanda Nanlu, Jinan, China 250100
- <sup>199</sup> Shanghai Institute of Applied Physics, Chinese Academy of Sciences, 2019 Jiaruo Rd.,  
Jiading, Shanghai, China 201800
- <sup>200</sup> Shinshu University, 3-1-1, Asahi, Matsumoto, Nagano 390-8621, Japan
- <sup>201</sup> Sobolev Institute of Mathematics, Siberian Branch of the Russian Academy of Sciences,  
4 Acad. Koptyug Avenue, 630090 Novosibirsk, Russia
- <sup>202</sup> Sokenai, The Graduate University for Advanced Studies, Shonan Village, Hayama,  
Kanagawa 240-0193, Japan
- <sup>203</sup> Stanford Linear Accelerator Center (SLAC), 2575 Sand Hill Road, Menlo Park, CA  
94025, USA
- <sup>204</sup> State University of New York at Binghamton, Department of Physics, PO Box 6016,  
Binghamton, NY 13902, USA
- <sup>205</sup> State University of New York at Buffalo, Department of Physics & Astronomy, 239  
Franczak Hall, Buffalo, NY 14260, USA
- <sup>206</sup> State University of New York at Stony Brook, Department of Physics and Astronomy,  
Stony Brook, NY 11794-3800, USA
- <sup>207</sup> Sumitomo Heavy Industries, Ltd., Natsushima-cho, Yokosuka, Kanagawa 237-8555,  
Japan
- <sup>208</sup> Sungkyunkwan University (SKKU), Natural Science Campus 300, Physics Research  
Division, Chunchun-dong, Jangan-gu, Suwon, Kyunggi-do 440-746, Korea
- <sup>209</sup> Swiss Light Source (SLS), Paul Scherrer Institut (PSI), PSI West, CH-5232 Villigen  
PSI, Switzerland
- <sup>210</sup> Syracuse University, Department of Physics, 201 Physics Building, Syracuse, NY  
13244-1130, USA
- <sup>211</sup> Tata Institute of Fundamental Research, School of Natural Sciences, Homi Bhabha Rd.,  
Mumbai 400005, India
- <sup>212</sup> Technical Institute of Physics and Chemistry, Chinese Academy of Sciences, 2 North 1st  
St., Zhongguancun, Beijing, China 100080
- <sup>213</sup> Technical University of Lodz, Department of Microelectronics and Computer Science, al.  
Politechniki 11, 90-924 Lodz, Poland
- <sup>214</sup> Technische Universität Dresden, Institut für Kern- und Teilchenphysik, D-01069  
Dresden, Germany
- <sup>215</sup> Technische Universität Dresden, Institut für Theoretische Physik, D-01062 Dresden,  
Germany
- <sup>216</sup> Tel-Aviv University, School of Physics and Astronomy, Ramat Aviv, Tel Aviv 69978,  
Israel
- <sup>217</sup> Texas A&M University, Physics Department, College Station, 77843-4242 TX, USA
- <sup>218</sup> Texas Tech University, Department of Physics, Campus Box 41051, Lubbock, TX  
79409-1051, USA
- <sup>219</sup> The Henryk Niewodniczanski Institute of Nuclear Physics (NINP), High Energy Physics  
Lab, ul. Radzikowskiego 152, PL-31342 Cracow, Poland
- <sup>220</sup> Thomas Jefferson National Accelerator Facility (TJNAF), 12000 Jefferson Avenue,  
Newport News, VA 23606, USA
- <sup>221</sup> Tohoku Gakuin University, Faculty of Technology, 1-13-1 Chuo, Tagajo, Miyagi  
985-8537, Japan

- <sup>222</sup> Tohoku University, Department of Physics, Aoba District, Sendai, Miyagi 980-8578, Japan
- <sup>223</sup> Tokyo Management College, Computer Science Lab, Ichikawa, Chiba 272-0001, Japan
- <sup>224</sup> Tokyo University of Agriculture Technology, Department of Applied Physics, Naka-machi, Koganei, Tokyo 183-8488, Japan
- <sup>225</sup> Toyama University, Department of Physics, 3190 Gofuku, Toyama-shi 930-8588, Japan
- <sup>226</sup> TRIUMF, 4004 Wesbrook Mall, Vancouver, BC V6T 2A3, Canada
- <sup>227</sup> Tufts University, Department of Physics and Astronomy, Robinson Hall, Medford, MA 02155, USA
- <sup>228</sup> Universidad Autònoma de Madrid (UAM), Facultad de Ciencias C-XI, Departamento de Física Teórica, Cantoblanco, Madrid 28049, Spain
- <sup>229</sup> Universitat Autònoma de Barcelona, Institut de Física d'Altes Energies (IFAE), Campus UAB, Edifici Cn, E-08193 Bellaterra, Barcelona, Spain
- <sup>230</sup> University College of London (UCL), High Energy Physics Group, Physics and Astronomy Department, Gower Street, London WC1E 6BT, UK
- <sup>231</sup> University College, National University of Ireland (Dublin), Department of Experimental Physics, Science Buildings, Belfield, Dublin 4, Ireland
- <sup>232</sup> University de Barcelona, Facultat de Física, Av. Diagonal, 647, Barcelona 08028, Spain
- <sup>233</sup> University of Abertay Dundee, Department of Physics, Bell St, Dundee, DD1 1HG, UK
- <sup>234</sup> University of Auckland, Department of Physics, Private Bag, Auckland 1, New Zealand
- <sup>235</sup> University of Bergen, Institute of Physics, Allegaten 55, N-5007 Bergen, Norway
- <sup>236</sup> University of Birmingham, School of Physics and Astronomy, Particle Physics Group, Edgbaston, Birmingham B15 2TT, UK
- <sup>237</sup> University of Bristol, H. H. Wills Physics Lab, Tyndall Ave., Bristol BS8 1TL, UK
- <sup>238</sup> University of British Columbia, Department of Physics and Astronomy, 6224 Agricultural Rd., Vancouver, BC V6T 1Z1, Canada
- <sup>239</sup> University of California Berkeley, Department of Physics, 366 Le Conte Hall, #7300, Berkeley, CA 94720, USA
- <sup>240</sup> University of California Davis, Department of Physics, One Shields Avenue, Davis, CA 95616-8677, USA
- <sup>241</sup> University of California Irvine, Department of Physics and Astronomy, High Energy Group, 4129 Frederick Reines Hall, Irvine, CA 92697-4575 USA
- <sup>242</sup> University of California Riverside, Department of Physics, Riverside, CA 92521, USA
- <sup>243</sup> University of California Santa Barbara, Department of Physics, Broida Hall, Mail Code 9530, Santa Barbara, CA 93106-9530, USA
- <sup>244</sup> University of California Santa Cruz, Department of Astronomy and Astrophysics, 1156 High Street, Santa Cruz, CA 05060, USA
- <sup>245</sup> University of California Santa Cruz, Institute for Particle Physics, 1156 High Street, Santa Cruz, CA 95064, USA
- <sup>246</sup> University of Cambridge, Cavendish Laboratory, J J Thomson Avenue, Cambridge CB3 0HE, UK
- <sup>247</sup> University of Colorado at Boulder, Department of Physics, 390 UCB, University of Colorado, Boulder, CO 80309-0390, USA
- <sup>248</sup> University of Delhi, Department of Physics and Astrophysics, Delhi 110007, India
- <sup>249</sup> University of Delhi, S.G.T.B. Khalsa College, Delhi 110007, India
- <sup>250</sup> University of Dundee, Department of Physics, Nethergate, Dundee, DD1 4HN, Scotland, UK

- <sup>251</sup> University of Edinburgh, School of Physics, James Clerk Maxwell Building, The King's Buildings, Mayfield Road, Edinburgh EH9 3JZ, UK
- <sup>252</sup> University of Essex, Department of Physics, Wivenhoe Park, Colchester CO4 3SQ, UK
- <sup>253</sup> University of Florida, Department of Physics, Gainesville, FL 32611, USA
- <sup>254</sup> University of Glasgow, Department of Physics & Astronomy, University Avenue, Glasgow G12 8QQ, Scotland, UK
- <sup>255</sup> University of Hamburg, Physics Department, Institut für Experimentalphysik, Luruper Chaussee 149, 22761 Hamburg, Germany
- <sup>256</sup> University of Hawaii, Department of Physics and Astronomy, HEP, 2505 Correa Rd., WAT 232, Honolulu, HI 96822-2219, USA
- <sup>257</sup> University of Heidelberg, Kirchhoff Institute of Physics, Albert Überle Strasse 3-5, DE-69120 Heidelberg, Germany
- <sup>258</sup> University of Helsinki, Department of Physical Sciences, P.O. Box 64 (Vaino Auerin katu 11), FIN-00014, Helsinki, Finland
- <sup>259</sup> University of Hyogo, School of Science, Kouto 3-2-1, Kamigori, Ako, Hyogo 678-1297, Japan
- <sup>260</sup> University of Illinois at Urbana-Champaign, Department of Phys., High Energy Physics, 441 Loomis Lab. of Physics 1110 W. Green St., Urbana, IL 61801-3080, USA
- <sup>261</sup> University of Iowa, Department of Physics and Astronomy, 203 Van Allen Hall, Iowa City, IA 52242-1479, USA
- <sup>262</sup> University of Kansas, Department of Physics and Astronomy, Malott Hall, 1251 Wescoe Hall Drive, Room 1082, Lawrence, KS 66045-7582, USA
- <sup>263</sup> University of Liverpool, Department of Physics, Oliver Lodge Lab, Oxford St., Liverpool L69 7ZE, UK
- <sup>264</sup> University of Louisville, Department of Physics, Louisville, KY 40292, USA
- <sup>265</sup> University of Manchester, School of Physics and Astronomy, Schuster Lab, Manchester M13 9PL, UK
- <sup>266</sup> University of Maryland, Department of Physics and Astronomy, Physics Building (Bldg. 082), College Park, MD 20742, USA
- <sup>267</sup> University of Melbourne, School of Physics, Victoria 3010, Australia
- <sup>268</sup> University of Michigan, Department of Physics, 500 E. University Ave., Ann Arbor, MI 48109-1120, USA
- <sup>269</sup> University of Minnesota, 148 Tate Laboratory Of Physics, 116 Church St. S.E., Minneapolis, MN 55455, USA
- <sup>270</sup> University of Mississippi, Department of Physics and Astronomy, 108 Lewis Hall, PO Box 1848, Oxford, Mississippi 38677-1848, USA
- <sup>271</sup> University of Montenegro, Faculty of Sciences and Math., Department of Phys., P.O. Box 211, 81001 Podgorica, Serbia and Montenegro
- <sup>272</sup> University of New Mexico, New Mexico Center for Particle Physics, Department of Physics and Astronomy, 800 Yale Boulevard N.E., Albuquerque, NM 87131, USA
- <sup>273</sup> University of Notre Dame, Department of Physics, 225 Nieuwland Science Hall, Notre Dame, IN 46556, USA
- <sup>274</sup> University of Oklahoma, Department of Physics and Astronomy, Norman, OK 73071, USA
- <sup>275</sup> University of Oregon, Department of Physics, 1371 E. 13th Ave., Eugene, OR 97403, USA



- <sup>276</sup> *University of Oxford, Particle Physics Department, Denys Wilkinson Bldg., Keble Road, Oxford OX1 3RH England, UK*
- <sup>277</sup> *University of Patras, Department of Physics, GR-26100 Patras, Greece*
- <sup>278</sup> *University of Pavia, Department of Nuclear and Theoretical Physics, via Bassi 6, I-27100 Pavia, Italy*
- <sup>279</sup> *University of Pennsylvania, Department of Physics and Astronomy, 209 South 33rd Street, Philadelphia, PA 19104-6396, USA*
- <sup>280</sup> *University of Puerto Rico at Mayaguez, Department of Physics, P.O. Box 9016, Mayaguez, 00681-9016 Puerto Rico*
- <sup>281</sup> *University of Regina, Department of Physics, Regina, Saskatchewan, S4S 0A2 Canada*
- <sup>282</sup> *University of Rochester, Department of Physics and Astronomy, Bausch & Lomb Hall, P.O. Box 270171, 600 Wilson Boulevard, Rochester, NY 14627-0171 USA*
- <sup>283</sup> *University of Science and Technology of China, Department of Modern Physics (DMP), Jin Zhai Road 96, Hefei, China 230026*
- <sup>284</sup> *University of Silesia, Institute of Physics, Ul. Uniwersytecka 4, PL-40007 Katowice, Poland*
- <sup>285</sup> *University of Southampton, School of Physics and Astronomy, Highfield, Southampton S017 1BJ, England, UK*
- <sup>286</sup> *University of Strathclyde, Physics Department, John Anderson Building, 107 Rottenrow, Glasgow, G4 0NG, Scotland, UK*
- <sup>287</sup> *University of Sydney, Falkiner High Energy Physics Group, School of Physics, A28, Sydney, NSW 2006, Australia*
- <sup>288</sup> *University of Texas, Center for Accelerator Science and Technology, Arlington, TX 76019, USA*
- <sup>289</sup> *University of Tokushima, Institute of Theoretical Physics, Tokushima-shi 770-8502, Japan*
- <sup>290</sup> *University of Tokyo, Department of Physics, 7-3-1 Hongo, Bunkyo District, Tokyo 113-0033, Japan*
- <sup>291</sup> *University of Toronto, Department of Physics, 60 St. George St., Toronto M5S 1A7, Ontario, Canada*
- <sup>292</sup> *University of Tsukuba, Institute of Physics, 1-1-1 Ten'nodai, Tsukuba, Ibaraki 305-8571, Japan*
- <sup>293</sup> *University of Victoria, Department of Physics and Astronomy, P.O.Box 3055 Stn Csc, Victoria, BC V8W 3P6, Canada*
- <sup>294</sup> *University of Warsaw, Institute of Physics, Ul. Hoza 69, PL-00 681 Warsaw, Poland*
- <sup>295</sup> *University of Warsaw, Institute of Theoretical Physics, Ul. Hoza 69, PL-00 681 Warsaw, Poland*
- <sup>296</sup> *University of Washington, Department of Physics, PO Box 351560, Seattle, WA 98195-1560, USA*
- <sup>297</sup> *University of Wisconsin, Physics Department, Madison, WI 53706-1390, USA*
- <sup>298</sup> *University of Wuppertal, Gaußstraße 20, D-42119 Wuppertal, Germany*
- <sup>299</sup> *Université Claude Bernard Lyon-I, Institut de Physique Nucléaire de Lyon (IPNL), 4, rue Enrico Fermi, F-69622 Villeurbanne Cedex, France*
- <sup>300</sup> *Université de Genève, Section de Physique, 24, quai E. Ansermet, 1211 Genève 4, Switzerland*
- <sup>301</sup> *Université Louis Pasteur (Strasbourg I), UFR de Sciences Physiques, 3-5 Rue de l'Université, F-67084 Strasbourg Cedex, France*

- <sup>302</sup> *Université Pierre et Marie Curie (Paris VI-VII) (6-7) (UPMC), Laboratoire de Physique Nucléaire et de Hautes Energies (LPNHE), 4 place Jussieu, Tour 33, Rez de chaussée, 75252 Paris Cedex 05, France*
- <sup>303</sup> *Universität Bonn, Physikalisches Institut, Nußallee 12, 53115 Bonn, Germany*
- <sup>304</sup> *Universität Karlsruhe, Institut für Physik, Postfach 6980, Kaiserstrasse 12, D-76128 Karlsruhe, Germany*
- <sup>305</sup> *Universität Rostock, Fachbereich Physik, Universitätsplatz 3, D-18051 Rostock, Germany*
- <sup>306</sup> *Universität Siegen, Fachbereich für Physik, Emmy Noether Campus, Walter-Flex-Str.3, D-57068 Siegen, Germany*
- <sup>307</sup> *Università de Bergamo, Dipartimento di Fisica, via Salvecchio, 19, I-24100 Bergamo, Italy*
- <sup>308</sup> *Università degli Studi di Roma La Sapienza, Dipartimento di Fisica, Istituto Nazionale di Fisica Nucleare, Piazzale Aldo Moro 2, I-00185 Rome, Italy*
- <sup>309</sup> *Università degli Studi di Trieste, Dipartimento di Fisica, via A. Valerio 2, I-34127 Trieste, Italy*
- <sup>310</sup> *Università degli Studi di “Roma Tre”, Dipartimento di Fisica “Edoardo Amaldi”, Istituto Nazionale di Fisica Nucleare, Via della Vasca Navale 84, 00146 Roma, Italy*
- <sup>311</sup> *Università dell’Insubria in Como, Dipartimento di Scienze CC.FF.MM., via Vallegio 11, I-22100 Como, Italy*
- <sup>312</sup> *Università di Pisa, Dipartimento di Fisica ‘Enrico Fermi’, Largo Bruno Pontecorvo 3, I-56127 Pisa, Italy*
- <sup>313</sup> *Università di Salento, Dipartimento di Fisica, via Arnesano, C.P. 193, I-73100 Lecce, Italy*
- <sup>314</sup> *Università di Udine, Dipartimento di Fisica, via delle Scienze, 208, I-33100 Udine, Italy*
- <sup>315</sup> *Variable Energy Cyclotron Centre, 1/AF, Bidhan Nagar, Kolkata 700064, India*
- <sup>316</sup> *VINCA Institute of Nuclear Sciences, Laboratory of Physics, PO Box 522, YU-11001 Belgrade, Serbia and Montenegro*
- <sup>317</sup> *Vinh University, 182 Le Duan, Vinh City, Nghe An Province, Vietnam*
- <sup>318</sup> *Virginia Polytechnic Institute and State University, Physics Department, Blacksburg, VA 2406, USA*
- <sup>319</sup> *Visva-Bharati University, Department of Physics, Santiniketan 731235, India*
- <sup>320</sup> *Waseda University, Advanced Research Institute for Science and Engineering, Shinjuku, Tokyo 169-8555, Japan*
- <sup>321</sup> *Wayne State University, Department of Physics, Detroit, MI 48202, USA*
- <sup>322</sup> *Weizmann Institute of Science, Department of Particle Physics, P.O. Box 26, Rehovot 76100, Israel*
- <sup>323</sup> *Yale University, Department of Physics, New Haven, CT 06520, USA*
- <sup>324</sup> *Yonsei University, Department of Physics, 134 Sinchon-dong, Sudaemoon-gu, Seoul 120-749, Korea*
- <sup>325</sup> *Zhejiang University, College of Science, Department of Physics, Hangzhou, China 310027*  
\* deceased

# Acknowledgements

We would like to acknowledge the support and guidance of the International Committee on Future Accelerators (ICFA), chaired by A. Wagner of DESY, and the International Linear Collider Steering Committee (ILCSC), chaired by S. Kurokawa of KEK, who established the ILC Global Design Effort, as well as the World Wide Study of the Physics and Detectors.

We are grateful to the ILC Machine Advisory Committee (MAC), chaired by F. Willeke of DESY and the International ILC Cost Review Committee, chaired by L. Evans of CERN, for their advice on the ILC Reference Design. We also thank the consultants who participated in the Conventional Facilities Review at CalTech and in the RDR Cost Review at SLAC.

We would like to thank the directors of the institutions who have hosted ILC meetings: KEK, ANL/FNAL/SLAC/U. Colorado (Snowmass), INFN/Frascati, IIT/Bangalore, TRIUMF/U. British Columbia, U. Valencia, IHEP/Beijing and DESY.

We are grateful for the support of the Funding Agencies for Large Colliders (FALC), chaired by R. Petronzio of INFN, and we thank all of the international, regional and national funding agencies whose generous support has made the ILC Reference Design possible.

Each of the GDE regional teams in the Americas, Asia and Europe are grateful for the support of their local scientific societies, industrial forums, advisory committees and reviewers.



# CONTENTS

|          |   |           |
|----------|---|-----------|
| <b>1</b> | <b>Physics at a Terascale <math>e^+e^-</math> Linear Collider</b> | <b>1</b>  |
| 1.1      | Questions about the Universe . . . . .                            | 1         |
| 1.2      | The New Landscape of Particle Physics . . . . .                   | 3         |
| 1.3      | Precision Requirements for ILC . . . . .                          | 5         |
| 1.4      | Specifying Machine Parameters . . . . .                           | 5         |
| <b>2</b> | <b>The ILC Accelerator</b>  | <b>7</b>  |
| 2.1      | Superconducting RF . . . . .                                      | 8         |
| 2.2      | The ILC Baseline Design . . . . .                                 | 11        |
| 2.2.1    | Beam Parameters . . . . .   | 11        |
| 2.2.2    | Electron Source . . . . .   | 14        |
| 2.2.3    | Positron Source . . . . .   | 14        |
| 2.2.4    | Damping Rings . . . . .   | 16        |
| 2.2.5    | Ring to Main Linac (RTML) . . . . .                               | 17        |
| 2.2.6    | Main Linacs . . . . .   | 18        |
| 2.2.7    | Beam Delivery System . . . . .                                    | 20        |
| 2.3      | Sample Sites . . . . .  | 22        |
| <b>3</b> | <b>Detectors</b>  | <b>25</b> |
| 3.1      | Challenges for Detector Design and Technology . . . . .           | 25        |
| 3.2      | Detector Concepts . . . . .                                       | 27        |
| 3.2.1    | The Silicon Detector (SiD) Concept . . . . .                      | 28        |
| 3.2.2    | The Large Detector Concept (LDC) . . . . .                        | 29        |
| 3.2.3    | The GLD Concept . . . . .   | 30        |
| 3.2.4    | Fourth Concept (“4 <sup>th</sup> ”) Detector . . . . .            | 31        |
| 3.3      | Detector and Physics Performance . . . . .                        | 32        |
| 3.4      | Interfacing the Detector to the Machine . . . . .                 | 34        |
| <b>4</b> | <b>Value Estimates</b>  | <b>35</b> |
| 4.1      | The Accelerator . . . . .   | 35        |
| 4.2      | The Detectors . . . . .   | 36        |
| <b>5</b> | <b>Next Steps: R&amp;D and the Engineering Design Phase</b>       | <b>37</b> |
| 5.1      | Accelerator R&D . . . . .   | 37        |
| 5.2      | The Detector Roadmap: R&D and Engineering Designs . . . . .       | 39        |
| 5.3      | Towards the Engineering Design Report (EDR) . . . . .             | 39        |

## CONTENTS

|                        |           |
|------------------------|-----------|
| <b>Bibliography</b>    | <b>41</b> |
| <b>List of figures</b> | <b>45</b> |
| <b>List of tables</b>  | <b>47</b> |

# CHAPTER 1

## Physics at a Terascale $e^+e^-$ Linear Collider

### 1.1 QUESTIONS ABOUT THE UNIVERSE

- *What is the universe? How did it begin?*
- *What are matter and energy? What are space and time?*

These basic questions have been the subject of scientific theories and experiments throughout human history. The answers have revolutionized the enlightened view of the world, transforming society and advancing civilization. Universal laws and principles govern everyday phenomena, some of them manifesting themselves only at scales of time and distance far beyond everyday experience. Particle physics experiments using particle accelerators transform matter and energy, to reveal the basic workings of the universe. Other experiments exploit naturally occurring particles, such as solar neutrinos or cosmic rays, and astrophysical observations, to provide additional insights.

The triumph of 20th century particle physics was the development of the Standard Model. Experiments determined the particle constituents of ordinary matter, and identified four forces binding matter and transforming it from one form to another. This success leads particle physicists to address even more fundamental questions, and explore deeper mysteries in science. The scope of these questions is illustrated by the summary from the report *Quantum Universe*[1]:

1. *Are there undiscovered principles of nature?*
2. *How can we solve the mystery of dark energy?*
3. *Are there extra dimensions of space?*
4. *Do all the forces become one?*
5. *Why are there so many particles?*
6. *What is dark matter? How can we make it in the laboratory?*
7. *What are neutrinos telling us?*
8. *How did the universe begin?*
9. *What happened to the antimatter?*

## PHYSICS AT A TERASCALE $E^+E^-$ LINEAR COLLIDER

A worldwide particle physics program explores this fascinating scientific landscape. The International Linear Collider (ILC)[2] is expected to play a central role in an era of revolutionary advances[3] with breakthrough impact on many of these fundamental questions.

The Standard Model includes a third component beyond particles and forces that has not yet been verified, the Higgs mechanism that gives mass to the particles. Many scientific opportunities for the ILC involve the Higgs particle and related new phenomena at Terascale energies. The Standard Model Higgs field permeates the universe, giving mass to elementary particles, and breaking a fundamental electroweak force into two, the electromagnetic and weak forces (Figure 1.1). But quantum effects should destabilize the Higgs of the Standard Model, preventing its operation at Terascale energies. The proposed antidotes for this quantum instability mostly involve dramatic phenomena accessible to the ILC: new forces, a new principle of nature called supersymmetry, or even extra dimensions of space.

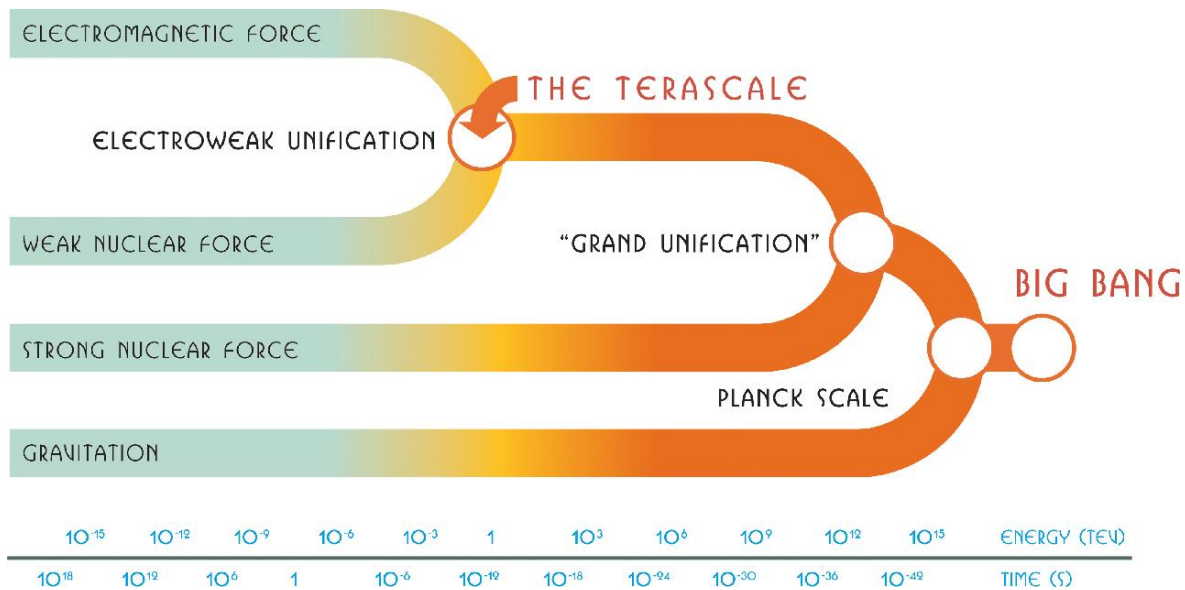


FIGURE 1.1. The electromagnetic and weak nuclear forces unify at the Terascale. The ILC will test unification at even high energy scales (from *Discovering the Quantum Universe*).

Thus the Higgs is central to a broad program of discovery. Is there really a Higgs? Or are there other mechanisms that give mass to particles and break the electroweak force? If there is a Higgs, does it differ from the Standard Model? Is there more than one Higgs particle? What new phenomena stabilize the Higgs at the Terascale?

Astrophysical data show that dark matter dominates the matter content of the universe, and cannot be explained by known particles. Dark matter may be comprised of new weakly interacting particles with Terascale masses. If such Terascale dark matter exists, experiments at the ILC should produce and study such particles, raising important questions (Figure 1.1). Do these new particles have all the properties of the dark matter? Can they alone account for all of the dark matter? How would they affect the evolution of the universe? How do they connect to new principles or forces of nature?

ILC experiments could test the idea that fundamental forces originate from a single “grand” unified force, and search for evidence of a related unified origin of matter involving



supersymmetry. They could distinguish among patterns of phenomena to judge different unification models, providing a telescopic view of the ultimate unification.

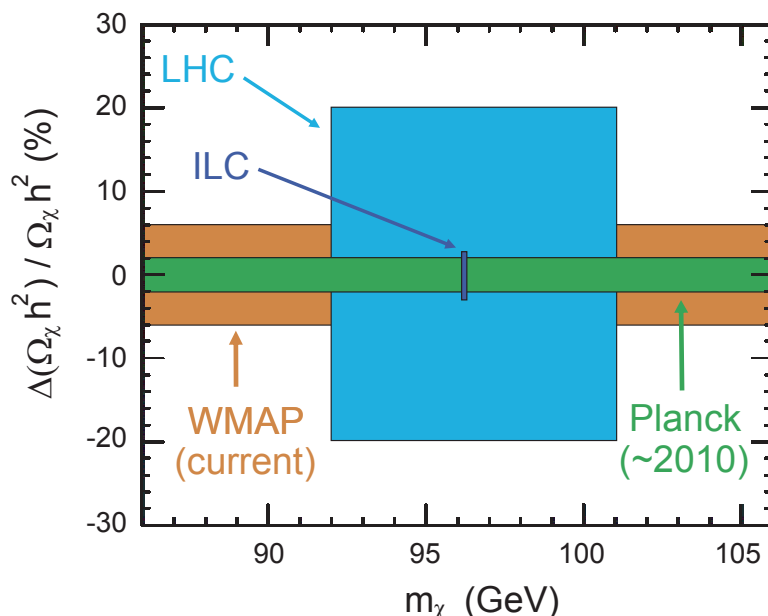


FIGURE 1.2. Accuracy of relic density ( $\Omega_\chi h^2$ ) and mass determinations for neutralino dark matter. Comparison of the LHC and ILC data with that of the WMAP and Planck satellites test neutralinos as the dark matter. (ALCPG Cosmology Subgroup, from chapter 7, volume 2: Physics at the ILC, ILC Reference Design Report)

## 1.2 THE NEW LANDSCAPE OF PARTICLE PHYSICS

During the next few years, experiments at CERN's Large Hadron Collider will have the first direct look at Terascale physics. While those results are unpredictable [4], they could considerably enhance the physics case for the ILC. Possible discoveries include the Higgs particle, a recurrence of the Z boson (the Z'), evidence for extra dimensions, or observation of supersymmetry (SUSY) particles. Like the discovery of an uncharted continent, exploration of the Terascale could transform forever the geography of our universe. Equally compelling will be the interplay of LHC discoveries with other experiments and observations. Particle physics should be entering a new era of intellectual ferment and revolutionary advance.

If there is a Higgs boson, it is almost certain to be found at the LHC and its mass measured by the ATLAS and CMS experiments. If there is a multiplet of Higgs bosons, there is a good chance the LHC experiments will see more than one. However it will be difficult for the LHC to measure the spin and parity of the Higgs particle and thus to establish its essential nature; the ILC can make these measurements accurately. If there is more than one decay channel of the Higgs, the LHC experiments will determine the ratio of branching fractions (roughly 7-30%); the ILC will measure these couplings to quarks and vector bosons at the few percent level, and thus reveal whether the Higgs is the simple Standard Model object, or something more complex.

This first look at Terascale physics by the LHC can have three possible outcomes. The first possibility is that a Higgs boson consistent with Standard Model properties has been found. Then the ILC will be able to make a more complete and precise experimental analysis to verify if it is indeed Standard Model or something else. The second possibility is that a Higgs boson is found with gross features at variance with the Standard Model. Such discrepancies might be a Higgs mass significantly above Standard Model expectations, a large deviation in the predicted pattern of Higgs decay, or the discovery of multiple Higgs particles. The ILC measurements of couplings and quantum numbers will point to the new physics at work. The third possibility is that no Higgs boson is seen. In this case, the ILC precision measurements of top quark, Z and W boson properties will point the way to an alternate theory. In all cases, the ILC will be essential to a full understanding of the Higgs and its relation to other new fundamental phenomena.

The ATLAS and CMS experiments at LHC will have impressive capabilities to discover new heavy particles. They could detect a new  $Z'$  gauge boson as heavy as 5 TeV[5], or squarks and gluinos of supersymmetry up to 2.5 TeV[4]. New particles with mass up to a few TeV associated with the existence of extra spatial dimensions could be seen[4]. The discovery of a  $Z'$  particle would indicate a new fundamental force of nature. The question would be to deduce the properties of this force, its origins, its relation to the other forces in a unified framework, and its role in the earliest moments of the universe. The ILC would play a definitive role in addressing these questions.

If supersymmetry is responsible for stabilizing the electroweak unification at the Terascale and for providing a light Higgs boson, signals of superpartner particles should be seen at the LHC. But are the new heavy particles actually superpartners, with the right spins and couplings? Is supersymmetry related to unification at a higher energy scale? What was its role in our cosmic origins? Definitive answers to these questions will require precise measurements of the superpartner particles and the Higgs particles. This will require the best possible results from the LHC and the ILC in a combined analysis.

Supersymmetry illustrates the possible interplay between different experiments and observations. Missing energy signatures at the LHC may indicate a weakly interacting massive particle consistent with a supersymmetric particle. Direct or indirect dark matter searches may see a signal for weakly interacting exotic particles in our galactic halo. Are these particles neutralinos, responsible for some or all of the dark matter? Does the supersymmetry model preferred by collider data predict the observed abundance of dark matter (Figure 1.1), or do assumptions about the early history of the universe need to change? ILC measurements will be mandatory for these analyses.

Alternative possible structures of the new physics include phenomena containing extra dimensions, introducing connections between Terascale physics and gravity. One possibility is that the weakness of gravity could be understood by the escape of the gravitons into the new large extra dimensions. Events with unbalanced momentum caused by the escaping gravitons could be seen at both the LHC and the ILC. The ILC could confirm this scenario by observing anomalous electron positron pair production caused by graviton exchange.

Another possible extra-dimensional model (warped extra-dimensions) postulates two three-dimensional branes separated along one of the new dimensions. In this scenario, new resonances could appear at the colliders, and again pair production at the ILC would be critical to confirmation. The measurement of the couplings to leptons at the ILC would reveal the nature of the new states.

In these differing scenarios, the ILC has a critical role to play in resolving the confusing

possible interpretations. In some scenarios the new phenomena are effectively hidden from the LHC detectors, but are revealed as small deviations in couplings that could be measured at the ILC. In some cases the LHC experiments could definitively identify the existence of extra dimensions. Then the ILC would explore the size, shape, origins and impact of this expanded universe. A powerful feature of the ILC is its capability to explore new physics in a model independent way.

### 1.3 PRECISION REQUIREMENTS FOR ILC

ILC has an unprecedented potential for precision measurements, with new windows of exploration for physics beyond the Standard Model. This implies new requirements on theoretical and experimental accuracies. This in turn drives the need for more precise theoretical calculations for standard, Higgs and supersymmetry processes at the Terascale. There must be a corresponding effort to eliminate all known instrumental limitations which could compromise the precision of the measurements. These would include limits on the accuracy of momentum resolution, jet reconstruction, or reconstruction of short lived particles.

The ILC will search for invisible particles, candidates for the Dark Matter. This requires that the detector be as hermetic as possible. Machine backgrounds must be well controlled to reach the highest precision. The luminosity and polarisation of the beams must also be accurately known.

### 1.4 SPECIFYING MACHINE PARAMETERS

The accelerator described in Chapter 2 has been designed to meet the basic parameters required for the planned physics program [6]. The initial maximum center of mass energy is  $\sqrt{s} = 500$  GeV. Physics runs are possible for every energy above  $\sqrt{s} = 200$  GeV and calibration runs with limited luminosity are possible at  $\sqrt{s} = 91$  GeV. The beam energy can be changed in small steps for mass measurement threshold scans.

The total luminosity required is  $500 \text{ fb}^{-1}$  within the first four years of operation and  $1000 \text{ fb}^{-1}$  during the first phase of operation at 500 GeV. The electron beam must have a polarisation larger than 80%. The positron source should be upgradable to produce a beam with more than  $\pm 50\%$  polarisation[7]. Beam energy and polarisation must be stable and measurable at a level of about 0.1%.

An  $e^+e^-$  collider is uniquely capable of operation at a series of energies near the threshold of a new physical process. This is an extremely powerful tool for precision measurements of particle masses and unambiguous particle spin determinations. In a broad range of scenarios, including those with many new particles to explore and thresholds to measure, it is possible to achieve precision for all relevant observables in a reasonable time span.

All of the physics scenarios studied indicate that a  $\sqrt{s} = 500$  GeV collider can have a great impact on understanding the physics of the Terascale. An energy upgrade up to  $\sqrt{s} \sim 1$  TeV opens the door to even greater discoveries. With modest modifications, the ILC can also offer other options if required by physics, although these are not all explicitly included in the RDR design. For GigaZ, the ILC would run on the Z-resonance with high luminosity and both beams polarised, producing  $10^9$  hadronic Z decays in less than a year. The ILC could also run at the W-pair production threshold for a high precision W-mass measurement[8]. Both linacs could accelerate electrons for an  $e^-e^-$  collider[9], measuring the mass of a particular

## PHYSICS AT A TERASCALE $E^+E^-$ LINEAR COLLIDER

supersymmetric particle, the selectron, if it exists in the ILC energy range. Colliding electrons with a very intense laser beam near the interaction point can produce a high energy, high quality photon beam, resulting in an  $e^- \gamma$  or  $\gamma \gamma$  collider[10]. After operating below or at 500 GeV for a number of years, the ILC could be upgraded to higher energy or be modified for one of the options. It would then operate for several years in the new configuration.

## CHAPTER 2

# The ILC Accelerator

The ILC is based on 1.3 GHz superconducting radio-frequency (SCRF) accelerating cavities. The use of the SCRF technology was recommended by the International Technology Recommendation Panel (ITRP) in August 2004 [11], and shortly thereafter endorsed by the International Committee for Future Accelerators (ICFA). In an unprecedented milestone in high-energy physics, the many institutes around the world involved in linear collider R&D united in a common effort to produce a global design for the ILC. In November 2004, the 1st International Linear Collider Workshop was held at KEK, Tsukuba, Japan. The workshop was attended by some 200 physicists and engineers from around the world, and paved the way for the 2nd ILC Workshop in August 2005, held at Snowmass, Colorado, USA, where the ILC Global Design Effort (GDE) was officially formed. The GDE membership reflects the global nature of the collaboration, with accelerator experts from all three regions (Americas, Asia and Europe). The first major goal of the GDE was to define the basic parameters and layout of the machine – the Baseline Configuration. This was achieved at the first GDE meeting held at INFN, Frascati, Italy in December 2005 with the creation of the Baseline Configuration Document (BCD). During the next 14 months, the BCD was used as the basis for the detailed design work and value estimate culminating in the completion of the second major milestone, the publication of the draft ILC Reference Design Report (RDR).

The technical design and cost estimate for the ILC is based on two decades of world-wide Linear Collider R&D, beginning with the construction and operation of the SLAC Linear Collider (SLC). The SLC is acknowledged as a proof-of-principle machine for the linear collider concept. The ILC SCRF linac technology was pioneered by the TESLA collaboration<sup>1</sup>, culminating in a proposal for a 500 GeV center-of-mass linear collider in 2001 [12]. The concurrent (competing) design work on a normal conducting collider (NLC with X-band [13] and GLC with X- or C-Band [14]), has advanced the design concepts for the ILC injectors, Damping Rings (DR) and Beam Delivery System (BDS), as well as addressing overall operations, machine protection and availability issues. The X- and C-band R&D has led to concepts for RF power sources that may eventually produce either cost and/or performance benefits. Finally, the European XFEL [15] to be constructed at DESY, Hamburg, Germany, will make use of the TESLA linac technology, and represents a significant on-going R&D effort of great benefit for the ILC.

The current ILC baseline assumes an average accelerating gradient of 31.5 MV/m in the cavities to achieve a center-of-mass energy of 500 GeV. The high luminosity requires the

---

<sup>1</sup>Now known as the TESLA Technology Collaboration (TTC); see <http://tesla.desy.de>

use of high power and small emittance beams. The choice of 1.3 GHz SCRF is well suited to the requirements, primarily because the very low power loss in the SCRF cavity walls allows the use of long RF pulses, relaxing the requirements on the peak-power generation, and ultimately leading to high wall-plug to beam transfer efficiency.

The primary cost drivers are the SCRF Main Linac technology and the Conventional Facilities (including civil engineering). The choice of gradient is a key cost and performance parameter, since it dictates the length of the linacs, while the cavity quality factor ( $Q_0$ ) relates to the required cryogenic cooling power. The achievement of 31.5 MV/m as the baseline average operational accelerating gradient – requiring a minimum performance of 35 MV/m during cavity mass-production acceptance testing – represents the primary challenge to the global ILC R&D

With the completion of the RDR, the GDE will begin an engineering design study, closely coupled with a prioritized R&D program. The goal is to produce an Engineering Design Report (EDR) by 2010, presenting the matured technology, design and construction plan for the ILC, allowing the world High Energy Physics community to seek government-level project approvals, followed by start of construction in 2012. When combined with the seven-year construction phase that is assumed in studies presented in RDR, this timeline will allow operations to begin in 2019. This is consistent with a technically driven schedule for this international project.

## 2.1 SUPERCONDUCTING RF

The primary cost driver for the ILC is the superconducting RF technology used for the Main Linacs, bunch compressors and injector linacs. In 1992, the TESLA Collaboration began R&D on 1.3 GHz technology with a goal of reducing the cost per MeV by a factor of 20 over the then state-of-the-art SCRF installation (CEBAF). This was achieved by increasing the operating accelerating gradient by a factor of five from 5 MV/m to 25 MV/m, and reducing the cost per meter of the complete accelerating module by a factor of four for large-scale production.

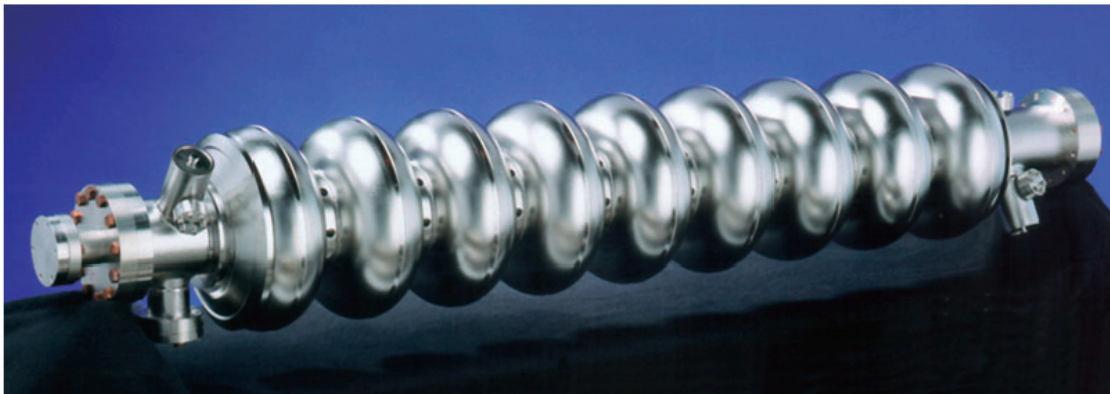


FIGURE 2.1. A TESLA nine-cell 1.3 GHz superconducting niobium cavity.

The TESLA cavity R&D was based on extensive existing experience from CEBAF (Jefferson Lab), CERN, Cornell University, KEK, Saclay and Wuppertal. The basic element of the technology is a nine-cell 1.3 GHz niobium cavity, shown in Figure 2.1. Approximately

160 of these cavities have been fabricated by industry as part of the on-going R&D program at DESY; some 17,000 are needed for the ILC.

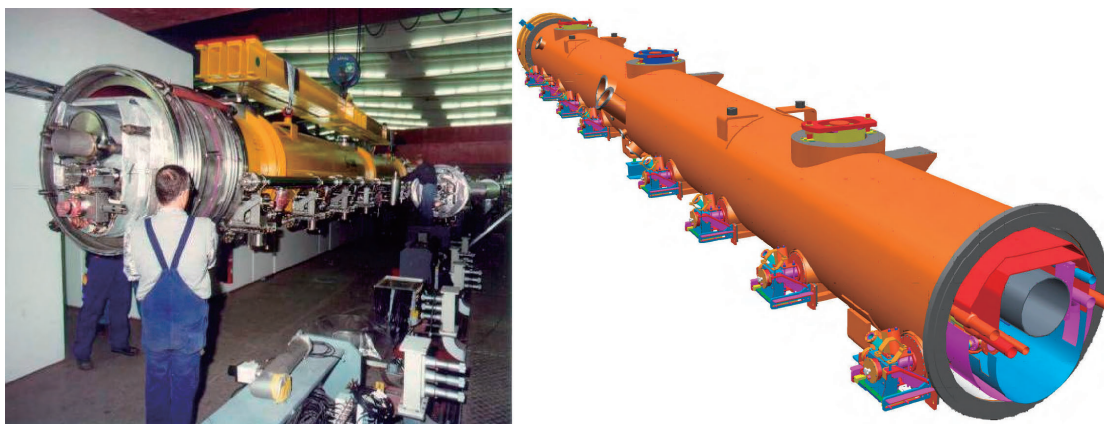


FIGURE 2.2. SCRF Cryomodules. Left: an 8 cavity TESLA cryomodule is installed into the FLASH linac at DESY. Right: design for the 4th generation ILC prototype cryomodule, due to be constructed at Fermilab National Laboratory.

A single cavity is approximately 1 m long. The cavities must be operated at 2 K to achieve their performance. Eight or nine cavities are mounted together in a string and assembled into a common low-temperature cryostat or *cryomodule* (Figure 2.2), the design of which is already in the third generation. Ten cryomodules have been produced to-date, five of which are currently installed in the VUV free-electron laser (FLASH)<sup>2</sup> at DESY, where they are routinely operated. DESY is currently preparing for the construction of the European XFEL facility, which will have a  $\sim 20$  GeV superconducting linac containing 116 cryomodules.

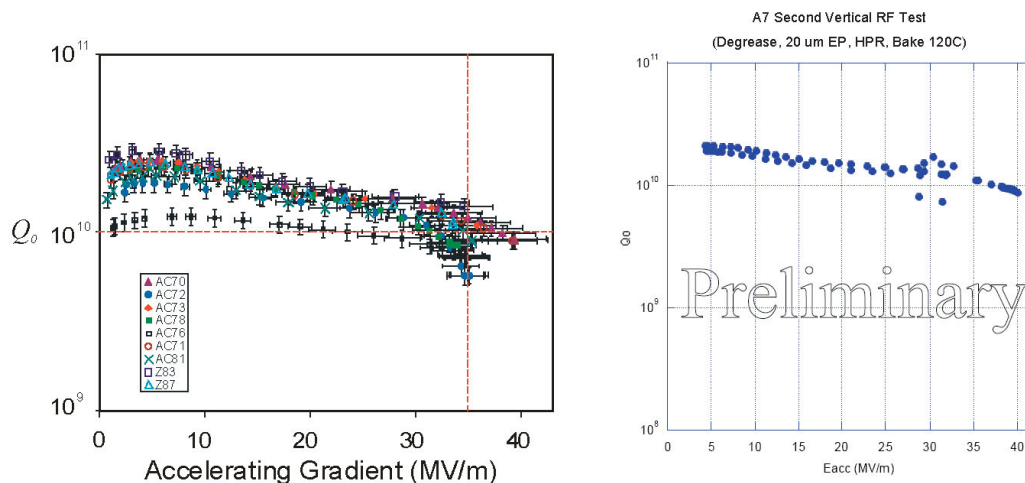


FIGURE 2.3. High-performance nine-cell cavities. Left: Examples of DESY nine-cell cavities achieving  $\geq 35$  MV/m. Right: Recent result from Jefferson Lab of nine-cell cavity achieving 40 MV/m.

The ILC community has set an aggressive goal of routinely achieving<sup>3</sup> 35 MV/m in nine-cell cavities, with a minimum production yield of 80%. Several cavities have already achieved

<sup>2</sup>Originally known as the TESLA Test Facility (TTF).

<sup>3</sup>Acceptance test.



## THE ILC ACCELERATOR

these and higher gradients (see Figure 2.3), demonstrating proof of principle. Records of over 50 MV/m have been achieved in single-cell cavities at KEK and Cornell[16]. However, it is still a challenge to achieve the desired production yield for nine-cell cavities at the mass-production levels ( $\sim 17,000$  cavities) required.

The key to high-gradient performance is the ultra-clean and defect-free inner surface of the cavity. Both cavity preparation and assembly into cavity strings for the cryomodules must be performed in clean-room environments (Figure 2.4).



FIGURE 2.4. Clean room environments are mandatory. Left: the assembly of eight nine-cell TESLA cavities into a cryomodule string at DESY. Right: an ICHIRO nine-cell cavity is prepared for initial tests at the Superconducting RF Test Facility (STF) at KEK.

The best cavities have been achieved using electropolishing, a common industry practice which was first developed for use with superconducting cavities by CERN and KEK. Over the last few years, research at Cornell, DESY, KEK and Jefferson Lab has led to an agreed standard procedure for cavity preparation, depicted in Figure 2.5. The focus of the R&D is now to optimize the process to guarantee the required yield. The ILC SCRF community has developed an internationally agreed-upon plan to address the priority issues.

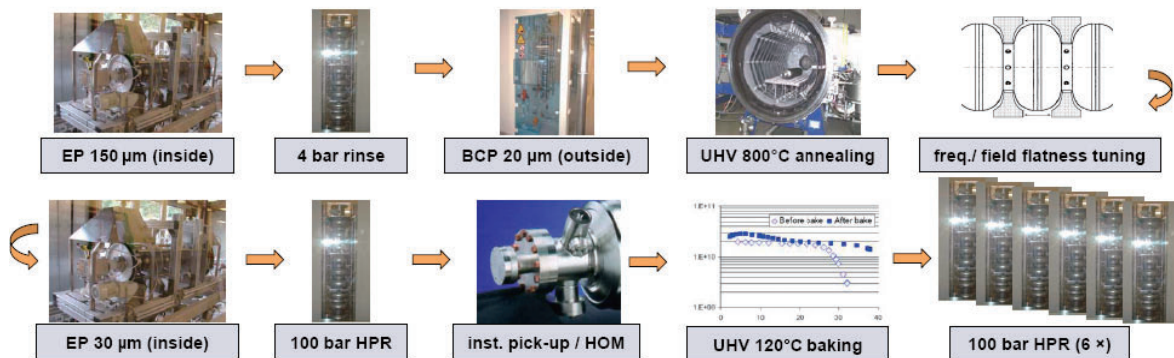


FIGURE 2.5. Birth of a nine-cell cavity: basic steps in surface treatment needed to achieve high-performance superconducting cavities. (EP = electropolishing; HPR = high-pressure rinsing.)

The high-gradient SCRF R&D required for ILC is expected to ramp-up world-wide over



the next years. The U.S. is currently investing in new infrastructure for nine-cell cavity preparation and string and cryomodule assembly. These efforts are centered at Fermilab (ILC Test Accelerator, or ILCTA), together with ANL, Cornell University, SLAC and Jefferson Lab. In Japan, KEK is developing the Superconducting RF Test Facility (STF). In Europe, the focus of R&D at DESY has shifted to industrial preparation for construction of the XFEL. There is continued R&D to support the high-gradient program, as well as other critical ILC-related R&D such as high-power RF couplers (LAL, Orsay, France) and cavity tuners (CEA Saclay, France; INFN Milan, Italy).

The quest for high-gradient and affordable SCRF technology for high-energy physics has revolutionized accelerator applications. In addition to the recently completed Spallation Neutron Source (SNS) in Oak Ridge, Tennessee and the European XFEL under construction, many linac-based projects utilizing SCRF technology are being developed, including 4th-generation light sources such as single-pass FELs and energy-recovery linacs. For the large majority of new accelerator-based projects, SCRF has become the technology of choice.

## 2.2 THE ILC BASELINE DESIGN

The overall system design has been chosen to realize the physics requirements with a maximum CM energy of 500 GeV and a peak luminosity of  $2 \times 10^{34} \text{ cm}^{-2}\text{s}^{-1}$ . Figure 2.6 shows a schematic view of the overall layout of the ILC, indicating the location of the major sub-systems:

- a polarized electron source based on a photocathode DC gun;
- an undulator-based positron source, driven by the 150 GeV main electron beam;
- 5 GeV electron and positron damping rings (DR) with a circumference of 6.7 km, housed in a common tunnel at the center of the ILC complex;
- beam transport from the damping rings to the main linacs, followed by a two-stage bunch compressor system prior to injection into the main linac;
- two 11 km long main linacs, utilizing 1.3 GHz SCRF cavities, operating at an average gradient of 31.5 MV/m, with a pulse length of 1.6 ms;
- a 4.5 km long beam delivery system, which brings the two beams into collision with a 14 mrad crossing angle, at a single interaction point which can be shared by two detectors.

The total footprint is  $\sim 31$  km. The electron source, the damping rings, and the positron auxiliary (‘keep-alive’) source are centrally located around the interaction region (IR). The plane of the damping rings is elevated by  $\sim 10$  m above that of the BDS to avoid interference.

To upgrade the machine to  $E_{\text{cms}} = 1$  TeV, the linacs and the beam transport lines from the damping rings would be extended by another  $\sim 11$  km each. Certain components in the beam delivery system would also need to be augmented or replaced.

### 2.2.1 Beam Parameters

The nominal beam parameter set, corresponding to the design luminosity of  $2 \times 10^{34} \text{ cm}^{-2}\text{s}^{-1}$  at  $E_{\text{cms}} = 500$  GeV is given in Table 2.1. These parameters have been chosen to optimize between known accelerator physics and technology challenges throughout the whole accelerator complex. Examples of such challenges are:

## THE ILC ACCELERATOR

- beam instability and kicker hardware constraints in the damping rings;
- beam current, beam power, and pulse length limitations in the main linacs;
- emittance preservation requirements, in the main linacs and the BDS;
- background control and kink instability issues in the interaction region.

Nearly all high-energy physics accelerators have shown unanticipated difficulties in reaching their design luminosity. The ILC design specifies that each subsystem support a range of beam parameters. The resulting flexibility in operating parameters will allow identified

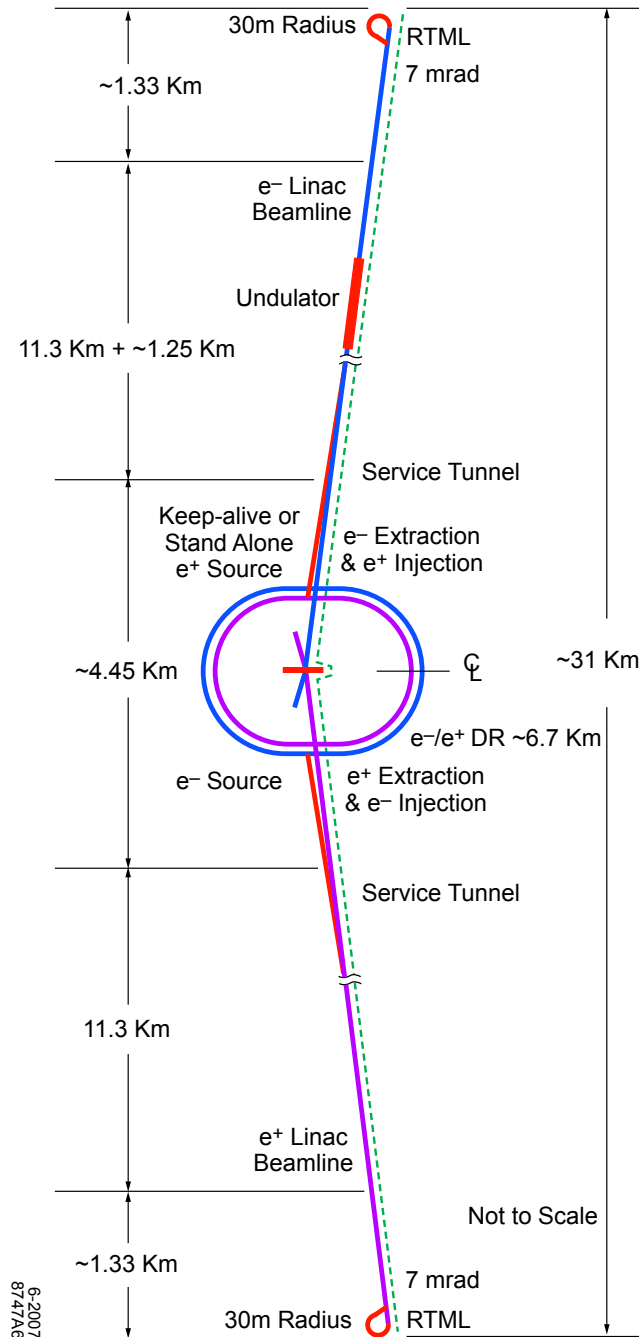


FIGURE 2.6. Schematic layout of the ILC complex for 500 GeV CM.

TABLE 2.1

Basic design parameters for the ILC (<sup>a</sup> values at 500 GeV center-of-mass energy).

| Parameter  | Unit                          |                    |
|--|-------------------------------|--------------------|
| Center-of-mass energy range                            | GeV                           | 200 - 500          |
| Peak luminosity <sup>a)</sup>                          | $\text{cm}^{-2}\text{s}^{-1}$ | $2 \times 10^{34}$ |
| Average beam current in pulse                          | mA                            | 9.0                |
| Pulse rate   | Hz                            | 5.0                |
| Pulse length (beam)                                    | ms                            | $\sim 1$           |
| Number of bunches per pulse                            |                               | 1000 - 5400        |
| Charge per bunch                                       | nC                            | 1.6 - 3.2          |
| Accelerating gradient <sup>a)</sup>                    | MV/m                          | 31.5               |
| RF pulse length  | ms                            | 1.6                |
| Beam power (per beam) <sup>a)</sup>                    | MW                            | 10.8               |
| Typical beam size at IP <sup>a)</sup> ( $h \times v$ ) | nm                            | $640 \times 5.7$   |
| Total AC Power consumption <sup>a)</sup>               | MW                            | 230                |

problems in one area to be compensated for in another. The nominal IP beam parameters and design ranges are presented in Table 2.2.

TABLE 2.2

Nominal and design range of beam parameters at the IP. The min. and max. columns do not represent consistent sets of parameters, but only indicate the span of the design range for each parameter. (Nominal vertical emittance assumes a 100% emittance dilution budget from the damping ring to the IP.)

|   | min  | nominal. | max. | unit             |
|---|------|----------|------|------------------|
| Bunch population                            | 1    | 2        | 2    | $\times 10^{10}$ |
| Number of bunches                           | 1260 | 2625     | 5340 |                  |
| Linac bunch interval                        | 180  | 369      | 500  | ns               |
| RMS bunch length                            | 200  | 300      | 500  | $\mu\text{m}$    |
| Normalized horizontal emittance at IP       | 10   | 10       | 12   | mm-mrad          |
| Normalized vertical emittance at IP         | 0.02 | 0.04     | 0.08 | mm-mrad          |
| Horizontal beta function at IP              | 10   | 20       | 20   | mm               |
| Vertical beta function at IP                | 0.2  | 0.4      | 0.6  | mm               |
| RMS horizontal beam size at IP              | 474  | 640      | 640  | nm               |
| RMS vertical beam size at IP                | 3.5  | 5.7      | 9.9  | nm               |
| Vertical disruption parameter               | 14   | 19.4     | 26.1 |                  |
| Fractional RMS energy loss to beamstrahlung | 1.7  | 2.4      | 5.5  | %                |

## 2.2.2 Electron Source

### Functional Requirements

The ILC polarized electron source must:

- generate the required bunch train of polarized electrons ( $> 80\%$  polarization);
- capture and accelerate the beam to 5 GeV;
- transport the beam to the electron damping ring with minimal beam loss, and perform an energy compression and spin rotation prior to injection.

### System Description

The polarized electron source is located on the positron linac side of the damping rings. The beam is produced by a laser illuminating a photocathode in a DC gun. Two independent laser and gun systems provide redundancy. Normal-conducting structures are used for bunching and pre-acceleration to 76 MeV, after which the beam is accelerated to 5 GeV in a superconducting linac. Before injection into the damping ring, superconducting solenoids rotate the spin vector into the vertical, and a separate superconducting RF structure is used for energy compression. The layout of the polarized electron source is shown in Figure 2.7.

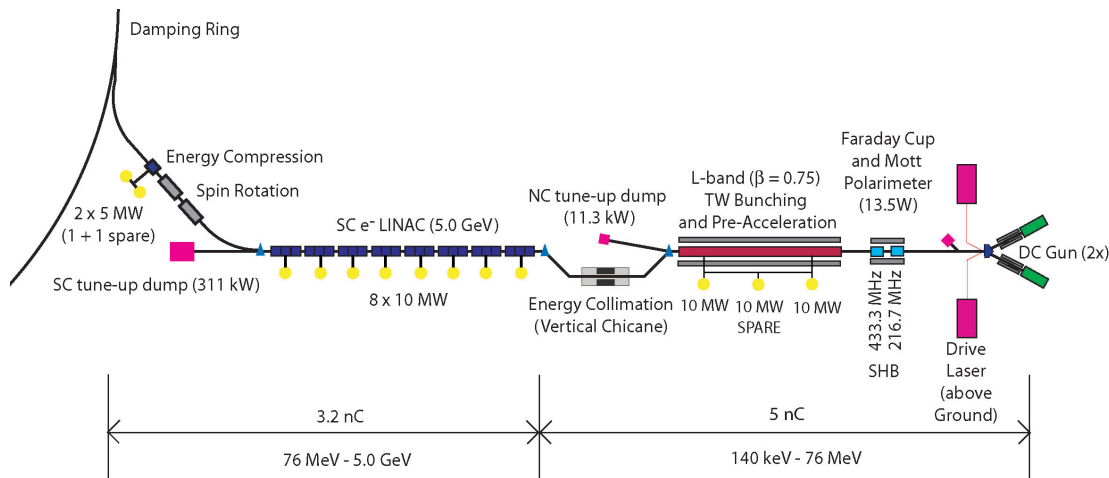


FIGURE 2.7. Schematic View of the Polarized Electron Source.

### Challenges

The SLC polarized electron source already meets the requirements for polarization, charge and lifetime. The primary challenge for the ILC electron source is the 1 ms long bunch train, which demands a laser system beyond that used at any existing accelerator.

## 2.2.3 Positron Source

### Functional requirements

The positron source must perform several critical functions:

- generate a high-power multi-MeV photon production drive beam in a suitably short-period, high K-value helical undulator;

- produce the needed positron bunches in a metal target that can reliably deal with the beam power and induced radioactivity;
- capture and accelerate the beam to 5 GeV ;
- transport the beam to the positron damping ring with minimal beam loss, and perform an energy compression and spin rotation prior to injection.

### System Description

The major elements of the ILC positron source are shown in Figure 2.8. The source uses photoproduction to generate positrons. After acceleration to 150 GeV, the electron beam is diverted into an offset beamline, transported through a 150-meter helical undulator, and returned to the electron linac. The high-energy ( $\sim 10$  MeV) photons from the undulator are directed onto a rotating 0.4 radiation-length Ti-alloy target  $\sim 500$  meters downstream, producing a beam of electron and positron pairs. This beam is then matched using an optical-matching device into a normal conducting (NC) L-band RF and solenoidal-focusing capture system and accelerated to 125 MeV. The electrons and remaining photons are separated from the positrons and dumped. The positrons are accelerated to 400 MeV in a NC L-band linac with solenoidal focusing. The beam is transported 5 km through the rest of the electron main linac tunnel, brought to the central injector complex, and accelerated to 5 GeV using superconducting L-band RF. Before injection into the damping ring, superconducting solenoids rotate the spin vector into the vertical, and a separate superconducting RF structure is used for energy compression.

The baseline design is for unpolarized positrons, although the beam has a polarization of 30%, and beamline space has been reserved for an eventual upgrade to 60% polarization.

To allow commissioning and tuning of the positron systems while the high-energy electron beam is not available, a low-intensity auxiliary (or “keep-alive”) positron source is provided. This is a conventional positron source, which uses a 500 MeV electron beam impinging on a heavy-metal target to produce  $\sim 10\%$  of the nominal positron beam. The keep-alive and primary sources use the same linac to accelerate from 400 MeV to 5 GeV.

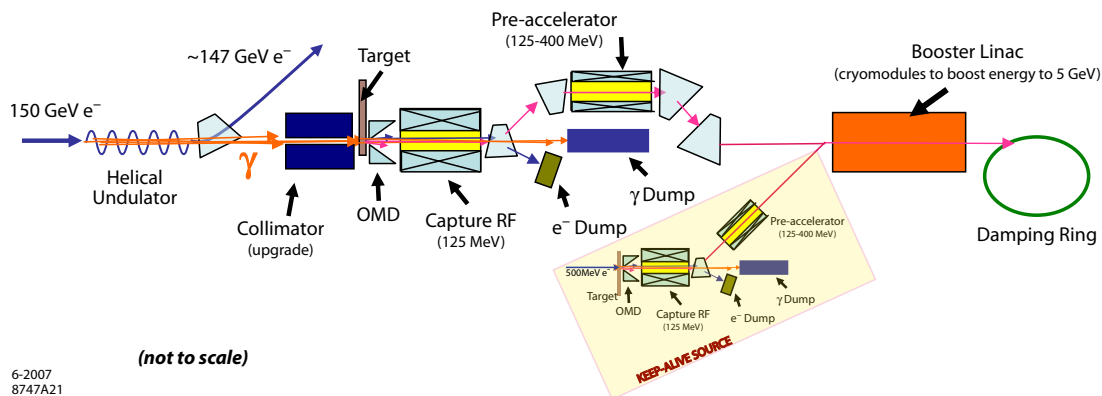


FIGURE 2.8. Overall Layout of the Positron Source.

### Challenges

The most challenging elements of the positron source are:

- the 150 m long superconducting helical undulator, which has a period of 1.15 cm and a K-value of 0.92, and a 6 mm inner diameter vacuum chamber;

- the Ti-alloy target, which is a cylindrical wheel 1.4 cm thick and 1 m in diameter, which must rotate at 100 m/s in vacuum to limit damage by the photon beam;
- the normal-conducting RF system which captures the positron beam, which must sustain high accelerator gradients during millisecond-long pulses in a strong magnetic field, while providing adequate cooling in spite of high RF and particle-loss heating.

The target and capture sections are also high-radiation areas which present remote handling challenges.

## 2.2.4 Damping Rings

### Functional requirements

The damping rings must perform four critical functions:

- accept  $e^-$  and  $e^+$  beams with large transverse and longitudinal emittances and damp to the low emittance beam required for luminosity production (by five orders of magnitude for the positron vertical emittance), within the 200 ms between machine pulses;
- inject and extract individual bunches without affecting the emittance or stability of the remaining stored bunches;
- damp incoming beam jitter (transverse and longitudinal) and provide highly stable beams for downstream systems;
- delay bunches from the source to allow feed-forward systems to compensate for pulse-to-pulse variations in parameters such as the bunch charge.

### System Description

The ILC damping rings include one electron and one positron ring, each 6.7 km long, operating at a beam energy of 5 GeV. The two rings are housed in a single tunnel near the center of the site, with one ring positioned directly above the other. The plane of the DR tunnel is located  $\sim 10$  m higher than that of the beam delivery system. This elevation difference gives adequate shielding to allow operation of the injector system while other systems are open to human access.

The damping ring lattice is divided into six arcs and six straight sections. The arcs are composed of TME cells; the straight sections use a FODO lattice. Four of the straight sections contain the RF systems and the superconducting wigglers. The remaining two sections are used for beam injection and extraction. Except for the wigglers, all of the magnets in the ring, are normal-conducting. Approximately 200 m of superferric wigglers are used in each damping ring. The wigglers are 2.5 m long devices, operating at 4.5K, with a peak field of 1.67 T.

The superconducting RF system is operated CW at 650 MHz, and provides 24 MV for each ring. The frequency is chosen to be half the linac RF frequency to easily accommodate different bunch patterns. The single-cell cavities operate at 4.5 K and are housed in eighteen 3.5 m long cryomodules. Although a number of 500 MHz CW RF systems are currently in operation, development work is required for this 650 MHz system, both for cavities and power sources.

The momentum compaction of the lattice is relatively large, which helps to maintain single bunch stability, but requires a relatively high RF voltage to achieve the design RMS bunch length (9 mm). The dynamic aperture of the lattice is sufficient to allow the large emittance injected beam to be captured with minimal loss.

## Challenges

The principal challenges in the damping ring are:

- control of the electron cloud effect in the positron damping ring. This effect, which can cause instability, tune spread, and emittance growth, has been seen in a number of other rings and is relatively well understood. Simulations indicate that it can be controlled by proper surface treatment of the vacuum chamber to suppress secondary emission, and by the use of solenoids and clearing electrodes to suppress the buildup of the cloud.
- control of the fast ion instability in the electron damping ring. This effect can be controlled by limiting the pressure in the electron damping ring to below 1 nTorr, and by the use of short gaps in the ring fill pattern.
- development of a very fast rise and fall time kicker for single bunch injection and extraction in the ring. For the most demanding region of the beam parameter range, the bunch spacing in the damping ring is  $\sim 3$  ns, and the kicker must have a rise plus fall time no more than twice this. Short stripline kicker structures can achieve this, but the drive pulser technology still needs development.

## 2.2.5 Ring to Main Linac (RTML)

### Functional requirements

The RTML must perform several critical functions for each beam:

- transport the beam from the damping ring to the upstream end of the linac;
- collimate the beam halo generated in the damping ring;
- rotate the polarization from the vertical to any arbitrary angle required at the IP;
- compress the long Damping Ring bunch length by a factor of  $30 \sim 45$  to provide the short bunches required by the Main Linac and the IP;

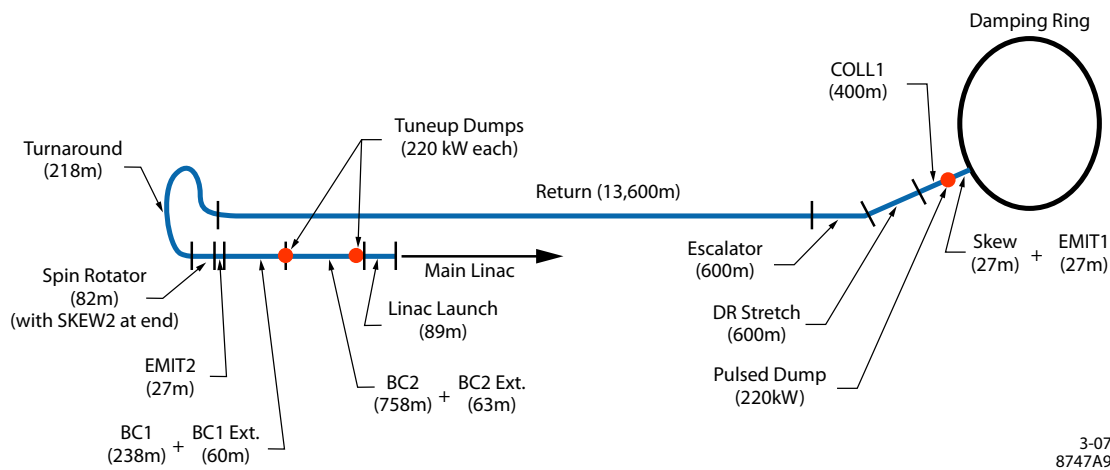


FIGURE 2.9. Schematic of the RTML.

### System Description

The layout of the RTML is identical for both electrons and positrons, and is shown in Figure 2.9. The RTML consists of the following subsystems:

- an  $\sim 15$  km long 5 GeV transport line;
- betatron and energy collimation systems;
- a  $180^\circ$  turn-around, which enables feed-forward beam stabilization;
- spin rotators to orient the beam polarization to the desired direction;
- a 2-stage bunch compressor to compress the beam bunch length from several millimeters to a few hundred microns as required at the IP.

The bunch compressor includes acceleration from 5 GeV to 13-15 GeV in order to limit the increase in fractional energy spread associated with bunch compression.

### Challenges

The principal challenges in the RTML are:

- control of emittance growth due to static misalignments, resulting in dispersion and coupling. Simulations indicate that the baseline design for beam-based alignment can limit the emittance growth to tolerable levels.
- suppression of phase and amplitude jitter in the bunch compressor RF, which can lead to timing errors at the IP. RMS phase jitter of  $0.24^\circ$  between the electron and positron RF systems results in a 2% loss of luminosity. Feedback loops in the bunch compressor low-level RF system should be able to limit the phase jitter to this level.

## 2.2.6 Main Linacs

### Functional requirements

The two main linacs accelerate the electron and positron beams from their injected energy of 15 GeV to the final beam energy of 250 GeV, over a combined length of 23 km. The main linacs must:

- accelerate the beam while preserving the small bunch emittances, which requires precise orbit control based on data from high resolution beam position monitors, and also requires control of higher-order modes in the accelerating cavities;
- maintain the beam energy spread within the design requirement of  $\sim 0.1\%$  at the IP;
- not introduce significant transverse or longitudinal jitter, which could cause the beams to miss at the collision point.

### System description

The ILC Main Linacs accelerate the beam from 15 GeV to a maximum energy of 250 GeV at an average accelerating gradient of 31.5 MV/m. The linacs are composed of RF units, each of which are formed by three contiguous SCRF cryomodules containing 26 nine-cell cavities. The layout of one unit is illustrated in Figure 2.10. The positron linac contains 278 RF units, and the electron linac has 282 RF units<sup>4</sup>.

<sup>4</sup>Approximately 3 GeV of extra energy is required in the electron linac to compensate for positron production.



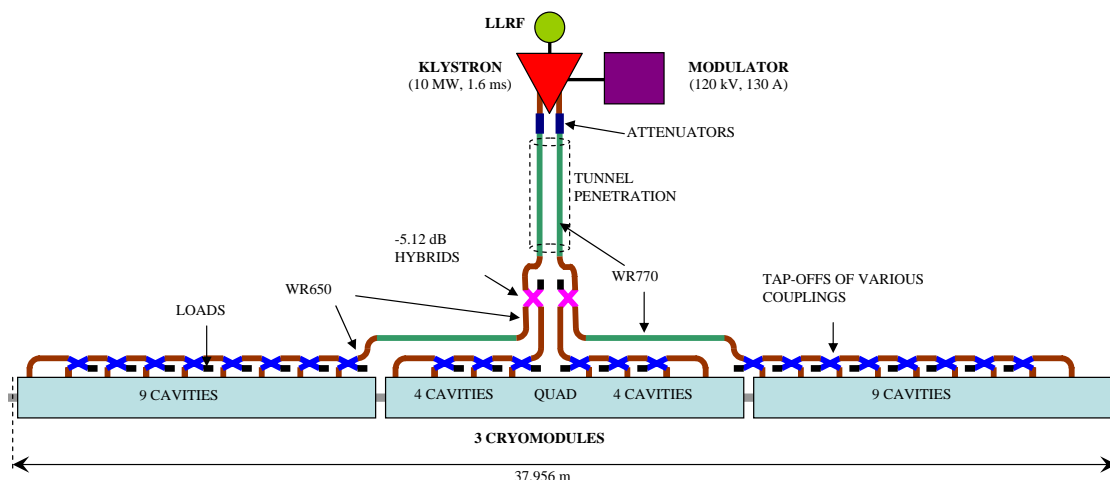


FIGURE 2.10. RF unit layout.

Each RF unit has a stand-alone RF source, which includes a conventional pulse-transformer type high-voltage (120 kV) modulator, a 10 MW multi-beam klystron, and a waveguide system that distributes the RF power to the cavities (see Figure 2.10). It also includes the low-level RF (LLRF) system to regulate the cavity field levels, interlock systems to protect the source components, and the power supplies and support electronics associated with the operation of the source.

The cryomodule design is a modification of the Type-3 version (Figure 2.2) developed and used at DESY. Within the cryomodules, a 300 mm diameter helium gas return pipe serves as a strongback to support the cavities and other beam line components. The middle cryomodule in each RF unit contains a quad package that includes a superconducting quadrupole magnet at the center, a cavity BPM, and superconducting horizontal and vertical corrector magnets. The quadrupoles establish the main linac magnetic lattice, which is a weak focusing FODO optics with an average beta function of  $\sim 80$  m. All cryomodules are 12.652 m long, so the active-length to actual-length ratio in a nine-cavity cryomodule is 73.8%. Every cryomodule also contains a 300 mm long high-order mode beam absorber assembly that removes energy through the 40-80 K cooling system from beam-induced higher-order modes above the cavity cutoff frequency.

To operate the cavities at 2 K, they are immersed in a saturated He II bath, and helium gas-cooled shields intercept thermal radiation and thermal conduction at 5-8 K and at 40-80 K. The estimated static and dynamic cryogenic heat loads per RF unit at 2 K are 5.1 W and 29 W, respectively. Liquid helium for the main linacs and the RTML is supplied from 10 large cryogenic plants, each of which has an installed equivalent cooling power of  $\sim 20$  kW at 4.5 K. The main linacs follow the average Earth's curvature to simplify the liquid helium transport.

The Main Linac components are housed in two tunnels, an accelerator tunnel and a service tunnel, each of which has an interior diameter of 4.5 meters. To facilitate maintenance and limit radiation exposure, the RF source is housed mainly in the service tunnel as illustrated in Figure 2.11.

The tunnels are typically hundreds of meters underground and are connected to the surface through vertical shafts<sup>5</sup>. Each of the main linacs includes three shafts, roughly 5 km apart

<sup>5</sup>Except for the Asian sample site: see Section 2.3.

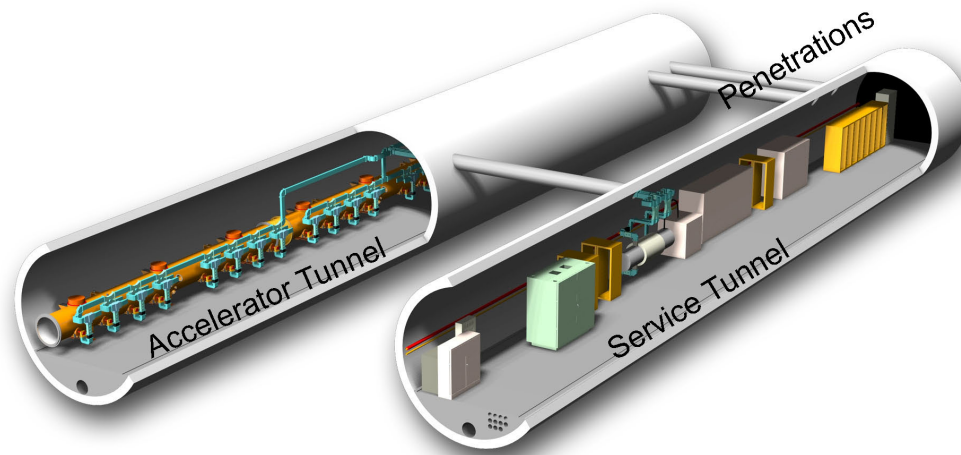


FIGURE 2.11. Cutaway view of the linac dual-tunnel configuration.

as dictated by the cryogenic system. The upstream shafts in each linac have diameters of 14 m to accommodate lowering cryomodules horizontally, and the downstream shaft in each linac is 9 m in diameter, which is the minimum size required to accommodate tunnel boring machines. At the base of each shaft is a 14,100 cubic meter cavern for staging installation; it also houses utilities and parts of the cryoplant, most of which are located on the surface.

### Challenges

The principal challenges in the main linac are:

- achieving the design average accelerating gradient of 31.5 MV/m. This operating gradient is higher than that typically achievable today and assumes further progress will be made during the next few years in the aggressive program that is being pursued to improve cavity performance.
- control of emittance growth due to static misalignments, resulting in dispersion and coupling. Beam-based alignment techniques should be able to limit the single-bunch emittance growth. Long-range multibunch effects are mitigated via HOM damping ports on the cavities, HOM absorbers at the quadrupoles, and HOM detuning. Coupling from mode-rotation HOMs is limited by splitting the horizontal and vertical betatron tunes.
- control of the beam energy spread. The LLRF system monitors the vector sum of the fields in the 26 cavities of each RF unit and makes adjustments to flatten the energy gain along the bunch train and maintain the beam-to-RF phase constant. Experience from FLASH and simulations indicate that the baseline system should perform to specifications.

## 2.2.7 Beam Delivery System

### Functional requirements

The ILC Beam Delivery System (BDS) is responsible for transporting the  $e^+e^-$  beams from the exit of the high energy linacs, focusing them to the sizes required to meet the ILC luminosity goals, bringing them into collision, and then transporting the spent beams to the main beam dumps. In addition, the BDS must perform several other critical functions:

- measure the linac beam and match it into the final focus;
- protect the beamline and detector against mis-steered beams from the main linacs;
- remove any large amplitude particles (beam-halo) from the linac to minimize background in the detectors;
- measure and monitor the key physics parameters such as energy and polarization before and after the collisions.

## System Description

The layout of the beam delivery system is shown in Figure 2.12. There is a single collision point with a 14 mrad total crossing angle. The 14 mrad geometry provides space for separate extraction lines but requires crab cavities to rotate the bunches in the horizontal plane for effective head-on collisions. There are two detectors in a common interaction region (IR) hall in a so-called “push-pull” configuration. The detectors are pre-assembled on the surface and then lowered into the IR hall when the hall is ready for occupancy.

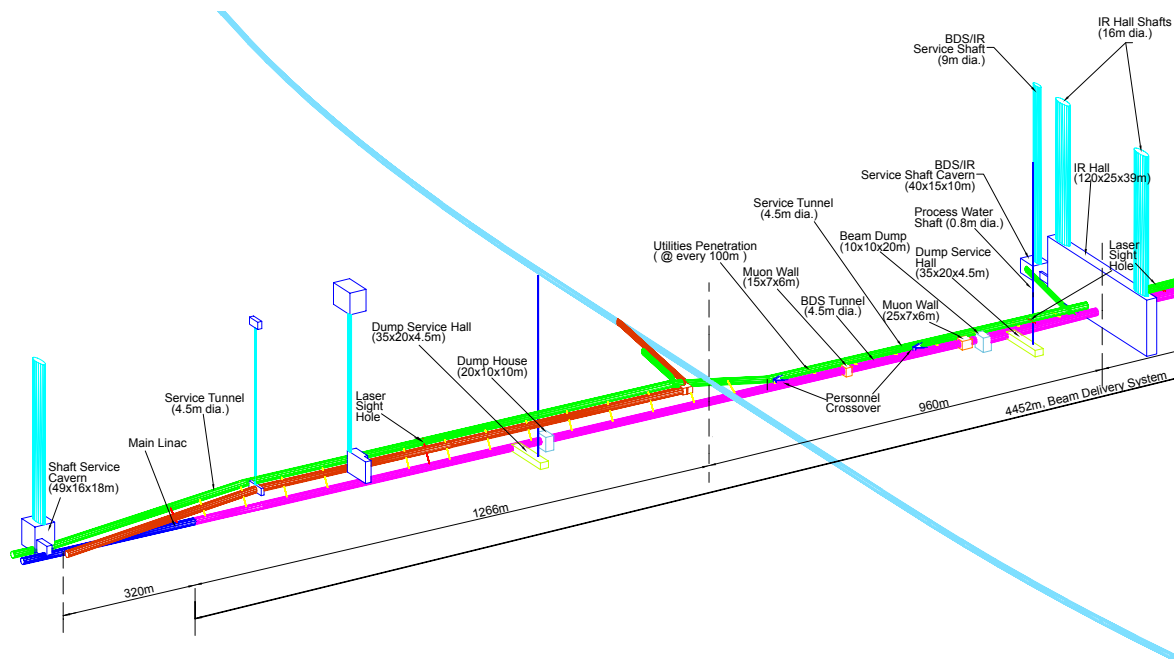


FIGURE 2.12. BDS layout, beam and service tunnels (shown in magenta and green), shafts, experimental hall. The line crossing the BDS beamline at right angles is the damping ring, located 10 m above the BDS tunnels.

The BDS is designed for 500 GeV center-of-mass energy but can be upgraded to 1 TeV with additional magnets.

The main subsystems of the beam delivery, starting from the exit of the main linacs, are:

- a section containing post-linac emittance measurement and matching (correction) sections, trajectory feedback, polarimetry and energy diagnostics;
- a fast pulsed extraction system used to extract beams in case of a fault, or to dump the beam when not needed at the IP;

## THE ILC ACCELERATOR

- a collimation section which removes beam halo particles that would otherwise generate unacceptable background in the detector, and also contains magnetized iron shielding to deflect muons;
- the final focus (FF) which uses strong compact superconducting quadrupoles to focus the beam at the IP, with sextupoles providing local chromaticity correction;
- the interaction region, containing the experimental detectors. The final focus quadrupoles closest to the IP are integrated into the detector to facilitate detector “push-pull”;
- the extraction line, which has a large enough bandwidth to cleanly transport the heavily disrupted beam to a high-powered water-cooled dump. The extraction line also contains important polarization and energy diagnostics.

### Challenges

The principal challenges in the beam delivery system are:

- tight tolerances on magnet motion (down to tens of nanometers), which make the use of fast beam-based feedback systems mandatory, and may well require mechanical stabilization of critical components (e.g. final doublets).
- uncorrelated relative phase jitter between the crab cavity systems, which must be limited to the level of tens of femtoseconds.
- control of emittance growth due to static misalignments, which requires beam-based alignment and tuning techniques similar to the RTML.
- control of backgrounds at the IP via careful tuning and optimization of the collimation systems and the use of the tail-folding octupoles.
- clean extraction of the high-powered disrupted beam to the dump. Simulations indicate that the current design is adequate over the full range of beam parameters.

## 2.3 SAMPLE SITES

Conventional Facilities and Siting (CFS) is responsible for civil engineering, power distribution, water cooling and air conditioning systems. The value estimate (see Section 4) for the CFS is approximately 38% of the total estimated project value.

In the absence of a single agreed-upon location for the ILC, a sample site in each region was developed. Each site was designed to support the baseline design described in Section 2.2. Although many of the basic requirements are identical, differences in geology, topography and local standards and regulations lead to different construction approaches, resulting in a slight variance in value estimates across the three regions. Although many aspects of the CFS (and indeed machine design) will ultimately depend on the specific host site chosen, the approach taken here is considered sufficient for the current design phase, while giving a good indication of the influence of site-specific issues on the project as a whole.

Early in the RDR process, the regional CFS groups agreed upon a matrix of criteria for any sample site. All three sites satisfied these criteria, including the mandatory requirement that the site can support the extension to the 1 TeV center-of-mass machine.

The three sample sites have the following characteristics:

- The Americas sample site lies in Northern Illinois near Fermilab. The site provides a range of locations to position the ILC in a north-south orientation. The site chosen

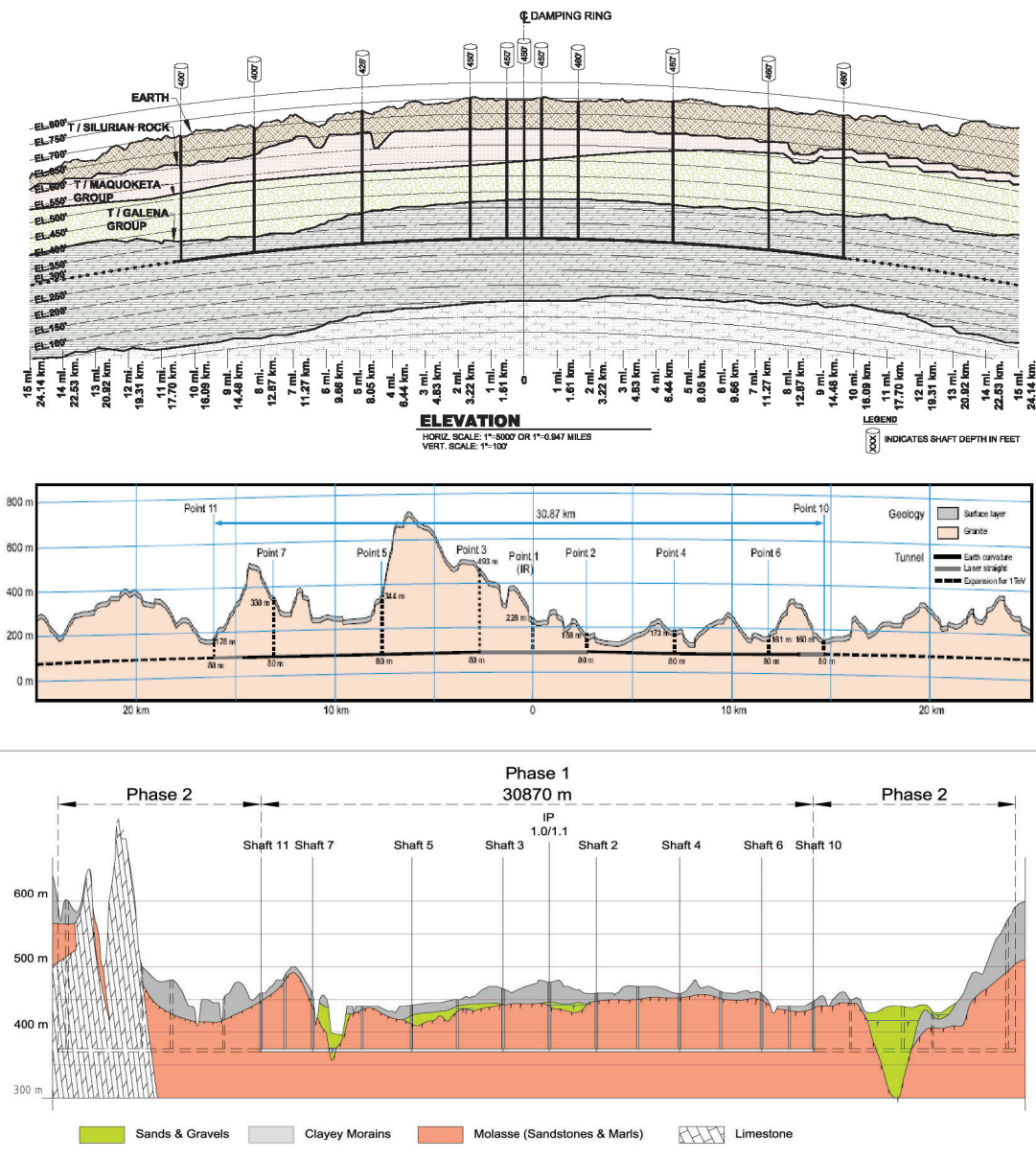


FIGURE 2.13. Geology and tunnel profiles for the three regional sites, showing the location of the major access shafts (tunnels for the Asian site). Top: the Americas site close to Fermilab. Middle: the Asian site in Japan. Bottom: the European site close to CERN.

has approximately one-quarter of the machine on the Fermilab site. The surface is primarily flat. The long tunnels are bored in a contiguous dolomite rock strata (Galena Platteville), at a typical depth of 30-100 m below the surface.

- The Asian site has been chosen from several possible ILC candidate sites in Japan. The sample site has a uniform terrain located along a mountain range, with a tunnel depth ranging from 40 m to 600 m. The chosen geology is uniform granite highly suited to modern tunneling methods. One specific difference for the Asian site is the use of long sloping access tunnels instead of vertical shafts, the exception being the experimental hall at the Interaction Region, which is accessed via two 112 m deep vertical shafts. The sloping access tunnels take advantage of the mountainous location.

## THE ILC ACCELERATOR

- The European site is located at CERN, Geneva, Switzerland, and runs parallel to the Jura mountain range, close to the CERN site. The majority of the machine is located in the ‘Molasse’ (a local impermeable sedimentary rock), at a typical depth of 370 m.

The elevations of the three sample sites are shown in Figure 2.13. The tunnels for all three sites would be predominantly constructed using Tunnel Boring Machines (TBM), at typical rates of 20–30 m per day. The Molasse of the European site near CERN requires a reinforced concrete lining for the entire tunnel length. The Asian site (granite) requires rock bolts and a 5 cm ‘shotcrete’ lining. The US site is expected to require a concrete lining for only approximately 20% of its length, with rock-bolts being sufficient for permanent structural support.

A second European sample site near DESY, Hamburg, Germany, has also been developed. This site is significantly different from the three reported sites, both in geology and depth (25 m deep), and requires further study.

In addition, the Joint Institute for Nuclear Research has submitted a proposal to site the ILC in the neighborhood of Dubna, Russian Federation.

The three sites reported in detail here are all ‘deep-tunnel’ solutions. The DESY and Dubna sites are examples of ‘shallow’ sites. A more complete study of shallow sites – shallow tunnel or cut-and-cover – will be made in the future as part of the Engineering Design phase.

## CHAPTER 3

# Detectors

The challenge for the ILC detectors is to optimize the scientific results from a broad experimental program aimed at understanding the mechanism of mass generation and electroweak symmetry breaking. This includes the search for supersymmetric particles, and their detailed study if they are found, and the hunt for signs of extra space-time dimensions and quantum gravity. Precision measurements of Standard Model processes can reveal new physics at energy scales beyond direct reach. The detectors must also be prepared for the unexpected.

Experimental conditions at the ILC provide an ideal environment for the precision study of particle production and decay, and offer the unparalleled cleanliness and well-defined initial conditions conducive to recognizing new phenomena. Events are recorded without trigger bias, with detectors designed for optimal physics performance. The physics poses challenges, pushing the limits of jet energy resolution, tracker momentum resolution, and vertex impact parameter resolution. Multi-jet final states and supersymmetry (SUSY) searches put a premium on hermeticity and full solid angle coverage. Although benign by LHC standards, the ILC environment poses challenges of its own.

The World Wide Study of Physics and Detectors for Future Linear Colliders has wrestled with these challenges for more than a decade, advancing the technologies needed for ILC detectors. Different concepts for detectors have evolved[12, 17], as the rapid collider progress has spurred the experimental community. Four concept reports[18, 19, 20, 21] were presented in Spring, 2006. All of these detectors meet the ILC physics demands, and can be built with technologies that are within reach today. There is a growing community involved in refining and optimizing these designs, and advancing the technologies. Full detector engineering designs and proof of principle technology demonstrations can be completed on the timetable proposed for the ILC Engineering Design Report as long as there is adequate support for detector R&D and integrated detector studies.

### 3.1 CHALLENGES FOR DETECTOR DESIGN AND TECHNOLOGY

The relatively low radiation environment of the ILC allows detector designs and technologies not possible at the LHC, but the demanding physics goals still challenge the state of the art, particularly in readout and sensor technologies.

Many interesting ILC physics processes appear in multi-jet final states, often accompanied

by charged leptons or missing energy. Precision mass measurements require a jet energy resolution of  $\frac{\sigma_{E_{jet}}}{E_{jet}} = \frac{30\%}{\sqrt{E_{jet}}}$  for  $E_{jet}$  up to approximately 100 GeV, and  $\frac{\sigma_{E_{jet}}}{E_{jet}} \leq 3\%$  beyond, more than a factor of 2 better than achieved at LEP/SLC.

Detailed studies of leptons from W and Z decays require efficient electron and muon ID and accurate momentum measurements over the largest possible solid angle. Excellent identification of electrons and muons within jets is critical because they indicate the presence of neutrinos from heavy quark decays, and tag the jet flavor and quark charge.

The jet mass resolution appears achievable if the detector has an excellent, highly efficient, nearly hermetic tracking system and a finely segmented calorimeter. Charged tracks reconstructed in the tracker can be isolated in the calorimeter, and their contributions removed from the calorimeter energy measurement. This “particle flow” concept has motivated the development of high granularity calorimeters, and highly efficient tracking systems. The main challenge is the separation of neutral and charged contributions within a dense jet environment.

It is possible to satisfy the calorimeter granularity required for the particle flow concept with electromagnetic cell sizes of about  $1 \times 1 \text{ cm}^2$ , and comparable or somewhat larger hadronic cells. An electromagnetic energy resolution of  $\sim 15\%/\sqrt{E}$  and a hadronic resolution of  $\sim 40\%/\sqrt{E}$  is sufficient.

The momentum resolution required to satisfy the demands of particle flow calorimetry and missing energy measurements is particularly challenging and exceeds the current state of the art. Good momentum resolution from the beam energy down to very low momentum is needed over the full solid angle. Pattern recognition must be robust and highly efficient even in the presence of backgrounds. This requires minimal material to preserve lepton ID and permit high performance calorimetry.

“Higgs-strahlung” production in association with a Z is a particularly powerful physics channel. It allows precision Higgs mass determination, precision studies of the Higgs branching fractions, measurement of the production cross section and accompanying tests of SM couplings, and searches for invisible Higgs decays. The resolution of the recoil mass from a Z decaying to leptons depends on beam energy accuracy, beam energy spread and tracking precision. Figure 3.1 shows an example of the recoil mass distribution[22] opposite the Z. The tracker is also critical to mass determination of kinematically accessible sleptons and neutralinos, and accurate measurements of the center of mass energy.

Vertex detection identifies heavy particle decay vertices, enabling flavor and charge tagging. Multilayer vertex detection also provides efficient stand-alone pattern recognition, momentum measurement for soft tracks, and seeds for tracks in outer trackers. The ILC physics goals push vertex detector efficiency, angular coverage, and impact parameter resolution beyond the current state of the art, even surpassing the SLD CCD vertex detector[23]. The ILC beamstrahlung  $e^+e^-$  pairs present a background of up to 100 hits/mm<sup>2</sup>/train for the innermost detector elements. It is essential to reduce the number of background hits, either by time-slicing the bunch train into pieces of less than 150 bunch crossings, or by discriminating charged tracks from background. The simultaneous challenges of rapid readout, constrained power budget, transparency and high resolution are being actively addressed by several efforts. The ILCs low data rates and low radiation loads allow consideration of new technologies that reach beyond LHC capabilities.

The very forward region of the ILC detector is instrumented with a calorimeter (BeamCal) that extends calorimeter hermeticity to small angles. To search for new particles, this instru-



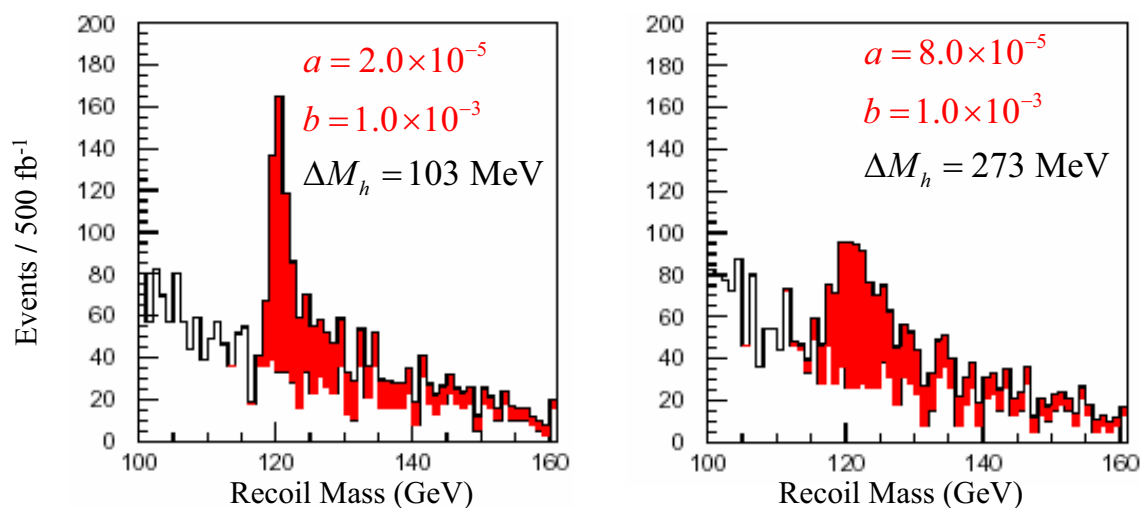


FIGURE 3.1. Higgs recoil mass spectra for tracker momentum resolution,  $\frac{\delta p_t}{p_t} = a \oplus \frac{b}{p_t \sin \theta}$ , for 120 GeV Higgs mass,  $\sqrt{s} = 350$  GeV, and  $500 \text{ fb}^{-1}$ .

ment must veto electrons in a high radiation and high background environment. Measurement of the energy deposited by beamstrahlung pairs and photons in the BeamCal and associated photon calorimeter (GamCal) provides a bunch-by-bunch luminosity measurement that can be used for intra-train luminosity optimization. Beam parameters can also be determined from the shapes of the observed energy depositions given sufficiently fast readout electronics and adequate high bandwidth resolution. Near the beampipe the absorbed radiation dose is up to 10 MGy per year.

Polarimetry and beam energy spectrometry must be able to achieve very low systematic errors, with beam energy measured to 200 ppm, and polarization to 0.1%. High-field superconducting solenoid designs must be refined, with development of new conductors. The solenoid design must also accommodate dipole and solenoid compensation, have high field uniformity, and support push-pull. Muon detectors must be developed.

Detector system integration depends on engineering and design work in several areas. Stable, adjustable, vibration free support of the final quadrupoles is needed. Support of the fragile beampipe with its massive masking is also a concern. The detectors are required to move on and off beamline quickly and reproducibly (“push-pull”). The detectors must be calibrated, aligned, and accessed, without compromising performance.

Research and development on all of these detector issues must be expanded in order to achieve the needed advances.

## 3.2 DETECTOR CONCEPTS

Four detector concepts are being studied as candidate detectors for the ILC experimental program. These represent complementary approaches and technology choices. Each concept is designed with an inner vertex detector, a tracking system based on either a gaseous Time Projection Chamber or silicon detectors, a calorimeter to reconstruct jets, a muon system, and a forward system of tracking and calorimetry. Table 3.1 presents some of the key parameters

## DETECTORS

of each of the four detector concepts. GLD, LDC and SiD employ particle flow for jet energy measurements. SiD has the strongest magnetic field and the smallest radius, while LDC and GLD rely on smaller fields with larger tracking radii. Each approach uses different emphasis to address the optimization. The 4<sup>th</sup> concept employs a dual-readout fiber calorimeter and a novel outer muon system.

TABLE 3.1  
Some key parameters of the four detector concepts.

| Concept         | Tracking Technology | Solenoidal Field Strength (Tesla) | Solenoid Radius, Length (m) | Vertex Inner Radius (mm) | ECAL Barrel Inner Radius, Half-Length (m) | Overall Detector Outer Radius, Half-Length (m) |
|-----------------|---------------------|-----------------------------------|-----------------------------|--------------------------|---|--|
| GLD             | TPC/Si              | 3                                 | 4                           | 20                       | 2.1                                       | 7.20   |
|                 |                     |                                   | 9.5                         |                          | 2.8                                       | 7.50   |
| LDC             | TPC/Si              | 4                                 | 3                           | 16                       | 1.60                                      | 6.00   |
|                 |                     |                                   | 6.6                         |                          | 2.3                                       | 6.20   |
| SiD             | Silicon             | 5                                 | 2.5                         | 14                       | 1.27                                      | 6.45   |
|                 |                     |                                   | 5.5                         |                          | 1.27                                      | 5.89   |
| 4 <sup>th</sup> | TPC or drift        | 3.5                               | 3                           | 15                       | 1.5                                       | 5.50   |
|                 |                     |                                   | 8                           |                          | 1.8                                       | 6.50   |

Software models of the detectors have produced realistic simulations of the physics performance, making it clear that the detectors can do the physics. The community is also preparing for the evolution to collaborations.

### 3.2.1 The Silicon Detector (SiD) Concept

The SiD concept is based on silicon tracking and a silicon-tungsten sampling calorimeter, complemented by a powerful pixel vertex detector, outer hadronic calorimeter, and muon system. Silicon detectors are fast and robust, and can be finely segmented. Most SiD systems can record backgrounds from a single bunch crossing accompanying a physics event, maximizing event cleanliness. The vertex detector, the tracker and the calorimeter can all absorb significant radiation bursts without “tripping” or sustaining damage, maximizing running efficiency. The SiD Starting Point[18] is illustrated in Figure 3.2.

A highly pixellated silicon-tungsten electromagnetic calorimeter and a multilayer, highly segmented hadron calorimeter, inside the solenoid, are chosen to optimize particle flow calorimetry. Cost and performance considerations dictate a 5 Tesla solenoid, at relatively small radius.

SiD tracking works as an integrated system, incorporating the pixellated vertex detector (5 barrels and 4 endcap layers), the central silicon microstrip tracker (5 layers, barrels and endcaps), and the electromagnetic calorimeter. The vertex detector plays a key role in pattern

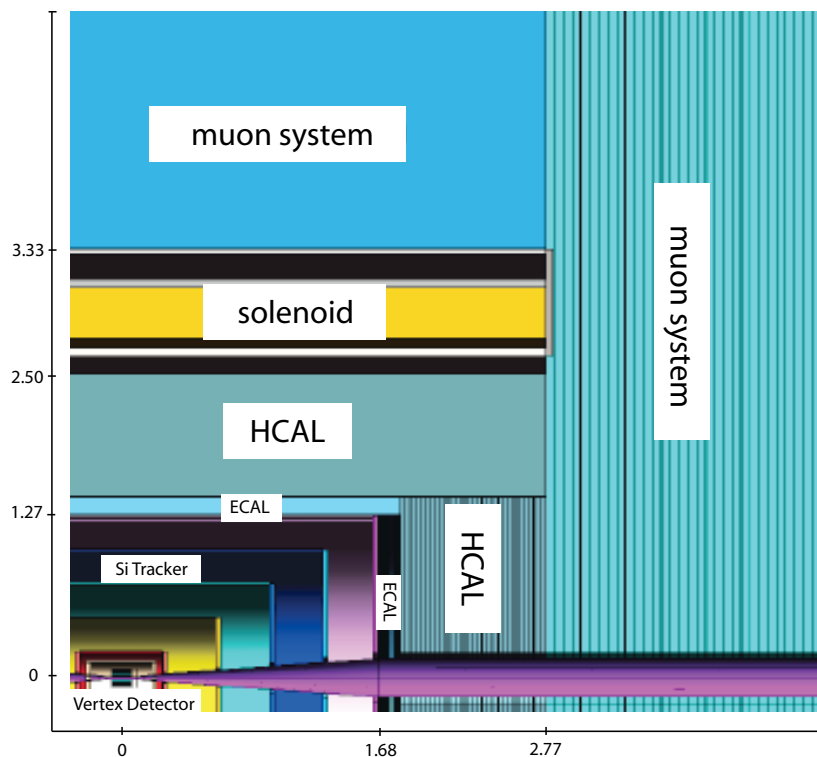


FIGURE 3.2. Illustration of a quadrant of SiD.

recognition; tracks produced by decays beyond the second layer of the central tracker, but within the ECAL, are captured with a calorimeter-assisted tracking algorithm. The resolution of the combined system is  $\frac{\sigma_p}{p^2} < 2 \times 10^{-5} \text{ GeV}^{-1}$  at high momentum.

The SiD electromagnetic calorimeter consists of layers of tungsten and large-area silicon diode detectors in one mm gaps. The hadronic calorimeter sandwich employs steel absorber plates and resistive plate chambers (RPCs). Options include tungsten absorber, glass RPCs, GEM foils, Micromegas, and scintillating tiles with silicon photomultipliers. Muon detectors (following  $6\lambda$  at 3.5 m radius) fill some gaps between iron plates of the flux return. Two technologies are under consideration for the muon system, strip-scintillator detectors and RPCs.

### 3.2.2 The Large Detector Concept (LDC)

The LDC[19] is based on a precision, highly redundant and reliable Time Projection Chamber (TPC) tracking system, and particle flow as a means to complete event reconstruction, all inside a large volume magnetic field of up to 4 Tesla, completed by a precision muon system covering nearly the complete solid angle outside the coil. A view of the simulated detector is shown in Figure 3.3 (left).

The TPC provides up to 200 precise measurements along a track, supplemented by Si-based tracking detectors. A silicon vertex detector gives unprecedented precision in the reconstruction of long lived particles.

The proposed LDC detector has the following components:

- a five layer pixel-vertex detector
- a system of silicon strip and pixel detectors extending the vertex detector

## DETECTORS

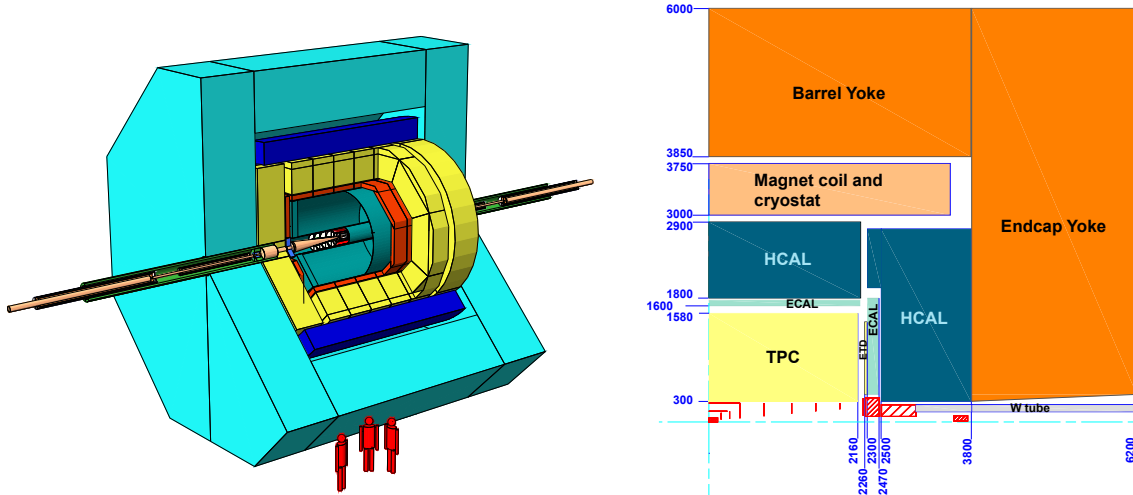


FIGURE 3.3. View of the LDC detector concept, as simulated with the MOKKA simulation package (left). 1/4 view of the LDC detector concept (right).

- a large volume TPC
  - a system of “linking” detectors behind the endplate of the TPC and in between the TPC outer radius and the ECAL inner radius
  - a granular Si-W electromagnetic calorimeter
  - a granular Fe-Scintillator hadronic calorimeter, gas hadronic calorimeter is an option
  - a system of high precision extremely radiation hard calorimetric detectors in the very forward region, to measure luminosity and to monitor collision quality
  - a large volume superconducting coil, with longitudinal B-field of 4 Tesla
  - an iron return yoke, instrumented to serve as a muon filter and detector.
- A schematic view of one quarter of this detector is shown in Figure 3.3 (right).

### 3.2.3 The GLD Concept

The GLD detector[20] concept has a large gaseous tracker and finely granulated calorimeter within a large bore 3 Tesla solenoid. Figure 3.4 shows a schematic view of two different quadrants of the baseline design of GLD.

The baseline design has the following sub-detectors:

- a Time Projection Chamber as a large gaseous central tracker
- a highly segmented electromagnetic calorimeter placed at large radius and based on a tungsten-scintillator sandwich structure
- a highly segmented hadron calorimeter with a lead-scintillator sandwich structure and radial thickness of  $\sim 6\lambda$
- forward electromagnetic calorimeters which provide nearly full solid angle coverage down to very forward angles
- a precision silicon (FPCCD) micro-vertex detector
- silicon inner and endcap trackers
- a beam profile monitor in front of a forward electromagnetic calorimeter
- a scintillator strip muon detector interleaved with the iron plates of the return yoke
- a solenoidal magnet to generate the 3 Tesla magnetic field.

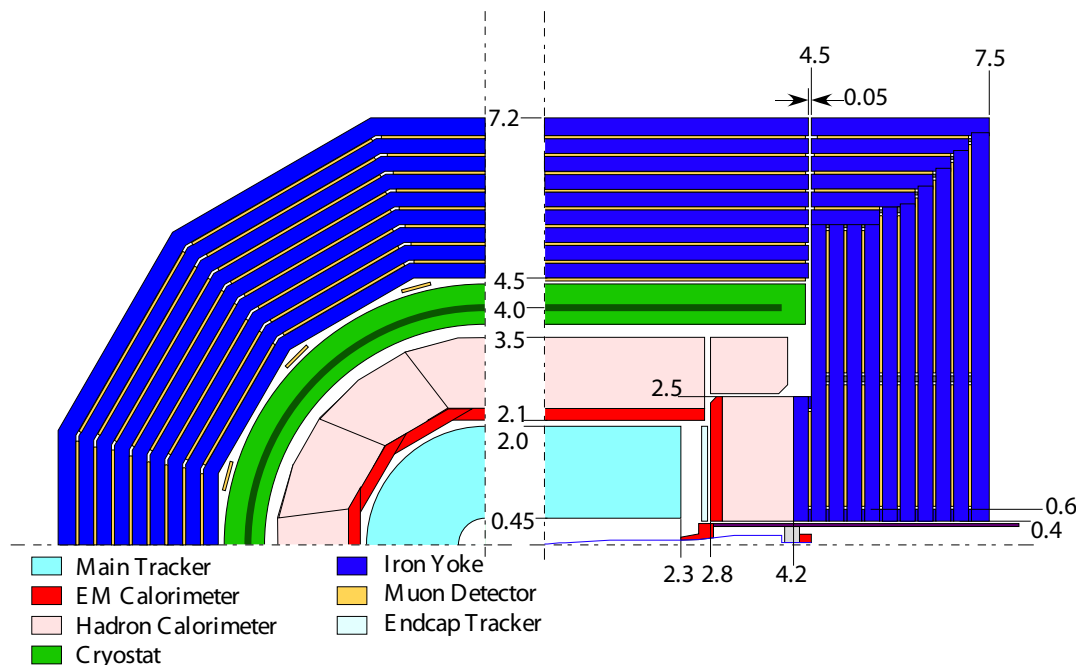


FIGURE 3.4. Schematic view of two different quadrants of the GLD Detector. The left figure shows the  $\phi$  view and the right shows the rz view. Dimensions are given in meters. The vertex detector and the silicon inner tracker are not shown.

### 3.2.4 Fourth Concept (“4<sup>th</sup>”) Detector

The Fourth Concept detector[21] consists of four essential detector systems. The calorimeter is a spatially fine-grained dual-readout fiber sampling calorimeter augmented with the ability to measure the neutron content of a shower. The dual fibers are scintillation and Cerenkov for separation of hadronic and electromagnetic components of hadronic showers[24]. A separate crystal calorimeter with dual readout in front of the fiber calorimeter is being studied.

The muon system is a dual-solenoid magnetic field configuration in which the flux from the inner solenoid is returned through the annulus between this inner solenoid and an outer solenoid. The magnetic field between the two solenoids back-bends the muons for a second measurement of the momentum (with drift tubes after the calorimeter).

The iron-free magnetic field is confined to a cylinder with negligible fringe fields and with the capability to control the fields at the beam. The twist compensation solenoid just outside the wall of coils is shown in Figure 3.5 (right). The iron-free configuration may allow mounting of all beam line elements on a single support, which could reduce the effect of vibrations at the final focus (FF) as the beams move coherently up and down together. In addition, the FF elements can be brought close to the vertex chamber for better control of the beam crossing. The iron-free magnetic field configuration allows any crossing angle.

The pixel vertex detector is the SiD detector design. The Time Projection Chamber (TPC) is very similar to those being developed by the GLD and LDC concepts.

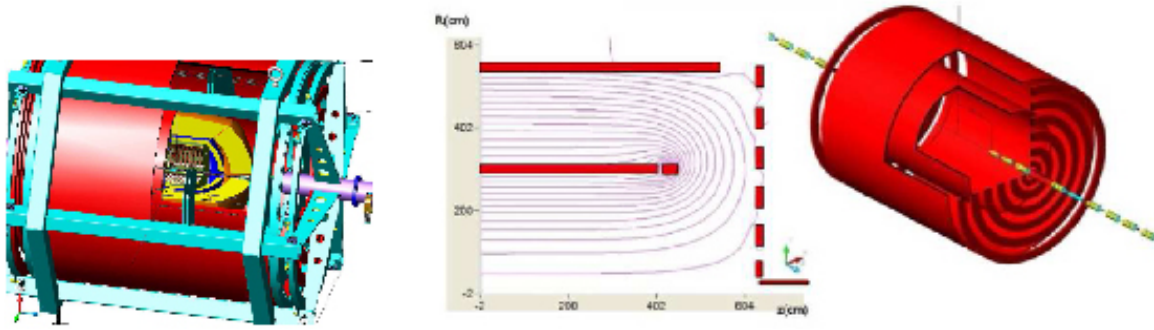


FIGURE 3.5. Cut-away view of the 4th Detector (left). Drawings showing the two solenoids and the “wall of coils” and resulting field lines in an r-z view (right). This field is uniform to 1% at 3.5 T in the TPC tracking region, and also uniform and smooth at -1.5 T in the muon tracking annulus between the solenoids.

### 3.3 DETECTOR AND PHYSICS PERFORMANCE

Significant progress has been made in the development of complete simulation and reconstruction software systems for the ILC detectors, lending reality and credibility to studies of detector performance and physics studies. These are available in software repositories[25].

The detectors have tracking systems composed of a number of different sub-systems. Using realistic algorithms, and including a simulation of the expected background rates, track reconstruction efficiencies close to 99% have been demonstrated, with momentum resolutions of  $\frac{\sigma_{p_t}}{p_t} < 1 \times 10^{-4} \text{ GeV}^{-1}$ .

Below 1 TeV the best event reconstruction resolution is believed to result from a particle flow algorithm. Simulations have shown jet-energy resolutions are near the goal of  $\frac{\sigma_{E_{jet}}}{E_{jet}} = \frac{30\%}{\sqrt{E_{jet}}}$  for  $E_{jet}$  up to approximately 100 GeV, and  $\frac{\sigma_{E_{jet}}}{E_{jet}} \leq 3\%$  beyond. Table 3.2 presents some recent results for jet energy resolution using particle flow in detailed, realistic simulations [26].

TABLE 3.2  
Jet energy resolutions based on simulations of LDC.

| $E_{jet}$ | $\sigma_{E_{jet}}$ |
|-----------|--------------------|
| 45 GeV    | 4.4%               |
| 100 GeV   | 3.0%               |
| 180 GeV   | 3.1%               |
| 250 GeV   | 3.4%               |

Figure 3.6 presents a calculation of the energy rms for 90% of  $\sqrt{s} = 91.2 \text{ GeV}$  events (RMS90) as a function of the production angle of the jets for GLD. In the barrel the averaged energy resolution is 2.97 GeV, which corresponds to 3.3%.

Particle Flow Algorithm (PFA) resolution is expected to improve as the calorimeter radius and magnetic field increase. In order to achieve the PFA performance goal with an acceptable detector cost, SiD adopts the strongest magnetic field with the smallest radius, GLD the

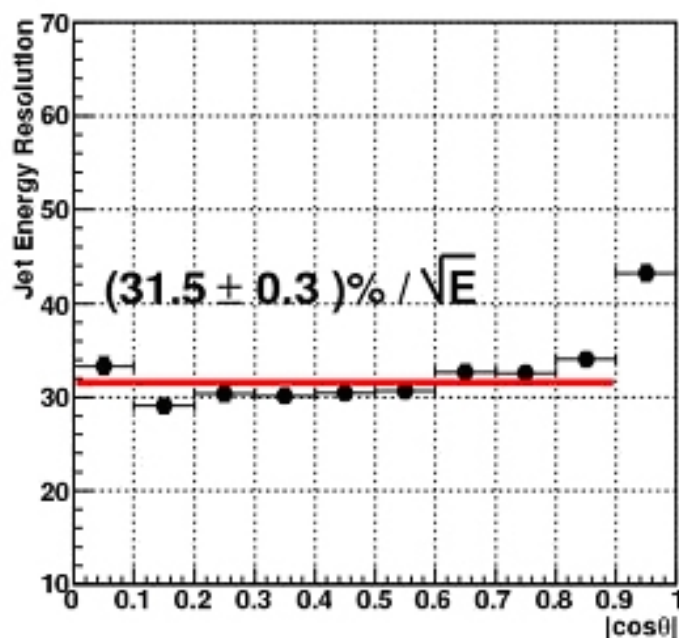


FIGURE 3.6. Energy resolution for 90% of events (RMS90) as a function of  $|\cos\theta_q|$  for  $e^+e^- \rightarrow q\bar{q}$  (light quarks) events at  $\sqrt{s} = 91.2$  GeV in the GLD detector.

weakest magnetic field but the largest radius, with LDC in between. The performances as a function of TPC radius for a few magnetic field values are shown in Figure 3.7. As expected, the jet energy resolution improves with increasing calorimeter radius when the magnetic field is fixed.

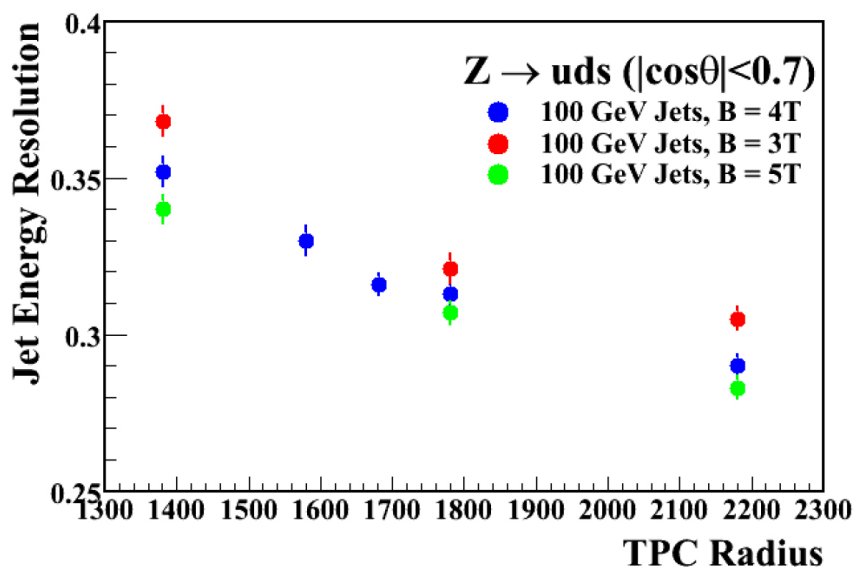


FIGURE 3.7. The jet energy resolution expressed as  $\sigma_{jet} \sqrt{E_{jet}}$ , as a function of the TPC radius for a few magnetic field values. The TPC radius is equivalent to the inner radius of calorimeter.

Study of Higgs boson properties could be a major focus of the ILC physics program. The challenging measurement of the Higgs mass using the recoil mass method is presented in

Figure 3.1. In a related study, the precision on the mass measurement for a 120 GeV Higgs boson at  $\sqrt{s} = 350$  GeV is shown to be 135 MeV with SiD.

### 3.4 INTERFACING THE DETECTOR TO THE MACHINE

The interaction region is the interface between the detector and the accelerator. Its complexity motivates integration of the beam delivery system with the detector design.

The beams are delivered through the largest possible apertures en route to the collision point, but are constrained to pass through a beampipe of minimal radius at the IP to optimize vertex detector performance. A series of detectors record the remnants from the beam interactions in the very forward direction, monitor the beam properties, and measure the delivered luminosity. Tungsten masks shield most of the detector from the backgrounds produced in the collision.

Several beam processes create backgrounds which are potentially problematic for the detector. The main background is large numbers of very forward going photons and electron-positron pairs produced by “beamstrahlung”. Other backgrounds include synchrotron radiation, muons produced upstream of the IR when beam tails impinge on collimators, and neutrons created by the absorption of beamstrahlung photons and pairs on beamline elements.

To guide the disrupted beam and charged background particles out of the detector and to minimize backgrounds, the detector magnetic field is perturbed to point in the direction of the outgoing beam. This is done by superposing a small dipole field on the detector’s main solenoidal field. This Detector Integrated Dipole (DID) is beneficial once the crossing angle increases beyond a few mrad.

The detectors most sensitive to pair backgrounds are the vertex detector and the beamcal. The innermost layer of the vertex detector sits between 1.3 and 1.55 cm from the interaction point, and must contend with  $\sim 100$  particles/mm<sup>2</sup>/bunch train, which generates high occupancies. The beamcal must contend with an energy deposition of 100 TeV/ beam crossing, which results in a high radiation dose. The number of particles passing outside the vertex detector, at radii beyond 10 cm, is rather small. For a silicon based tracking system it is not a real concern. In a TPC based tracking system, where many bunches are integrated into one image of the tracker, the total occupancy is expected to be below one percent, and is not a problem.

The ILC reference design has one interaction region with beams crossing at 14 mrad, and is equipped with two detectors which can be moved quickly into and out of the interaction region (push-pull operation) to share luminosity. The option with two beam delivery systems continues to be investigated. Push-pull is being engineered to proceed efficiently, allowing for quick vacuum and cryogenic disconnects, signal and power umbilicals, and the means to reestablish alignment and calibration quickly. The two detectors provide redundancy, cross-checks and insurance against mishaps.

Precise knowledge of the beam energy and polarization is critical to the physics program, and they can be measured both upstream and downstream of the detector, using energy spectrometers and polarimeters.



## CHAPTER 4

# Value Estimates

### 4.1 THE ACCELERATOR

A preliminary cost analysis has been performed for the ILC Reference Design. A primary goal of the estimate was to allow cost-to-performance optimization in the Reference Design, before entering into the engineering design phase. Over the past year, the component costs were estimated, various options compared and the design evolved through about ten significant cost-driven changes, resulting in a cost reduction of about 25%, while still maintaining the physics performance goals.

The ILC cost estimates have been performed using a “value” costing system, which provides basic agreed-to value costs for components in ILC Units<sup>1</sup>, and an estimate of the explicit labor (in person hours) that is required to support the project. The estimates are based on making world-wide tenders (major industrialized nations), using the lowest reasonable price for the required quality. There are three classes of costs:

- site-specific costs, where a separate estimate was made in each of the three regions;
- conventional costs for items where there is global capability – here a single cost was determined;
- costs for specialized high-tech components (e.g. the SCRF linac technology), where industrial studies and engineering estimates were used.

The total estimated value for the shared ILC costs for the Reference Design is 4.79 Billion (ILC Units). An important outcome of the value costing has been to provide a sound basis for determining the relative value of the various components or work packages. This will enable equitable division of the commitments of the world-wide collaboration.

In addition, the site specific costs, which are related to the direct costs to provide the infrastructure required to site the machine, are estimated to be 1.83 Billion (ILC Units). These costs include the underground civil facilities, water and electricity distribution and buildings directly supporting ILC operations and construction on the surface. The costs were determined to be almost identical for the Americas, Asian, and European sample sites. It should be noted that the actual site-specific costs will depend on where the machine is constructed, and the facilities that already exist at that location.

---

<sup>1</sup>For this value estimate, 1 ILC Unit = 1 US 2007\$ (= 0.83 Euro = 117 Yen).

Finally, the explicit labor required to support the construction project is estimated at 24 million person-hours; this includes administration and project management, installation and testing. This labor may be provided in different ways, with some being contracted and some coming from existing labor in collaborating institutions.

The ILC Reference Design cost estimates and the tools that have been developed will play a crucial role in the engineering design effort, both in terms of studying options for reducing costs or improving performance, and in guiding value engineering studies, as well as supporting the continued development of a prioritized R&D program.

The total estimated value cost for the ILC, defined by the Reference Design, including shared value costs, site specific costs and explicit labor, is comparable to other recent major international projects, e.g. ITER, and the CERN LHC when the cost of pre-existing facilities are taken into account. The GDE is confident that the overall scale of the project has been reliably estimated and that cost growth can be contained in the engineering phase, leading to a final project cost consistent with that determined at this early stage in the design.

## 4.2 THE DETECTORS

Three detector concepts, GLD, LDC, and SiD, estimated the costs of their respective detector designs. Each used a complete work breakdown structure, and identified the significant costs associated with subsystems, and costs associated with assembly and installation. Estimates were guided by the GDE costing rules, and included approximately 35% contingency. The three estimates are reasonably consistent, but are divided differently between M&S and labor, a result of regional accounting differences.

The cost drivers for the M&S budgets are the calorimeters and the solenoidal magnet and flux return iron. Integration, transportation, and computing have been included, as have indirect costs associated with both M&S and labor.

The coil costs for each of the concepts were consistent with the costs for the BaBar, Aleph, and CMS coils when compared as a function of stored energy. The cost breakdowns across detector subsystems for each of three concepts differ concept to concept. This is to be expected, as SiD has costed electronics, installation, and management as separate items whereas LDC and GLD have embedded these in the subdetectors. In another example, GLD chooses to cost both hadron and electromagnetic calorimeters as a single item, since the detectors used are similar. LDC and SiD have separated these expenses, because the detection techniques are quite different.

Based on the SiD and LDC estimates, the value (M&S) cost is in the range 360-420 Million (ILC Units) each. GLD does not estimate M&S separately. Manpower for SiD and LDC (including contingency) is estimated at 1250-1550 person-years. Combining M&S and person-years, the total detector cost lies in the range of 460-560 Million (ILC Units) for any of the detector concepts. The cost scale for the two detectors envisioned for the ILC is about 10% of the cost of the machine.

## CHAPTER 5

# Next Steps: R&D and the Engineering Design Phase

### 5.1 ACCELERATOR R&D

For the last year, the focus of the core GDE activity has been on producing the RDR and value estimate. In parallel, ILC R&D programs around the world have been ramping up to face the considerable challenges ahead. The GDE Global R&D Board – a group of twelve GDE members from the three regions – has evaluated existing programs, and has convened task forces of relevant experts to produce an internationally agreed-upon prioritized R&D plan for the critical items. The highest-priority task force (S0/S1) addresses the SCRF accelerating gradient:

- S0: high-gradient cavity – aiming to achieve 35 MV/m nine-cell cavity performance with an 80% production yield;
- S1: high-gradient cryomodule – the development of one or more high-gradient ILC cryomodules with an average operational gradient of 31.5 MV/m.

The S0/S1 task force has already produced focused and comprehensive R&D plans. Other task forces (S2: test linac; S3: Damping Ring; S4: Beam Delivery System, etc.) are in the process of either completing their reports, or just beginning their work.

For the cost- and performance-critical SCRF, the primary focus of S0/S1 remains the baseline choice, the relatively mature TESLA nine-cell elliptical cavity. However, additional research into alternative cavity shapes and materials continues in parallel. One promising technique is the use of ‘large-grain’ niobium [27], as opposed to the small-grain material that has been used in the past (Figure 5.1). Use of large grain material may remove the need for electropolishing, since the same surface finish can potentially be achieved with Buffered Chemical Polishing (BCP) – a possible cost saving. Several single-cells have achieved gradients in excess of 35 MV/m (without electropolishing) and more recent nine-cell cavity tests have shown very promising results.

Various new and promising cavity shapes are also being investigated, primarily at KEK and Cornell. While the basic nine-cell form remains, the exact shape of the ‘cells’ is modified to reduce the peak magnetic field at the niobium surface. In principle these new shapes can achieve higher gradients, or higher quality factors ( $Q_0$ ). Single-cells at KEK (ICHIRO) and Cornell (reentrant) have achieved the highest gradients to date ( $\sim 50$  MV/m, see Figure 5.1).

## NEXT STEPS: R&D AND THE ENGINEERING DESIGN PHASE

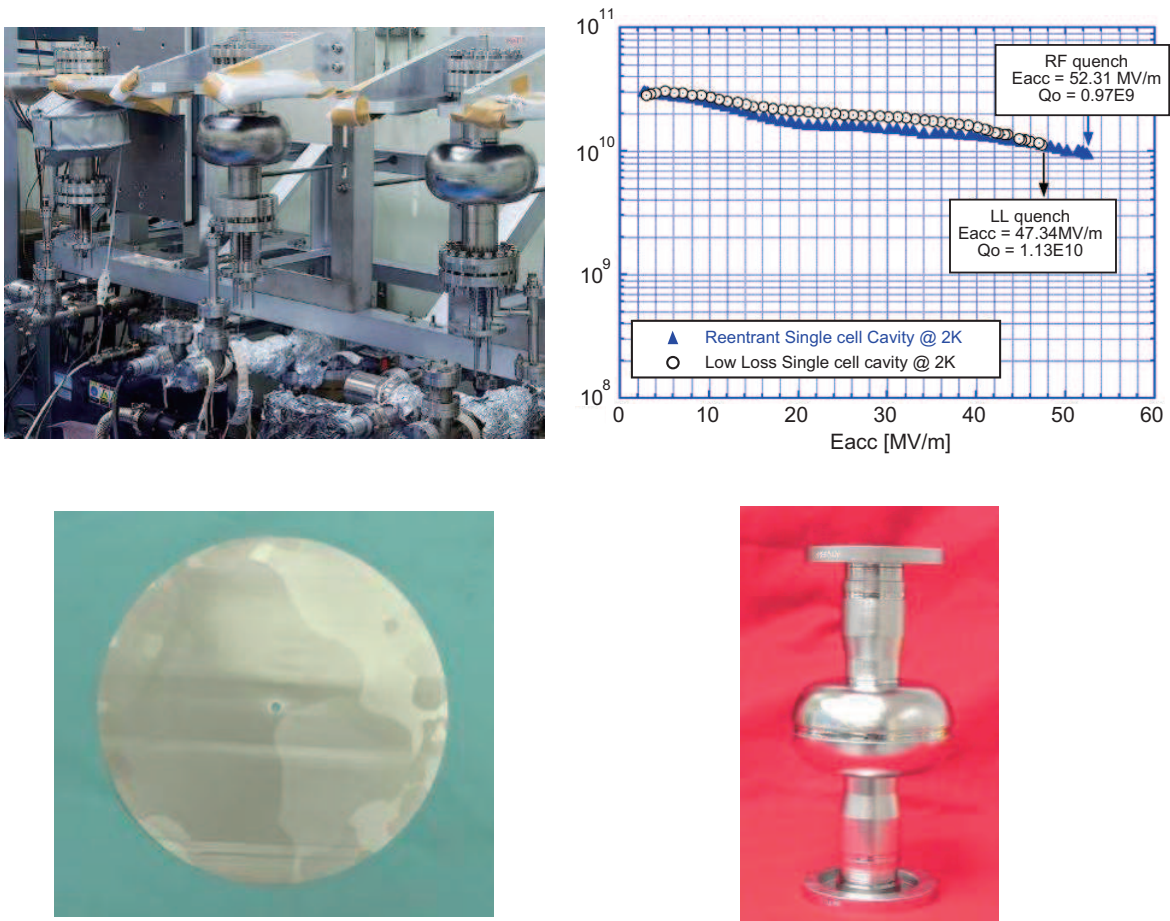


FIGURE 5.1. Cutting-edge SCRF R&D. Top-left: ICHIRO single-cells being prepared for testing at KEK. Top-right: world-record performance from novel shape single-cells (ICHIRO and Cornell's reentrant cavity). Bottom-left: large-grain niobium disk (Jefferson Lab). Bottom-right: single-cell cavity produced from large-grain niobium material (Jefferson Lab).

R&D towards making high-performance nine-cell cavities using these designs continues as future possible alternatives to the ILC baseline cavity.

The GDE formally supports R&D on alternative designs for components other than the cavities, where the new designs promise potential cost and/or performance benefits. Some key examples are alternative RF power source components, of which the Marx modulator is currently the most promising. In addition, R&D on critical technologies will continue through the EDR. Topics include items such as the damping ring kickers and electron-cloud mitigation techniques, the positron target and undulator, the magnets around the beam interaction point, and global issues that require very high availability such as the control system, the low-level RF, and the magnet power supplies.

## 5.2 THE DETECTOR ROADMAP: R&D AND ENGINEERING DESIGNS

The detector R&D and integrated detector design efforts must keep pace with progress on the ILC. The detector R&D program, which has already developed over many years, includes efforts in all regions, with inter-regional collaboration in some cases, and inter-regional coordination in all cases. The R&D is reviewed within the global context by the World Wide Study. This R&D is critical to the success of the ILC experimental program.

To focus integrated detector design efforts over the next few years, the current studies for four distinct concepts will be concentrated into two engineering design efforts, in time for the submission of two detector EDRs at the same time as the ILC machine EDR. The ILCSC will issue a call for Letters of Intent to the ILC detector community during Summer 2007 to initiate this process. The next steps are still being developed by the ILCSC, but will include appointing a Research Director, who will be responsible for developing the ILC experimental program, and establishing an International Detector Advisory Group, which will help define the two experiments suitable for engineering design. The resulting two detectors are expected to have complementary and contrasting strengths, as well as broad international participation. The two detector concepts should be defined by early 2009, and their engineering designs will then be completed over the next two or three years.

## 5.3 TOWARDS THE ENGINEERING DESIGN REPORT (EDR)

While investment into the critical R&D remains a priority, a significant ramping-up of global engineering resources will now be required to produce an engineered technical design by 2010. An important aspect of this work will be the refinement and control of the published cost estimate by value engineering. The EDR phase will also require a restructuring of the GDE to support the expanded scope. A more traditional project structure will be adopted based on the definition of a discrete set of Work Packages. The responsibility for achieving the milestones and deliverables of each Work Package will be assigned to either a single institute, or consortium of institutes, under the overall coordination of a central project management team. The Work Packages need to be carefully constructed to accommodate the direct needs of the Engineering Design phase, while at the same time reflecting the global nature of the project. An important goal of the current planning is to integrate the engineering design and fundamental R&D efforts, since these two aspects of the project are clearly not independent. The new project structure will be in place by mid 2007.

The GDE remains committed to the technically-driven schedule of supplying the EDR in 2010, making start of construction possible as early as 2012 consistent with expected early results from the LHC. The critical path and cost drivers have been clearly identified during the RDR phase, and they define the priorities for the next three years of the Engineering Design phase. The R&D program will be fine-tuned to mitigate the remaining identified technical risks of the design. A key element of the engineering activity will be the formation of a qualified industrial base in each region for the SCRF linac technology. A equally critical focus will be on the civil construction and conventional facilities the second primary cost driver where an early site selection would clearly be advantageous.

Finally, the GDE also remains committed to completing these challenging goals as a truly international organization, by building on and consolidating the successful collaboration

## NEXT STEPS: R&D AND THE ENGINEERING DESIGN PHASE

which produced the RDR. The support of the world-wide funding agencies is critical in this endeavor. The GDE together with the leaders of the particle physics community will continue to work with the regional funding agencies and governments to begin construction of this project in the early part of the next decade.

# BIBLIOGRAPHY

- [1] A. Albrecht, *et al.*, Report of the DOE/NSF High Energy Physics Advisory Panel (2004).
- [2] H. Shapiro *et al.*, “Report of the Committee on Elementary Particle Physics in the 21st Century,” Board of Physics and Astronomy, National Research Council, National Academies Press, Washington D.C. (2006); “The European Strategy for Particle Physics,” Report of CERN Council Strategy Group (2006); GLC Project: “Linear Collider for TeV Physics” ,KEK-REPORT-2003-7; I. Corbett *et al.*, “Report of the Consultative Group on High-Energy Physics,” OECD Global Science Forum (2002); S. Yamada *et al.*, “Report of the JLC Globalization Committee” (2002); Aguilar-Saavedra, J. A. *et al.*, “TESLA Technical Design Report Part III: Physics at an e+e- Linear Collider,” hep-ph/0106315; ACFA Linear Collider Working Group, “Particle Physics Experiments at JLC,” hep-ph/0109166; Abe, T. and *et al.*, “Linear Collider Physics Resource Book for Snowmass,” American Linear Collider Working Group (2001).
- [3] J. Bagger *et al.*, “Discovering the Quantum Universe: The Role of Particle Colliders,” Report of the DOE/NSF High Energy Physics Advisory Panel (2006).
- [4] ATLAS Collaboration, “ATLAS Physics Technical Design Report,” CERN-LHCC-99-14 and CERN-LHCC-99-15, <http://atlas.web.cern.ch/Atlas/GROUPS/PHYSICS/TDR/TDR.html>; “CMS Physics TDR,” CERN/LHCC/2006-021 (2006).
- [5] R. Cousins, J. Mumford and V. Valuev, “Forward-Backward Asymmetry of Simulated and Reconstructed Z-prime  $\rightarrow \mu^+\mu^-$  Events in CMS” CERN-CMS-NOTE-2005-022 (2005)
- [6] “Parameters for the Linear Collider,” [http://www.fnal.gov/directorate/icfa/LC\\_parameters.pdf](http://www.fnal.gov/directorate/icfa/LC_parameters.pdf) (2003) and <http://www.fnal.gov/directorate/icfa/para-Nov20-final.pdf> (2006).
- [7] G. Moortgat-Pick *et al.*, “The Role of Polarized Positrons and Electrons in Revealing Fundamental Interactions at the Linear Collider,” hep-ph/0507011 (2005).
- [8] R. Hawkings and K. Moenig, “Electroweak and CP violation physics at a Linear Collider Z-factory,” hep-ex/9910022 (1999).
- [9] C. A. Heusch, “The International Linear Collider in its Electron-Electron Version,” Int. J. Mod. Phys.A20 (2005).
- [10] I. F. Ginzburg, G. L. Kotkin, V. G. Serbo and V. I. Telnov, JETP Lett. 34 (1981) 491; Badelek, B. *et al.*, hep-ex/0108012.

## BIBLIOGRAPHY

- [11] ITRP Recommendation, [http://www.fnal.gov/directorate/icfa/ITRP\\_Report\\_Final.pdf](http://www.fnal.gov/directorate/icfa/ITRP_Report_Final.pdf) (2004).
- [12] R. Brinkmann *et al.*, eds., “TESLA Technical Design Report,” DESY-2001-011 (March, 2001).
- [13] T. O. Raubenheimer *et al.*, eds., “Zeroth Order Design Report for the Next Linear Collider,” SLAC-R-474 (1996); N. Phinney, ed., “2001 Report on the Next Linear Collider: A report submitted to Snowmass ’01,” SLAC-R-571 (2001).
- [14] “GLC project: Linear Collider for TeV Physics,” KEK-Report-2003-7, <http://lcdev.kek.jp/Roadmap/> (2003)
- [15] M. Altarelli *et al.*, “The European X-Ray Free-Electron Laser Technical Design Report,” DESY 2006-097 (2006).
- [16] F. Furuta *et al.*, “Experimental Comparison at KEK of High Gradient Performance of Different Single-Cell Superconducting Cavity Designs,” EPAC06 (2006); R. L. Geng *et al.*, “High-Gradient Activities at Cornell: Re-entrant Cavities,” SRF 2005 (2005).
- [17] K. Abe *et al.*, “Particle Physics Experiments at JLC,” KEK-Report-2001-11 and hep-ph/0109166 (2001); T. Abe *et al.*, “Linear Collider Physics Resource Book for Snowmass 2001,” BNL-52627, CLNS01/1279, FERMILAB-Pub-01/058-E, LBNL-47813, SLAC-R-570, UCRL-ID-143810-DR (2001).
- [18] The SiD Concept Group, “SiD Detector Outline Document, <http://physics.uoregon.edu/~lc/wwstudy/concepts/> (2006).
- [19] The LDC Concept Group, “LDC Detector Outline Document,” <http://www.ilcldc.org> (2006).
- [20] GLD Concept Study Group, “GLD Detector Outline Document,” physics/0607154 (2006).
- [21] The 4th Concept Group, “Detector Outline Document,” <http://physics.uoregon.edu/~lc/wwstudy/concepts/> (2006).
- [22] H. J. Schreiber, “Branching fraction measurements of the SM higgs with a mass of 160 GeV at future linear colliders,” LC-PHSM-2000-035 (2000); T. Barklow, “Physics impact of detector performance,” 2005 ILC Workshop, <http://www-conf.slac.stanford.edu/lcws05/program/talks/18mar2005.ppt> (2005); H.-J. Yang and K. Riles, “Impact of tracker design on higgs and slepton measurements,” physics/0506198 (2005).
- [23] T. Abe, “A Study of Topological Vertexing for Heavy Quark Tagging” , SLAC-PUB-8775 (2001).
- [24] N. Akchurin *et al.*, NIM **A537**, 537-561 (2005).
- [25] F. Gaede *et al.*, <http://ilcsoft.desy.de/marlin>; T. Johnson *et al.*, “lcorg.sim: A Java-based Reconstruction and Analysis Toolkit,” <http://www.lcsim.org>; C. Gatto *et al.*, <http://www.fisica.unile.it/~danieleb/IlcRoot>.



- [26] M. Thomson, Paris ILC Software Meeting (2007).
- [27] P. Kneisel *et al.*, “Preliminary Results from Single Crystal and Very Large Crystal Niobium Cavities,” PAC05 (2005).

## BIBLIOGRAPHY

# LIST of FIGURES

|      |   |    |
|------|---|----|
| 1.1  | The electromagnetic and weak nuclear forces unify at the Terascale. . . . . | 2  |
| 1.2  | Relic density and mass determinations for neutralino dark matter. . . . .   | 3  |
| 2.1  | A TESLA nine-cell 1.3 GHz superconducting niobium cavity. . . . .           | 8  |
| 2.2  | SCRF Cryomodules. . . . .   | 9  |
| 2.3  | High-performance nine-cell cavities. . . . .                                | 9  |
| 2.4  | Clean room environments are mandatory. . . . .                              | 10 |
| 2.5  | Birth of a nine-cell cavity. . . . .  | 10 |
| 2.6  | Schematic layout of the ILC complex for 500 GeV CM. . . . .                 | 12 |
| 2.7  | Schematic View of the Polarized Electron Source. . . . .                    | 14 |
| 2.8  | Overall Layout of the Positron Source. . . . .                              | 15 |
| 2.9  | Schematic of the RTML. . . . .  | 17 |
| 2.10 | RF unit layout. . . . .   | 19 |
| 2.11 | Cutaway view of the linac dual-tunnel configuration. . . . .                | 20 |
| 2.12 | BDS layout, beam and service tunnels. . . . .                               | 21 |
| 2.13 | Geology and tunnel profiles for the three regional sites. . . . .           | 23 |
| 3.1  | Higgs recoil mass spectra . . . . .   | 27 |
| 3.2  | Illustration of a quadrant of SiD. . . . .                                  | 29 |
| 3.3  | View of the LDC detector concept . . . . .                                  | 30 |
| 3.4  | Schematic view of two different quadrants of the GLD Detector. . . . .      | 31 |
| 3.5  | Cut-away view of the 4th Detector . . . . .                                 | 32 |
| 3.6  | RMS90 as a function of $ \cos \theta_q $ . . . . .                          | 33 |
| 3.7  | The jet energy resolution . . . . .   | 33 |
| 5.1  | Cutting-edge SCRF R&D. . . . .  | 38 |

## LIST OF FIGURES

# LIST of TABLES

|     |  |    |
|-----|--|----|
| 2.1 | Basic design parameters for the ILC. . . . .                   | 13 |
| 2.2 | Nominal and design range of beam parameters at the IP. . . . . | 13 |
| 3.1 | Some key parameters of the four detector concepts. . . . .     | 28 |
| 3.2 | Jet energy resolutions based on simulations of LDC. . . . .    | 32 |